Targeted whole genome sequencing protocols for African and classical swine fever viruses.

by

Chester Dale McDowell

B.S., Kansas State University, 2009
M.S., Kansas State University, 2012
D.V.M., Kansas State University, 2020

AN ABSTRACT OF A DISSERTATION

submitted in partial fulfillment of the requirements for the degree

DOCTOR OF PHILOSOPHY

Department of Diagnostic Medicine and Pathobiology
College of Veterinary Medicine

KANSAS STATE UNIVERSITY
Manhattan, Kansas

2025

Abstract

The increasing availability and feasibility of sequencing has facilitated the advancement of infectious disease research including pathogen discovery, phylogenetic characterization, and viral evolution. Sequencing data combined with clinical disease, virulence, and viral dynamics data, can reveal a more complete understanding of viral evolution for the development of novel and effective control measures. Furthermore, experimental infection studies contribute to our understanding of clinical disease and viral dynamics when there is limited information such as with a novel pathogen or viral strain and provide critical reagents to evaluate the performance of available diagnostics and to develop new ones.

African swine fever (ASF) an infectious viral disease caused by African swine fever virus (ASFV) that causes high mortality in domestic swine and wild boar (Sus scrofa). Since the outbreak in 2007 in the country of Georgia, ASFV has continues to spread and remains as a current global threat. In 2019, an African swine fever virus (ASFV) outbreak was reported in Mongolia; due to the limited information from field observations, we conducted an experimental infection of domestic pigs to further evaluate and characterize the progression of clinical disease, virulence, and pathology of an ASFV Mongolia/2019 field isolate (ASFV-MNG19). The study demonstrated that ASFV-MNG19 is a virulent genotype II ASFV strain that causes acute ASF in domestic swine. Controlled experimental studies like this one, are important to evaluate the genetics, virulence and clinical progression of emerging viruses and different variants/strains described in the field, and to aid in the development and validation of diagnostic tools used by regulatory agencies for the rapid detection and implementation of mitigation strategies.

Targeted whole genome sequencing protocols are crucial for the rapid identification and complete genetic characterization of emerging and high consequence viral pathogens for

outbreak investigations and understanding viral evolution for the development of novel and effective control measures. Such protocols are lacking for two high consequences viral pathogens affecting swine, ASFV and classical swine fever virus (CSFV). In order to fill this gap, we developed independent panels of primers spanning the genomes of ASFV and CSFV to generate approximately 10kB and 6kB amplicons, respectively, providing whole genome amplification. The targeted protocols for these viruses were tested using cell culture-derived viruses and clinical samples generated by our experimental infection studies in swine. These protocols resulted in an average coverage greater than 1000X for ASFV with 99% of the genome covered, and 10,000X-20,000X for CSFV with 97% to 99% of the genomes covered when sequenced on the Oxford Nanopore MinION platform. These protocols will be important tools to assist in early pathogen detection and genetic characterization of these high consequence swine viruses in outbreak and surveillance situations globally and within the United States, should an outbreak occur.

Targeted whole genome sequencing protocols were also developed for the emerging zoonotic viral pathogen, SARS-CoV-2, to evaluate the viral competition between ancestral and novel variants in a susceptible host. We conducted a competition experiment whereby adult white-tailed deer (WTD) were co-infected with a lineage A and lineage B alpha variant SARS-CoV-2 isolates. The percent composition of lineage A and B viruses were evaluated using lineage A and B-specific RT-qPCR assays and targeted whole genome sequencing with a BLAST-based analysis. Using the developed protocols, we obtained that the SARS-CoV-2 lineage B alpha variant had improved fitness compared to the lineage A virus in adult WTD. This study demonstrates that sequencing data and bioinformatic pipelines can be used to evaluate strain composition in the presence of a co-infection. The targeted whole genome sequencing

protocols developed here can be applied to investigate co-infection competition studies or to evaluate emerging viral variants through single nucleotide variant analysis, providing more information on the viral dynamics and evolution of these high consequence pathogens.

Targeted whole genome sequencing protocols for African and classical swine fever viruses.

by

Chester Dale McDowell

B.S., Kansas State University, 2009
M.S., Kansas State University, 2012
D.V.M., Kansas State University, 2020

A DISSERTATION

submitted in partial fulfillment of the requirements for the degree

DOCTOR OF PHILOSOPHY

Department of Diagnostic Medicine and Pathobiology
College of Veterinary Medicine

KANSAS STATE UNIVERSITY
Manhattan, Kansas

2025

Approved by:

Major Professor
Prof. Jürgen A. Richt, Ph.D., D.V.M

Copyright

© Chester McDowell 2025.

Abstract

The increasing availability and feasibility of sequencing has facilitated the advancement of infectious disease research including pathogen discovery, phylogenetic characterization, and viral evolution. Sequencing data combined with clinical disease, virulence, and viral dynamics data, can reveal a more complete understanding of viral evolution for the development of novel and effective control measures. Furthermore, experimental infection studies contribute to our understanding of clinical disease and viral dynamics when there is limited information such as with a novel pathogen or viral strain and provide critical reagents to evaluate the performance of available diagnostics and to develop new ones.

African swine fever (ASF), an infectious viral disease caused by African swine fever virus (ASFV) that causes high mortality in domestic swine and wild boar (Sus scrofa). Since the outbreak in 2007 in the country of Georgia, ASFV has continues to spread and remains as a current global threat. In 2019, an African swine fever virus (ASFV) outbreak was reported in Mongolia; due to the limited information from field observations, we conducted an experimental infection of domestic pigs to further evaluate and characterize the progression of clinical disease, virulence, and pathology of an ASFV Mongolia/2019 field isolate (ASFV-MNG19). The study demonstrated that ASFV-MNG19 is a virulent genotype II ASFV strain that causes acute ASF in domestic swine. Controlled experimental studies like this one, are important to evaluate the genetics, virulence and clinical progression of emerging viruses and different variants/strains described in the field, and to aid in the development and validation of diagnostic tools used by regulatory agencies for the rapid detection and implementation of mitigation strategies.

Targeted whole genome sequencing protocols are crucial for the rapid identification and complete genetic characterization of emerging and high consequence viral pathogens for

outbreak investigations and understanding viral evolution for the development of novel and effective control measures. Such protocols are lacking for two high consequences viral pathogens affecting swine, ASFV and classical swine fever virus (CSFV). In order to fill this gap, we developed independent panels of primers spanning the genomes of ASFV and CSFV to generate approximately 10kB and 6kB amplicons, respectively, providing whole genome amplification. The targeted protocols for these viruses were tested using cell culture-derived viruses and clinical samples generated by our experimental infection studies in swine. These protocols resulted in an average coverage greater than 1000X for ASFV with 99% of the genome covered, and 10,000X-20,000X for CSFV with 97% to 99% of the genomes covered when sequenced on the Oxford Nanopore MinION platform. These protocols will be important tools to assist in early pathogen detection and genetic characterization of these high consequence swine viruses in outbreak and surveillance situations globally and within the United States, should an outbreak occur.

Targeted whole genome sequencing protocols were also developed for the emerging zoonotic viral pathogen, SARS-CoV-2, to evaluate the viral competition between ancestral and novel variants in a susceptible host. We conducted a competition experiment whereby adult white-tailed deer (WTD) were co-infected with a lineage A and lineage B alpha variant SARS-CoV-2 isolates. The percent composition of lineage A and B viruses were evaluated using lineage A and B-specific RT-qPCR assays and targeted whole genome sequencing with a BLAST-based analysis. Using the developed protocols, we obtained that the SARS-CoV-2 lineage B alpha variant had improved fitness compared to the lineage A virus in adult WTD. This study demonstrates that sequencing data and bioinformatic pipelines can be used to evaluate strain composition in the presence of a co-infection. The targeted whole genome sequencing

protocols developed here can be applied to investigate co-infection competition studies or to evaluate emerging viral variants through single nucleotide variant analysis, providing more information on the viral dynamics and evolution of these high consequence pathogens.

Table of Contents

List of Figures xiv
List of Tables xv
Acknowledgements xvi
Dedication xvii
Chapter 1 - Introduction 1
1.1: African Swine Fever virus 1
1.1.2. Viral Characteristics 1
1.1.3 Epidemiology 2
1.1.4. Route of Transmission 4
1.1.5. Clinical Disease 5
1.1.6. Diagnostics 7
1.1.6.1 Detection of ASFV virus and viral antigen 8
1.1.6.2. Detection of ASFV Genome 10
1.1.6.3. Antibody Detection of ASFV 12
1.1.6.4. Genotyping and Serotyping of ASFV via Sequencing 14
1.1.7. ASFV Control and Mitigation Strategies 15
1.2: Classical Swine Fever virus 16
1.2.1. Viral Characteristics 17
1.2.2. Epidemiology 18
1.2.3. Clinical Disease 20
1.2.3.1. Acute disease 21
1.2.3.2. Chronic disease 21
1.2.3.3. Persistent disease 22
1.2.4. Diagnostics 22
1.2.4.1. Detection of CSFV Genome 23
1.2.4.2. Detection of CSFV Antigen and Antibodies 24
1.2.4.3. Genotyping of CSFV 26
1.2.5. Current Control Strategies 27
1.3. Severe Acute Respiratory Syndrome Coronavirus 2 (SARS-CoV-2) 28

1.3.1. Viral Characteristics 29
1.3.2. Epidemiology 30
1.3.3. Clinical Disease 32
1.3.4. Diagnostics 33
1.3.4.1. Detection of SARS-CoV-2 Genome 33
1.3.4.2. Targeted Whole Genome Sequencing SARS-CoV-2 34
1.3.4.3. Detection of SARS-CoV-2 Antigen and Antibodies 35
1.3.5. Control Strategies 37
1.4. Nucleic Acid Sequencing: Technologies and Approaches 38
1.4.1. The Generations of Sequencing Technologies 38
1.4.1.1. First-Generation Sequencing 38
1.4.1.2. Second-Generation Sequencing 39
1.4.1.3. Third-Generation Sequencing 42
1.4.2. Sequencing Approaches 45
1.4.2.1. Metagenomic Sequencing 45
1.4.2.2. Targeted Sequencing 46
1.5. Bioinformatic Analysis 47
1.5.1. *De Novo* Assembly 48
1.5.2. Read Alignment to Reference Genome (Read Mapping) 49
1.5.3. Single Nucleotide Polymorphism Analysis: Variant Calling 50
Chapter 2 - Experimental Infection of Domestic Pigs with African Swine Fever Virus Isolated in 2019 in Mongolia 52
Abstract 52
2.1. Introduction 53
2.2. Materials and Methods 55
2.2.1. Cell Culture and Challenge Material Preparation 55
2.2.2. Next Generation Sequencing (NGS) 56
2.2.3. Ethics Statement for Use of Animals 57
2.2.4. Study Design 57
2.2.5. Clinical Signs and Samples 59
2.2.6. Quantitative Real-Time PCR Assay for ASFV DNA 59

2.2.7. Gross and Histological Pathology 61
2.3. Results 62
2.3.1. Whole-Genome Sequencing of the ASFV-MNG19 Isolate 62
2.3.2. Clinical Observations Following Challenge with ASFV-MNG19 Isolate 65
2.3.3. Detection and Quantitation of ASFV DNA by qPCR 67
2.3.4. Viral Titrations in Blood and OP Swabs 69
2.3.5. Gross Pathologic Lesions 70
2.3.6. Histopathological Lesions 72
2.4. Discussion 74
Chapter 3 - Targeted Whole Genome Sequencing of African Swine Fever Virus and Classical Swine Fever Virus on the MinION Portable Sequencing Platform 78
Abstract 78
3.1. Introduction 79
3.2 Material/Methods 82
3.2.1 Samples/Source of samples 82
3.2.2 Ethics Statement for Use of Animals 83
3.2.3 Nucleic acid Extraction and Quantitative Real-time PCR 83
3.2.3.1 ASFV DNA Extraction and Quantitation 83
3.2.3.2 CSFV RNA Extraction and Quantitation 84
3.2.4 Primer Design 85
3.2.4.1 African Swine Fever Virus 86
3.2.4.2 Classical Swine Fever Virus 88
3.2.5 Whole Genome Amplification 89
3.2.5.1 African Swine Fever Virus 89
3.2.5.2 Classical Swine Fever Virus 90
3.2.6 Sequencing Library Preparation and MinION Sequencing 90
3.3 Results 91
3.3.1 ASFV AmpliSeq Results 91
3.3.2 CSFV AmpliSeq Results 97
3.4 Discussion 103
3.5 Conclusions 105

Chapter 4 - Assessment of SARS-CoV-2 Strain Competition in Co-Infected Adult White-tailed Deer by Targeted Whole Genome Sequencing 106
Abstract 106
4.1. Introduction 107
4.2. Material Methods 108
4.2.1. Samples Tested 108
4.2.2. Next-Generation Sequencing 109
4.2.3. Strain Specific RT-qPCR for Strain Differentiation 110
4.3 Results 113
4.3.1. SARS-CoV-2 Strain Competition Analysis by Sequencing 113
4.3.2. Strain Specific RT-qPCR 116
4.3.3. Strain Specific RT-qPCR for Clinical Samples 117
4.4 Discussion 118
Chapter 5 - Concluding Remarks 121
References 126

List of Figures

Figure 1.1. The global distribution of ASFV. 4
Figure 1.2. Global distribution of CSFV, 2024. 19
Figure 2.1. ASFV-MNG19 Challenge Study Schematic. 58
Figure 2.2. Phylogenetic tree of whole-genome sequences of ASFVs. 64
Figure 2.3. Clinical Observations of ASFV-MNG19 Infected Pigs. 66
Figure 2.4. Quantitative real-time PCR for ASFV DNA detected in blood, OP swabs, and oral fluids. 68
Figure 2.5. Viral titers in blood and OP swabs. 69
Figure 2.6. Gross pathology lesions following ASFV-MNG19 infection. 71
Figure 2.7. Histological lesions following ASFV-MNG19 infection. 73
Figure 3.1. Genome map of the ASFV genome displaying nineteen 10kB amplicons. 86
Figure 3.2. Genome map of CSFV genome displaying the two ~6 kB amplicons generated from the two primer pairs. 88
Figure 3.3. Coverage graphs of reads mapped to the ASFV genome. 93
Figure 3.4. Coverage graphs of reads mapped to the CSFV genome. 99
Figure 4.1. Strain specific RT-qPCR primer and probe schematic. 111
Figure 4.2. SARS-CoV-2 strain specific spike RT-qPCR. 112
Figure 4.3. Schematic for the generation of known viral RNA populations. 113
Figure 4.4. NGS results of nasal swabs collected from adult WTD co-infected with SARS-CoV-2 ancestral strain (WA1) and alpha VOC (B.1.1.7). 115
Figure 4.5. NGS of respiratory tissues collected at 4 DPC from WTD co-infected with SARS-CoV-2 ancestral strain (WA1) and alpha VOC (B.1.1.7). 116
Figure 4.6. Quantification of WA1 and B.1.1.7 within a known viral RNA population. 117

List of Tables

Table 1.1. CSF disease forms and associated clinical signs. 22
Table 2.1. The ten sequences with the highest similarity to ASFV-MNG19. 62
Table 3.1. ASFV primers and associated pools 87
Table 3.2. CSFV Primers 88
Table 3.3. Sequencing data for ASFV samples tested with ASFV AmpliSeq 96
Table 3.4. Sequencing data for 11 CSFV strains tested with CSFV AmpliSeq 100
Table 3.5. Sequencing data for clinical CSFV samples tested with CSFV AmpliSeq 102
Table 4.1. Strain composition of clinical swabs analyzed by RT-qPCR. 118
Table 4.2. Strain composition of respiratory tissue analyzed by RT-qPCR. 118

Acknowledgements

I would like to acknowledge Dr. Jürgen Richt for his years of mentorship and support in both my academic and professional careers. Drs. Jianfai Bai, Roman Pogranichniy, and William Wilson for serving on my supervisory committee. Dr. Natasha Gaudreault for the advice and guidance she provided throughout my Ph.D. program. Drs. Jayme Neto-Souza, Patricia Assato, and Taeyong Kwon for their support developing the ASFV and CSFV NGS protocols. Members of Dr. Richt's lab group both past and present for their support with animal studies, sample processing, data analysis and guidance. The USDA-NSTP program for the financial support of this Ph.D./DVM program. USDA-APHIS for providing financial support for the ASFV and CSFV NGS project. This project would not have been possible without all their support.

Dedication

I would like to dedicate this dissertation to Dr. Thomas McDowell, Ilona McDowell and my friends, for their continued support throughout my life and during my academic endeavors.

Chapter 1 - Introduction

1.1: African Swine Fever virus

African swine fever (ASF) is an infectious viral disease that causes high mortality in domestic swine and wild boars (*Sus scrofa)*. Outbreaks have devastating economic impacts on affected regions and countries threatening swine health and the swine industry worldwide (McDowell et al., 2022a). Currently there is one live-attenuated vaccine (NAVET-ASFVAC) licensed for use in Vietnam (Borca et al., 2021; X. H. Tran et al., 2022). Due to the lack of a globally available vaccines the current outbreak control measures include the culling of infected and in contact animals, quarantine of sites and zones, movement restrictions, and export restrictions (Sánchez-Cordón et al., 2018). These outbreaks can have lastly socio-economic impacts on affected countries. ASF is a World Organization for Animal Health (WOAH) and United States Department of Agriculture (USDA) notifiable disease due to the devastating impacts outbreaks have on both the swine populations and affected countries.

1.1.2. Viral Characteristics

The causative agent of ASF is African swine fever virus (ASFV) belonging to the *Asfarviridae* family, genus *Asfivirus*, and currently the only known DNA arbovirus. The viral particle encapsulates a 170-192 kilobases (kB) double-stranded DNA genome encoding more than 150 genes (Dixon et al., 2013, 2019; Vilem et al., 2020a; X. Wang et al., 2022a). The major differences in genome size between strains are the result of the loss and gain of multi-gene families (MGFs) and variations of tandem repeats in non-coding regions (Dixon et al., 2013; Gaudreault, Madden, et al., 2020). The significance and function of many of the non-structural and structural proteins encoded by the ASFV genome remains unknown (Dixon et al., 2013).

The ASFV virion has a multi-layered structure that consists of the nucleoid, core shell, inner envelope, capsid, and host-derived outer envelope 175-215 nm in diameter encapsulating its DNA genome (Chapman et al., 2008; Salas & Andrés, 2013). The viral capsid is decorated with a major capsid protein, p72, and four minor proteins, M1249L, p17, p49, and H240R (N. Wang et al., 2019).

ASFV has multiple genotypes and serotypes with varying virulence between and within genotypes. Historically, there were 24 known genotypes of ASFV based on the partial sequence of p72; recent retrospective studies of ASFV sequences suggest there may be only 6 to 7 genotypes including a recently characterized genotype I/II recombinant virus in China (Spinard, Dinhobl, et al., 2023; D. Zhao et al., 2023a). ASFV also has 8 known serogroups that are based on the CD2v and C-type Lectin sequence (Malogolovkin et al., 2015). The majority of ASFV genotypes have remained confined to Africa. Historically, genotype I and genotype II viruses have been the only viruses to result in outbreaks outside of Africa (Costard et al., 2013). Currently, genotype II viruses are spreading across the globe.

1.1.3 Epidemiology

Since ASFV was first identified in Kenya in 1921, it has remained endemic in sub-Saharan African countries (Eustace Montgomery, 1921). The *Orinthodoros* soft tick serves as the only known vector for ASFV. The *Orinthodoros* tick is a key component of ASFVs sylvatic cycle that is maintained between warthogs (*Phacochoerus africanus*) and *Orinthodoros moubata* in Africa (Gaudreault, Madden, et al., 2020). The *Orinthodoros erraticus* tick present in Europe have been demonstrated to be a competent vector for ASFV through experimental infection and potential role as a reservoir during the Iberian Peninsula outbreak (Costard et al., 2013; Diaz et

al., 2012; Oleaga et al., 1990). The first occurrence of ASFV outside continental Africa was a genotype I virus that resulted in outbreaks in Europe, Russia, and South America between the 1950 and 1980s; by the 1990s ASFV was confined to Africa and Sardinia where it remains endemic (Costard et al., 2013; Gaudreault, Madden, et al., 2020). In 2007 an outbreak of genotype II virus occurred in the country of Georgia where it spread through domestic swine (*Sus scrofa domesticus*) and wild boar (S*us scrofa*) populations across the Caucasus region and eventually into Russia and Eastern Europe (Cwynar et al., 2019; Gogin et al., 2013; Sánchez-Vizcaíno et al., 2013), Figure 1.1. ASFV continued to circulate and spread within wild boar populations, eventually reaching the People's Republic of China in 2018. By the end 2019 ASFV had been reported in neighboring and regional countries which include Mongolia, Vietnam, Cambodia, the Korean Peninsula, Loas, Myanmar, Timor-Leste, Papua New Guinea, the Philippines, Indonesia, and Serbia (Ankhanbaatar et al., 2021; H. J. Kim et al., 2020; Mighell & Ward, 2021; Milićević et al., 2019). In 2020 ASFV outbreaks were reported in India, Germany, and Greece (Brellou et al., 2021; Rajukumar et al., 2021; Sauter-Louis et al., 2021). In 2021 Malaysia, the Dominic Republic and Haiti reported outbreaks of a genotype II virus (Gonzales et al., 2021; Khoo et al., 2021; Ramirez-Medina et al., 2022). The outbreak in Dominic Republic and Haiti is of major concern to the Americas due to the proximity. From 2022-2023 outbreaks have occurred in Nepal, Thailand, Bangladesh, Singapore, and Sweden (Koh et al., 2023; Rajala et al., 2023; Subedi et al., 2022). As ASFV continues its global spread, outbreaks continue to be reported in previously ASFV-free countries. All of these outbreaks have been caused by virulent genotype II viruses that are distantly related to the Georgia/2007 virus (Ankhanbaatar et al., 2021; H. J. Kim et al., 2020; Lee et al., 2021; Ramirez-Medina et al., 2022).

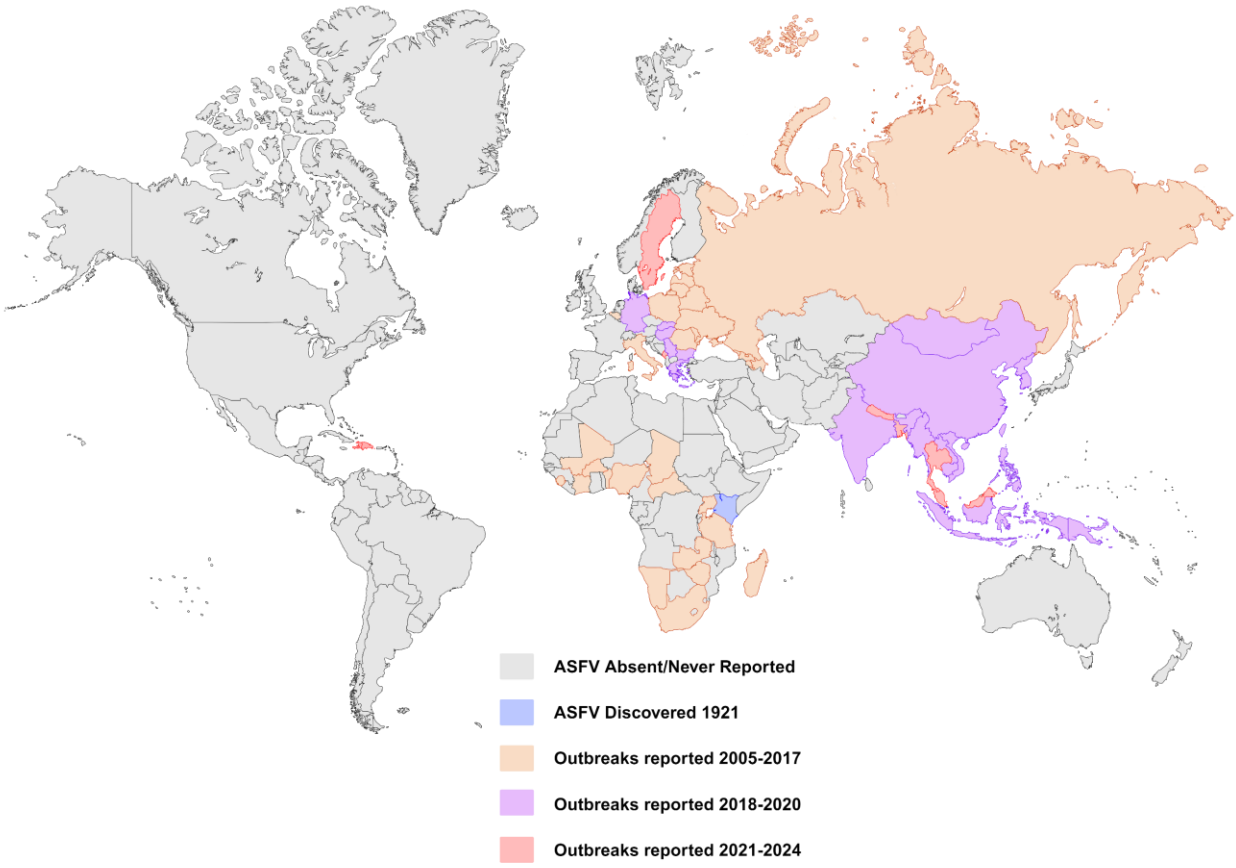

Figure 1.1. The global distribution of ASFV.

The data used for the map was curated from the WOAH World Animal Health Information System (https://wahis.woah.org/#/home, accessed 2024) and created with Biorender.com.

1.1.4. Route of Transmission

There are several routes of transmission that can occur during an ASFV outbreak or introduction. ASFV replicates to high titers in the blood of infected animals and is also shed in bodily secretion and excretion such as urine, feces, and saliva, contributing to the direct and indirect routes of transmission of ASFV (Costard et al., 2013; Dixon et al., 2019). The direct route of transmission of ASFV within domestic herds occurs primarily via oral-nasal route along with skin abrasions. Indirect routes of transmission can arise through contact with surfaces or

fomites contaminated with blood, urine, feces, or other bodily fluids (Guinat et al., 2016). ASFV is transmitted within wild boar populations through similar routes (Gaudreault, Madden, et al., 2020). Contact with infected wild boar carcasses provides an additional route of transmission in wild boar populations and free-roaming domestic swine herds (Guinat et al., 2016; Probst et al., 2017). The direct and indirect routes of transmission play significant roles in the spread of ASFV within domestic swine and wild boar herds. Another route of transmission is the *Orinthodoros* soft ticks in Africa and Europe which can become infected and are capable of transmitting ASFV to domestic swine, however their role in transmission is thought to be limited (Dixon et al., 2019; Gaudreault, Madden, et al., 2020). Human activity can contribute to the short and long distances transmission of ASFV through the movement of swine and meat products. ASFV can persist in meat products for survival weeks to months serving as a potential route of transmission to domestic swine if ingested (Dixon et al., 2019; Guinat et al., 2016). The environmental stability of ASFV, especially under extreme conditions, provides other indirect routes of transmission that can contribute to the spread of ASFV which include contaminated feed, equipment, vehicles, and clothing (Costard et al., 2013; Dixon et al., 2019). The movement of infected swine or contaminated pork products as well as swill-feeding have played significant roles in ASFV outbreaks and contributed to its global spread (Gaudreault, Madden, et al., 2020).

1.1.5. Clinical Disease

The clinical presentation of ASFV can vary depending on the virulence of the strain, age and immune status of the animal resulting in differing clinical presentation of ASF (Guinat et al., 2016). Following an incubation period of 4-19 days, the clinical presentation of ASF can be characterized as peracute, acute, subacute, or chronic (M. C. Gallardo et al., 2015). In general,

the peracute and acute forms are observed with highly virulent ASFV strains with near 100% mortality in 4-9 days post-infection (M. C. Gallardo et al., 2015). These forms usually present early in outbreaks due to the lethality and rapid spread in naïve herds. For peracute ASF sudden death can occur within 1-4 days after clinical signs develop with no apparent gross pathological lesions (M. C. Gallardo et al., 2015). The clinical course of acute ASF is approximately 4-5 days with progressive severity of clinical signs. Clinical signs include pyrexia, anorexia, lethargy, erythema and cyanotic skin lesions. As the disease progresses organ failure becomes apparent with the presentation of hemorrhagic diarrhea and vomiting in affected animals (M. C. Gallardo et al., 2015; Sánchez-Cordón et al., 2021; Sánchez-Vizcaíno et al., 2015). Death can occur within 1-2 days after anorexia, cyanosis, and ataxia develop. Gross lesions consist of hyperemic splenomegaly, hemorrhagic lymph nodes (gastrohepatic lymph nodes, renal lymph nodes, and mesenteric lymph nodes), ascites, and effusion of the thoracic cavity (M. C. Gallardo et al., 2015; Sánchez-Vizcaíno et al., 2015).

As ASFV becomes endemic within a population the clinical presentation becomes broader with increasing numbers of subacute, chronic, and subclinical infections but with a decline in mortality. The subacute form can be characterized by a persistent or fluctuating fever lasting up to 20 days. Infected animals may develop similar clinical signs described with the acute form but reduced severity, while others appear healthy. The morality rate of subacute ASF can range from 30-70% (Arias et al., 2018). Gross lesions are similar to acute ASF lesions described above but less severe. Chronic ASF presents with nonspecific clinical signs and lesions that can persist for several months and do not resemble typical ASF (M. C. Gallardo et al., 2015). During this time numerous clinical symptoms can develop such as skin ulcers, arthritis,

pneumonia, emaciation, delayed growth, and abortion. The subclinical form of ASF can develop through infection by a low virulent non-hemadsorbing ASFV strain which results in subclinical infections and seroconversion (Leitão et al., 2001). In both chronic and subclinical ASF, persistently infected animals continue to shed virus contributing to viral transmission (Penrith & Vosloo, 2009; Zimmerman et al., 2019). These animals contribute to maintaining ASFV in endemic areas in addition to sporadic outbreaks and introduction into disease-free countries (Arias et al., 2018; M. C. Gallardo et al., 2015).

1.1.6. Diagnostics

Since ASFV was discovered in 1921 numerous diagnostic techniques have been used and developed for the detection and surveillance of ASFV. Prior to molecular diagnostics, ASFV was primarily diagnosed by virus isolation, which is a laborious and time-consuming technique. With the development of molecular diagnostics, the time to obtain a diagnosis of ASFV was drastically shortened from days to hours in some cases. The Hemadsorption (HAD) test of ASFV is considered the definitive assay for ASFV detection, however it has been overshadowed by molecular diagnostic techniques (WOAH: Manual of Diagnostic Tests and Vaccines for Terrestrial Animals, 2023a). The diagnostics that have been developed for ASFV include polymerase chain reactions (PCR), both conventional and quantitative, immunoassays for detection of ASFV antigens or antibodies, and CRISPR-Cas based diagnostics (Z. Hu et al., 2023; Lim et al., 2023). Currently, the WOAH recommends real-time quantitative PCR (qPCR) for the diagnosis of ASFV due to the sensitivity, detection from multiple types of clinical samples, and detection early in infection (WOAH: Manual of Diagnostic Tests and Vaccines for Terrestrial Animals, 2023a). The ASFV qPCR is considered the gold standard for surveillance,

confirmation of clinical cases, and screening of populations. The other diagnostics can be used for the same purpose but have limitations that make them less suitable depending on the circumstances. The various diagnostic assays available are discussed below in more detail.

1.1.6.1 Detection of ASFV virus and viral antigen

Methods available for the detection of ASFV include hemadsorption and immunofluorescence assay (IFA). The hemadsorption (HAD) assay is considered a definitive diagnostic test for the detection of ASFV (De León et al., 2013; Lim et al., 2023). Virus isolation can be performed on anti-coagulated blood (EDTA), tissue suspensions (spleen, lymph nodes, lung, tonsil, kidney, and bone marrow) (WOAH: Manual of Diagnostic Tests and Vaccines for Terrestrial Animals, 2023a). Briefly, HAD is performed by inoculating primary monocyte-macrophage cells (i.e., pulmonary alveolar macrophage (PAM), PBMCs, bone marrow) isolated from naïve pigs with ASFV suspected samples (De León et al., 2013). Swine erythrocytes are added to infected cell cultures and incubated for up to 7-10 days with daily observation until hemadsorption is observed. The erythrocytes will adhere to the ASFV infected macrophages forming clusters of erythrocytes that can be visualized under a light microscope (De León et al., 2013). This assay is primarily performed by references laboratories and in research settings, due to the need for primary cell cultures and experienced technicians. Due to the time required to obtain a diagnosis, makes the HAD less feasible for the rapid diagnosis of ASFV in face of an outbreak. Also, some ASFV strains with a deletion of the EP402R gene, which encodes the CD2v protein that is responsible for HAD, can test negative with the HAD assay (Lim et al., 2023). These limitations associated with the HAD assay are the reasons that molecular based diagnostics are essential and favored for the diagnosis of ASFV.

IFA is another diagnostic assay that can be used for the detection of ASFV as well but does not require swine erythrocytes (Bool et al., 1969). Briefly, primary monocyte-macrophage cell cultures or less-susceptible cell cultures (i.e., MA-104 or Cos-1) are inoculated with suspected ASFV samples and incubated for up to 7-10 days (Hurtado et al., 2010; Rai et al., 2020). Following the incubation period, an ASFV-specific primary antibody is added that binds ASFV proteins in infected cells. A conjugated secondary antibody with a fluorophore binds the bound primary antibody. Results are determined by detection of fluorescing cells indicating ASFV infection in culture. As with HAD, this assay is time consuming, requires primary cell culture, and trained technicians. It is primarily performed by reference laboratories and researchers with the ability to work with live virus. ASFV IFAs can be conducted in parallel with the HAD assay in the case that a non-hemadsorbing strain is being tested (WOAH: Manual of Diagnostic Tests and Vaccines for Terrestrial Animals, 2023a). Due to the time constraints, requirement of primary cell cultures, and experienced technicians to perform both HAD and IFA for the detection of ASFV, diagnostics for the detection of viral antigen have been developed.

Detection of viral antigen can be completed by commercially available ELISA kit or lateral flow assays. The commercially available ELISA kit has been validated for use on blood, spleen, or lymph node samples. This system uses a sandwich ELISA where a plate is coated with a capsid-specific monoclonal antibody (MAb) that binds to ASFV in positive samples. Following the washing of the plate, a peroxidase-conjugated secondary MAb specific to another epitope of the capsid protein is added and binds ASFV. Detection of ASFV antigen is determined by addition of appropriate substrate resulting in a colorimetric change observed in the plate wells (C. Gallardo et al., 2015; WOAH: Manual of Diagnostic Tests and Vaccines for Terrestrial

Animals, 2023a). The major drawback of the antigen ELISA is the lower sensitivity (67.86%), and specificity (97.98%) compared to the gold standard PCR (C. Gallardo et al., 2015; Muzykina et al., 2024a). According to WOAH, results should be confirmed by PCR or HAD.

In recent years, lateral flow assays (LFA) have been developed for detection of ASFV antigen that allow for field-deployable, rapid, and easy-to-use diagnostics (Madden et al., 2022; Onyilagha et al., 2022). For example, some of these systems use ASFV specific MAbs bound to black beads that bind to one of the ASFV capsid proteins. The lateral flow strip contains a test line containing an ASFV specific MAb and MAb specific for a control protein at the control line. Briefly, the sample is mixed with the ASFV specific MAbs bound beads (Sastre et al., 2016). The mixture is added to the lateral flow strip, the samples migrate through the test strip via capillary diffusion. If ASFV is present in the sample a black line will appear, with results in 10-25 minutes. These tests have been demonstrated to have lower sensitivity than molecular assays (Muzykina et al., 2024b; Onyilagha et al., 2022). These tests can result in false negatives with low titer samples. Currently, the WOAH does not list LFAs for approved diagnostics, but these can provide information from a suspect herd or animals with moderate to severe clinical disease.

1.1.6.2. Detection of ASFV Genome

Real-time quantitative PCR (qPCR) are one of the most widely used molecular assays for the detection of viral infections globally and in many cases have become the gold standard for viral detection. These assays are highly specific to the target agent and highly sensitive with the ability to detect 10-100 copies of viral genetic material. These assays can be used on a variety of samples such as blood, swabs (nasal, oral, and rectal), bodily fluids, tissues, and waste stream samples. In the case of ASFV, qPCR is the gold standard for detection lending to the high

specificity and sensitivity (WOAH: Manual of Diagnostic Tests and Vaccines for Terrestrial Animals, 2023a). The qPCR enables the detection of ASFV in degraded samples, inactivated samples, or samples not suitable for virus isolation. Another major benefit of qPCR is the turnaround time for samples is approximately 4 hours with nucleic acid extraction. However, qPCR does come with some issues due to the sensitivity which include false negatives due to PCR inhibitors in the sample and potential for false positives as a result of cross-contamination. The most widely used qPCRs for ASFV targets the B646L gene that encodes the major capsid protein p72 of ASFV (Agüero et al., 2003; King et al., 2003; Zsak et al., 2005). Over the years, primers and probes have been modified to increase sensitivity of the assay as well as other gene targets such as the E183L gene encoding the p54 protein (Trinh et al., 2021). These assays are essential for the rapid detection of ASFV but require well equipped laboratories and temperature sensitive reagents limiting the field applications.

The field application of qPCR is currently being developed for rapid onsite detection of ASFV and other viral infections. Biomeme Inc. developed a portable thermal cycler called the Franklin that can run up to nine qPCR reactions with a companion syringe based nucleic acid extraction kit and lyophilized reagents. This system was tested by Daigle, et al. on clinical ASFV samples demonstrating similar sensitivity and specificity to the laboratory-based qPCR within 2 hours without a cold chain (Daigle et al., 2021; Lim et al., 2023). The advent of insulated isothermal PCR (iiPCR) has provided another avenue for field deployable ASFV diagnostics. These systems are based on Rayleigh-Bénard convection where a natural fluid flow is generated by heating the bottom end of a capillary tube. The traditional PCR steps of denaturation, annealing, and extension occur continuously as the fluid cycles through various temperature

levels within the vessel (Lim et al., 2023; H. N. T. Tran et al., 2021). Zou *et al.* developed an iiPCR for the detection of ASFV onsite with 100% sensitivity and specificity for the samples tested in this study (Zou et al., 2022) Loop-mediated isothermal amplification (LAMP) techniques have also been developed for ASFV detection which are the most promising due to speed, sensitivity, and cost-effectiveness (James et al., 2010; Parida et al., 2008; D. Wang et al., 2020). This methodology utilizes strand-displacement DNA polymerases to generate amplicons without a thermocycler. Amplicon detection can be visualized via agarose gel, fluorometry, or colorimetry (Asadi & Mollasalehi, 2021). A study by Tran, *et al*. using a colorimetric LAMP assay for the detection of ASFV in Vietnam demonstrated 100% sensitivity and specificity for samples tested in this study (D. H. Tran et al., 2021). These technologies have not yet been adopted by the WOAH but have been identified as promising techniques for field diagnostics (Bohorquez et al., 2023). In the future these technologies may provide the ability to conduct ASFV diagnostics in the field with similar sensitivity and specificity to laboratory-based techniques further enabling the rapid detection of ASFV.

1.1.6.3. Antibody Detection of ASFV

Serological assays for the detection of ASFV specific antibodies play critical roles in the surveillance and eradication efforts of ASFV in endemic areas along with areas where low-virulent and attenuated strains may be present, serving to identify asymptomatic or previously infected animals (WOAH: Manual of Diagnostic Tests and Vaccines for Terrestrial Animals, 2023a). Next to the qPCR, the detection of an immune response to ASFV is the most common diagnostic technique. The preferred assay for detecting antibodies is the ELISA, which is relatively inexpensive, easy to perform, and requires minimal specialized equipment. Currently,

there are several commercially available ELISA kits for ASFV antibody detection which come in indirect and competitive varieties (Caixia et al., 2022; Cao et al., 2021; Giménez-Lirola et al., 2016). Traditionally the indirect ELISA used soluble antigen isolated from infected cell cultures which require BSL-3 facilities. In order overcome this hurdle, recombinant ASFV proteins p72, p30, and p54 are used and have been demonstrated to have comparable or increased sensitivity and specificity compared to the native antigen (Cao et al., 2021; Gaudreault, Madden, et al., 2020; Giménez-Lirola et al., 2016; Lim et al., 2023). Briefly, ELISA plates coated with the target antigen are made in house or provided with the kit. Test sera, plasma, or meat juice is diluted and added to the plate in duplicate along with positive and negative controls per manufacturers protocol. Following an incubation period and washing steps, a horseradish-peroxidase (HRP) conjugated anti-swine antibody is added to all the wells, then incubated and washed. After the final wash step an HRP substrate is added eliciting a color change in wells containing bound antibodies. The antibody titer for each sample is determined through absorbance measurements compared to the controls (Pastor et al., 1990). Antibody based diagnostics for ASFV are commonly used for determining prevalence of virus within a herd and detection of subclinical or animals that recovered from disease prior to transportation which may not be detected by qPCR assays. However, these diagnostics may not be effective in the face of virulent ASFV strains that cause subacute and acute forms of disease, lending to the fact that an infected animal succumbs to the disease before an antibody response can be mounted (WOAH: Manual of Diagnostic Tests and Vaccines for Terrestrial Animals, 2023a). It is necessary that both qPCR and antibody-based diagnostics are utilized in ASFV outbreak mitigation strategies.

1.1.6.4. Genotyping and Serotyping of ASFV via Sequencing

The molecular and serological assays for ASFV allow for the detection and diagnosis of ASFV but provide minimal to no genetic information on circulating strains or outbreaks strains. This information is vital for determining the genotype associated with an outbreak and tracking the spread of ASFV. Historically, there were 26 known ASFV genotypes based on the partial sequencing of the B646L gene that encodes p72, the major capsid protein, specifically the variable region within the C-terminus (478 bp) (Bastos et al., 2003; Mulumba-Mfumu et al., 2017). ASFV strains are further discriminated from one another by sequencing of the envelope protein (p54), the central hypervariable region (CVR) of B602L (vial chaperone), and CD2v/C-type lectin for serotyping (C. Gallardo et al., 2009). The gene targets listed above are amplified using conventional PCR. The amplicons are isolated and purified from agarose gels. The amplicons can be sequencing using any available sequencing technology, traditionally this is sanger sequencing due to the low cost and availability. The genetic information gathered from the sequencing of these gene targets aids in determining the closest ancestry strain to determine the likely point of origin, which is vital for determining potential sources of ASFV introduction especially in a previously ASF-free country (Z. Li et al., 2022). While these gene targets provide important genetic information of ASFV strains, these do not provide the complete genomic picture of the virus. The reliance on sequencing partial and select genes is primarily due to the technological limitations of Sanger sequencing and genome size of ASFV; the expense and time needed to obtain whole genome sequences of ASFV was not feasible.

The feasibility of obtaining whole genome sequences of ASFV has greatly increased with advances in sequencing technology with the addition of second-generation (Illumina and ION

Torrent platforms) and third-generation sequencing platforms (Oxford Nanopore and PacBio platforms). These advances have increased the accuracy of sequencing providing the ability to sequence larger amplicons and whole viral genomes (Heather & Chain, 2016a). The Oxford Nanopore MinION and Illumina platforms have been used to obtain whole ASFV genome sequences via metagenomic approaches (Spinard, Dinhobl, et al., 2023; Spinard, O'Donnell, et al., 2023). Due to the abundance of host DNA present in metagenomic samples difficulties to obtain whole genome sequences of ASFV could arise in low titer samples and loss of sequencing reads to host DNA. However, it has allowed researchers and diagnosticians to procure whole ASFV sequences which provide more complete and detailed phylogenetic characterization of ASFV compared to the reliance of partial gene sequences (Ankhanbaatar et al., 2023; Le et al., 2023; Spinard, O'Donnell, et al., 2023). The availability of ASFV whole genome sequences will also provide a greater understanding of the viral evolution of ASFV.

1.1.7. ASFV Control and Mitigation Strategies

Currently ASFV outbreaks are controlled and mitigated following a stamp-out protocol/strategy and strict biosecurity procedures due to the lack of globally available vaccines and effective treatments for this devastating viral disease (McDowell et al., 2022a). This strategy relies on early and rapid detection of ASFV within a herd to contain the virus before spreading to other herds. Following, the detection of ASFV affected herds and farms are quarantined. All infected and contacted animals are culled. The movement of animals is restricted within the quarantined zones (USDA, 2023). Samples are regularly collected from other farms that fall within the quarantined area to detect subsequent ASFV positive animals. At the country level, the exportation of swine and pork products restricted to prevent the spread to other countries

(Dixon et al., 2020). In countries where ASFV is endemic, outbreaks are controlled in a similar fashion (Dixon et al., 2019). However, the presence of wild boar populations which can harbor ASFV brings up additional strategies of control that rely on surveillance and control of wild boar populations and biosecurity measures to reduce ASFV outbreaks (Dixon et al., 2013). Biosecurity measures that may be implemented to protect susceptible domestic swine herds can include decontamination of vehicles entering and leaving production operations, proper disposal of carcasses (domestic or feral), controlled access to the facilities, feed safety, and perimeter fencing around swine operations to reduce contact with wild boars (Heilmann et al., 2020; Y. Liu et al., 2021; USDA, 2023). The current control and mitigation strategies for ASFV have massive economic impacts on the pork industry both at the country and global levels. Until there is an effective globally available vaccine or treatment for ASFV, countries around the globe will have to rely on these control and mitigation strategies in the face of an ASFV outbreak.

1.2: Classical Swine Fever virus

Classical swine fever (CSF), also known as hog cholera, is a highly contagious febrile viral disease of domestic and feral swine (Ganges et al., 2020). Outbreaks can result in tremendous economic impacts on the swine industry of affected countries. Clinical signs of CSF vary in severity depending on affected age groups and can be non-specific (pyrexia, anorexia, and diarrhea) resembling other viral diseases such as ASFV (Blome, Staubach, et al., 2017). CSF is endemic in several regions of the world which include parts of Asia, Europe, and South America (Ganges et al., 2020). There are several commercially available vaccines for CSF that are utilized for vaccinating wild boar populations and as part of control/mitigation strategies (Moennig, 2015a; WOAH: Manual of Diagnostic Tests and Vaccines for Terrestrial Animals,

2023b). Current outbreak mitigation strategies for CSF-free countries include depopulation of infected herds, movement restrictions, and emergency vaccination for neighboring herds (USDA, 2013). Due to the devastating impacts that CSF can have on the global pork industry, it is a WOAH and USDA notifiable disease.

1.2.1. Viral Characteristics

Classical swine fever virus (CSFV) is the causative agent of Classical swine fever or "hog cholera" which belongs to the *pestivirus* genus within the *Flaviviridae* family. The *pestivirus* genus includes serval other important livestock viruses which are atypical porcine pestivirus, bovine viral diarrhea virus 1 and 2 (BVDV-1 and BVDV-2), and border disease virus (BDV) (Ganges et al., 2020). It is an enveloped virus containing a single stranded positive sense RNA genome that is ~12.3 kB in length. The positive sense RNA genome of CSFV is infectious allowing the direct translation of viral protein upon entry into the host's cell (Blome, Staubach, et al., 2017; Paton & Greiser-Wilke, 2003). The genome contains a single open reading frame that is flanked by two untranslated regions (UTR), resulting in a single polyprotein following translation. Viral proteins are generated via co- and post-translational processing by viral and cellular proteases that cleave the polyprotein into four structural and nine non-structural proteins (Beer et al., 2015). The four structural proteins form the viral particle which consist of the core protein (C), envelope glycoproteins E1, E2, and E^{rns}. The nine nonstructural proteins N^{pro}, p7, NS2-3, NS3, NS4A, NS4B, NS5A, and NS5B play a role in viral replication (Beer et al., 2015; Lattwein et al., 2012; H. J. Thiel et al., 1991).

Currently, there are three known genotypes with over 13 sub-genotypes of CSFV. The virulence varies between genotypes of CSFV and have been classified as highly virulent,

moderately virulent, low virulence, and avirulent. In general, the highly virulent strains belong to genotype-1, genotype-2 viruses are moderately virulent, and virulence is variable within genotype 3 (Mittelholzer et al., 2000; Yamashita et al., 2024). Genotyping of CSFV traditionally was completed by sequencing fragments of the 5'UTR (150 nucleotides), E2 (190 nucleotides) and NS5B (490 nucleotides) (Paton et al., 2000). The recent advances in sequencing technologies WOAH recommends whole genome sequencing or full-length E2 gene sequencing to provide reliable phylogenetic analysis, identify emerging strains and facilitate studies in viral evolution (Beer et al., 2015; Töpfer et al., 2013; WOAH: Manual of Diagnostic Tests and Vaccines for Terrestrial Animals, 2023b).

1.2.2. Epidemiology

CSFV was first described in 1833 with an outbreak that occurred in Ohio, USA (Birch, 1922). Following the initial outbreak, subsequent outbreaks were reported in 10 different states. CSFV was widespread across continental United States by the mid-19th century, it has been suggested that the rapid spread of CSFV was related to the development of railways during this time (Birch, 1922; Edwards et al., 2000; Ganges et al., 2020). While America was suffering from the rapid and devasting spread of CSFV, England reported the first cases in 1862. By the end of the 19th century CSFV had spread across Europe (Birch, 1922) and by the mid-20th century it had become a global presence (Cole et al., 1884). Since its emergence, 38 countries have been able to eradicate CSFV and maintain a CSFV-free status, which include North America, Oceania, and parts of the European union. CSFV remains endemic in parts Asia, South and Central America, and the Caribbean (Ganges et al., 2020). The most recent CSFV outbreaks have occurred in Korea, Russia, Colombia, Brazil and Japan (WOAH, 2024). Prior to this recent

outbreak, Japan had been CSFV-free for 32 years when it re-emerged in domestic and wild boar populations, suggesting re-introduction from outside Japan (Postel et al., 2019). CSFV remains a constant threat to CSFV-free countries or regions and the global pork industry due to the chance of introduction through importation of contaminated swine/pork products or wild boar populations harboring CSFV.

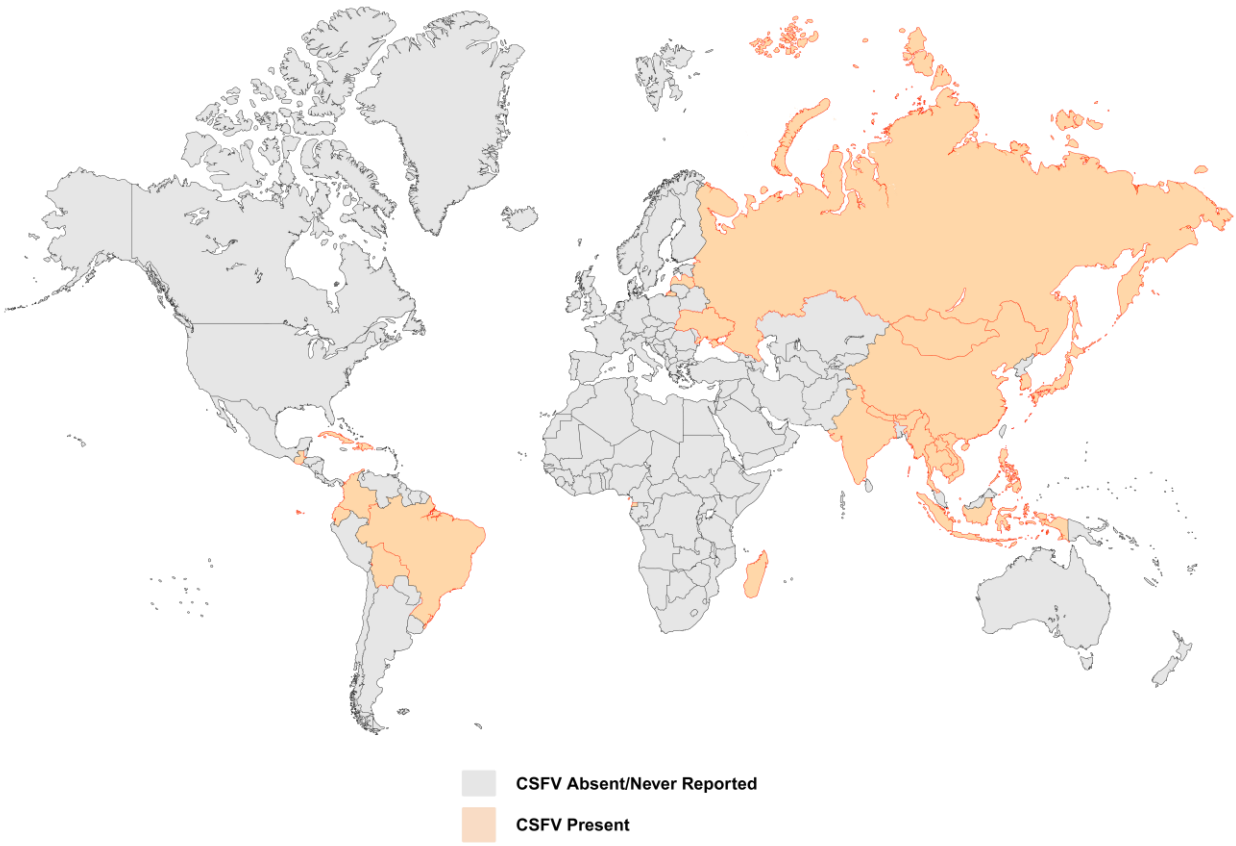

Figure 1.2. Global distribution of CSFV.

The map covers outbreaks reported from 2015-2024. The data used for the map was curated from the WOAH World Animal Health Information System (https://wahis.woah.org/#/home, accessed 2024) and created with Biorender.com.

Since the emergence of CSFV in the mid-19th century three genotypes and 13 subgenotypes of CSFV have been characterized. The global distribution of CSFV genotypes and subgenotypes has shown a distinct geographical pattern (Beer et al., 2015; Blome, Staubach, et al., 2017).The early outbreaks in the United States and Europe were caused by genotype 1 viruses, which continues to circulate in the Caribbean, Central and South America. Outbreaks of CSFV that have occurred in parts of Europe and Asia in the late 20th century belong to the genotype 2 group which has become the more prevalent genotype in these regions. Both genotype 1 and 2 viruses co-circulate in China, India, and Russia (Beer et al., 2015; Zhou, 2019). The genotype 3 viruses have been identified in Taiwan, Korea, and Japan (Beer et al., 2015; Blome, Staubach, et al., 2017). There is debate on the classification of a CSFV strain "congenital tremor" that was detected in Great Britain in 1964. Historically the "congenital tremor" is classified as a genotype 3 virus; however, it was recently suggested by *Rios, 2018* that this strain may be within its own genotype (Rios et al., 2018). As CSFV continues to circulate in endemic areas, there is a potential for the emergence of novel genotypes and/or subgenotypes.

1.2.3. Clinical Disease

CSF has several forms that can manifest in infected domestic and wild swine species. The viral strain, age, breed, and immune status factor into the disease manifestation which include acute, chronic, and persistent forms (Blome, Staubach, et al., 2017). The acute form of disease can occur with highly virulent strains and in younger pigs less than 12 weeks. Chronic form can result from infection with low virulent strains in any age group. Persistent form is a result of *in utero* infection occurring in late gestation (Moennig et al., 2003). These forms of disease are discussed in more detail below.

1.2.3.1. Acute disease

The acute form of CSF generally has a less than 4-week duration with two possible outcomes death or recovery; this form can result from highly virulent strains. However, 90% of infected animals succumb to the infection with juvenile animals being the most vulnerable exhibiting pyrexia of greater than 40° C (Moennig et al., 2003). Other early symptoms include lethargy, conjunctivitis, respiratory signs, anorexia, and diarrhea. As the infection progresses, animals can develop neurological symptoms which can include hindlimb paresis, convulsions, and ataxia (Moennig et al., 2003). CSFV results in generalized vasculitis which manifests as hemorrhages and cyanosis of the skin, particularly the ears, abdomen and extremities (WOAH: Manual of Diagnostic Tests and Vaccines for Terrestrial Animals, 2023b). Secondary infections can arise because of severe leukopenia that develops. These symptoms become milder and less specific with the increasing age of the pig, with adult pigs recovering. Infectious virus is shed in saliva, urine, and feces (Moennig et al., 2003).

1.2.3.2. Chronic disease

Chronic form is characterized by an infection that lasts longer than 4 weeks, this form is 100% fatal. It results from the animals' inability to mount an adequate immune response. The early symptoms resemble the acute form of disease with symptoms progressively becoming non-specific as infections continue which include chronic enteritis, undulating fever, and wasting (Moennig et al., 2003). Infected pigs can survive 2 to 4 months during which time they continually shed high viral loads (Ganges et al., 2020; Weesendorp et al., 2011). Chronically infected animals play a significant role in maintaining the virus in domestic herds and wild boar herds (Blome, Staubach, et al., 2017).

Table 1.1. CSF disease forms and associated clinical signs.

Disease Form	Early Clinical Signs	Late Clinical Signs	Duration
Acute CSF	Lethargy Conjunctivitis Respiratory distress Anorexia Diarrhea	Neurological signs: hindlimb paresis, convulsions, and/or ataxia Cyanosis: ears, abdomen, and extremities	< 4 weeks
Chronic CSF	Lethargy Conjunctivitis Respiratory distress Anorexia Diarrhea	Chronic enteritis Undulating fever Wasting	> 4 weeks, may survive 2 to 4 months

1.2.3.3. Persistent disease

The persistent form generally results from an infection *in utero* with a moderate to low virulent strain. Early gestational infections can result in abortions, stillbirths, mummification, or malformations (Bohórquez et al., 2020). However, if infection occurs around day 50-70 of gestation when the immune system is still developing, piglets are born appearing normal but are "poor growers" and exhibit neurological signs (Moennig et al., 2003). These persistently infected piglets shed high viral loads and serve as a viral reservoir (Van Oirschot & Terpstra, 1977).

1.2.4. Diagnostics

There are several diagnostic techniques available for CSFV which are approved by WOAH. These techniques include virus isolation, RT-PCR or RT-qPCR, ELISAs for antibody and antigen detection, and fluorescence antibody test (FAT) (WOAH: Manual of Diagnostic Tests and Vaccines for Terrestrial Animals, 2023b). For many of these diagnostics, if a positive result is obtained a secondary confirmatory assay must be completed. Several of the techniques

described are costly both in time and resources which can result in increased turnaround times for results which can be detrimental in the face of an outbreak.

1.2.4.1. Detection of CSFV Genome

The WOAH recommends RT-PCR and RT-qPCR for the detection of CSFV RNA for surveillance, confirmation of clinical cases, and screening of populations, due to the speed and sensitivity (WOAH: Manual of Diagnostic Tests and Vaccines for Terrestrial Animals, 2023b). These diagnostic tests can be performed on blood, serum, tissue homogenates, and cell culture. Over the years several gel-based RT-PCR assays have been developed for the identification and genotyping of CSFV, with these assays targeting the NS5B gene and 5'-UTR, respectively (Arce et al., 2009; Y. Zhao et al., 2019). These assays have been multiplexed for the differentiation of CSFV from other swine viruses or pesitviruses. These gel-based assays can have reduced sensitivity resulting in false negative samples which can result in devastating consequences. The use of RT-qPCR which uses primer and probes for detection of viral RNA, have become the preferred method for CSFV detection. Over the years at least 7 or more assays have been published (Haines et al., 2013; Y. L. Huang et al., 2009; Leifer et al., 2011; L. Liu et al., 2009; X. Shi et al., 2016; Zheng et al., 2020). Many of these assays target the highly conserved 5'-UTR (Haines et al., 2013; Leifer et al., 2011; L. Liu et al., 2009; X. Shi et al., 2016) and 3'-UTR (Y. L. Huang et al., 2009) with some targets to the E2 gene (Zheng et al., 2020). Due to the high-throughput capabilities of RT-qPCR many of the assays designed to target the 5'-UTR were also multiplexed for the detection of other swine viral pathogens such as African Swine fever, PRRSV, swine influenza virus (SIV), porcine circovirus virus (PCV), and others. RT-qPCR assays described for the detection and genotyping of CSFV targeted the 3'-UTR which contained

genotype-specific probes (Y. L. Huang et al., 2009). All the described assays were demonstrated to be highly specific and sensitive in the detection of CSFV RNA, however many of these assays fall short in differentiating vaccinated and unvaccinated with the exception of Liu *et. al.* which demonstrated differentiation of wild-type infection and C-strain vaccination through the incorporation of melt curve analysis (L. Liu et al., 2009). RT-qPCR is a highly sensitive and specific technique that has a high-throughput capacity and is rapid, but this technique requires costly qPCR thermal cyclers and dedicated laboratories. To alleviate the need for expensive thermal cyclers, groups have developed isothermal reverse transcriptase PCR and CRISPR/Cas based diagnostics which do not require sophisticated instruments (Bohórquez et al., 2024; Y. Zhang et al., 2022).

1.2.4.2. Detection of CSFV Antigen and Antibodies

Serological assays are routinely used for the detection and surveillance of CSFV in wild boars and previously infected domestic swine herds (Moennig & Becher, 2015). The two widely used assays for the detection of CSFV antibodies are virus neutralization test (VNT) and ELISA. The VNT is considered the gold standard for the detection and quantification of CSFV antibodies, lending to the high sensitivity and specificity of the assay (Ganges et al., 2020; Moennig, 2015b). Briefly, susceptible cell lines such as PK-15 or SK-6 are incubated with a mixture of serially diluted serum and a CSFV strain, commonly Alfort/187. However, due to the variability of antibodies titers with genotypes it is recommended to use recent genotype or circulating field isolates (WOAH: Manual of Diagnostic Tests and Vaccines for Terrestrial Animals, 2023b). Following the incubation period the virus/serum mixture is removed and replaced with growth media and incubated for 3-4 days. The cells are then fixed, after which a

CSFV specific monoclonal antibody or hyperimmune sera is added to the plate. The plate is then washed followed by the addition of horseradish peroxidase or fluorescently conjugated anti-murine or anti-porcine antibody to the plate. The secondary antibody is removed, a chromogen-substrate is added in the case of peroxidase conjugated antibody and rinsed. The plates are then visually evaluated under a light or fluorescent microscope with the cytoplasm of infected cells stained or fluorescing, respectively (Y. Li et al., 2013; Terpstra et al., 1984; WOAH: Manual of Diagnostic Tests and Vaccines for Terrestrial Animals, 2023b). The major drawbacks of VNT are the need for laboratories with the capacity to work with CSFV and trained personnel, and that it requires cell culture with infectious virus and is laborious. Despite these drawbacks it is a vital assay for confirming suspect positive ELISAs because it differentiates CSFV-specific antibodies from non-specific *pestivirus* antibodies.

ELISAs developed for the detection of CSFV antibodies are the other commonly used serological assay. These assays have multiplexing capabilities while being more rapid without the requirement for cell culture and live viruses compared to VNTs. These ELISAs are designed to detect antibodies specific to the E2 glycoprotein or E^{rns} specific antibodies (Aebischer et al., 2013; Kosmidou et al., 1995). Both ELISAs maybe used for the detection or surveillance of CSFV especially in countries that vaccinate domestic swine or wild boars using the DIVA (differentiating infected and vaccinated animals) compatible CP7_E2alf (Suvaxyn) vaccine (Blome, Wernike, et al., 2017). In this case, if the animals have been successfully vaccinated, they will have a positive titer for the E2 glycoprotein and negative for E^{rns}, where infected animals will have a titer for both proteins. This differentiation is essential for the evaluation of the effectiveness oral vaccination programs of wild boars as well as infected versus vaccinated

(Aebischer et al., 2013; Floegel-Niesmann, 2001; Meyer et al., 2017; Moennig & Becher, 2015). Due to the potential cross-reactivity of *pestivirus* antibodies ELISA results may need to be confirmed by VNT or RT-qPCR (WOAH: Manual of Diagnostic Tests and Vaccines for Terrestrial Animals, 2023b).

Several ELISAs have also been developed for the detection of CSFV antigen, which generally detects the viral glycoprotein, E^{rns}. They are primarily suited for monitoring at the herd level and may not be suited for determining CSFV-free status of individual animals due to the sensitivity and specificity (Ganges et al., 2020). Antigen ELISA results in any primary case of CSFV must be confirmed by virus isolation or RT-qPCR as required by WOAH (Ganges et al., 2020; WOAH: Manual of Diagnostic Tests and Vaccines for Terrestrial Animals, 2023b).

1.2.4.3. Genotyping of CSFV

Phylogenetic characterization of CSFV is a valuable molecular tool for discriminating viral isolates and aids in tracing the potential source of the outbreak. Historically, CSFV isolates were genotyped based on the sequence comparison of the 5'-UTR (150 nucleotides (nt)), partial E2 (190 nt) or 409 nt segment of the polymerase gene (NS5B) (Beer et al., 2015). These short sequencing methods were sufficient for classifying isolates into the three major genotypes and subgenotypes due to the limitations of sequencing technology at the time they were developed. However, with the advances in sequencing technology it is recommended to sequence the full E2 gene or whole genome for CSFV (Postel et al., 2012; WOAH: Manual of Diagnostic Tests and Vaccines for Terrestrial Animals, 2023b). The use of longer sequencing methods provides more detailed phylogenetic information and allows for the discrimination of closely related isolates. In

the case of whole genome sequencing, it allows researchers to further evaluate viral evolution through the role of viral quasispecies arising during infection (Töpfer et al., 2013).

1.2.5. Current Control Strategies

CSF has been successfully eradicated from several countries that have imposed strict control measures. However, the virus remains endemic in several central and south American countries, parts of Eastern Europe, along with Asia and India (Beer et al., 2015; Blome, Staubach, et al., 2017; Ganges et al., 2020). Current CSFV control measures rely on a stamp out strategy following diagnosis of infected animals/herds which includes culling infected and suscept animals, establishing quarantine zones and restricting animal movement within and out of these zones (Moennig, 2015b; Postel et al., 2018, 2019). The implementation of biosecurity measures serves a vital role in the reduction of CSFV introductions and controlling outbreaks which may include safe carcasses disposal, cleaning and disinfection of vehicles and equipment reducing the risk of contaminated fomites and mechanical vectors. Restrictions on swill and garbage feeding to reduce the risk of CSFV-contaminated feed into a naïve population (Postel et al., 2018). The implementation of biosecurity measures and control measures mentioned above are crucial in the control and prevention of CSFV outbreaks.

Vaccination for CSFV may be used in endemic countries and regions as part of a nation's mitigation strategy in the face of an outbreak (Blome, Moß, et al., 2017). There are several vaccines available for CSFV which include modified live vaccines (C-strain, Theiverval, and PAV250), the E2 subunit vaccine (Porcilis Pesti), and a marker vaccine (CP7_E2alf) (Blome, Moß, et al., 2017). The modified live vaccines are the most widely used due to efficacy and safety, but are not DIVA compatible (Blome, Moß, et al., 2017). The subunits and marker

vaccines are both DIVA compatible, however subunit vaccines fell out of favor due to lower efficacy and requiring two doses (Blome, Moß, et al., 2017; Ganges et al., 2020). The marker vaccine was demonstrated to be efficacious and safe via oral and intramuscular administration (Blome et al., 2014; Leifer et al., 2009). The emergency use of CSFV vaccines can play a role in controlling the spread of CSFV in combination with other control strategies (Postel et al., 2018).

Wild boar populations serve as a reservoir for CSFV which presents a constant threat of transmission to domestic herds. To mitigate this threat, several countries have implemented population control measures along with vaccination through oral bait vaccines (Blome, Moß, et al., 2017; Postel et al., 2018, 2019; Rossi et al., 2015). The oral immunization of wild boar has been applied in Germany, France, and Slovakia (Moennig & Becher, 2015). The combination of the strategies mentioned above along with rapid diagnosis and continuous surveillance of CSFV are currently the most effective strategies for reducing and mitigating CSFV outbreaks.

1.3. Severe Acute Respiratory Syndrome Coronavirus 2 (SARS-CoV-2)

The highly transmissible zoonotic virus severe acute respiratory syndrome coronavirus 2 (SARS-CoV-2) emerged in late 2019 and rapidly spread across the globe, resulting in one of the largest global pandemics since the 1918 influenza pandemic. Since the beginning of the pandemic greater than 777 million cases and 7 million deaths have been reported to the World Health Organization (WHO). As SARS-CoV-2 continues to circulate around the globe novel variants have emerged and continue to emerge perpetuating the threat to public health. SARS-CoV-2 has been demonstrated to have a broad host range through natural and experimental infections that can serve as potential secondary reservoirs that could harbor novel variants and future spillover events. (S. Cui et al., 2022; Meekins et al., 2021; Prince et al., 2021). The rapid

development of diagnostics, efficacious vaccines, surveillance and quarantine measures were vital to mitigating and controlling the SARS-CoV-2 pandemic. SARS-CoV-2 is globally endemic and remains a threat to public health.

1.3.1. Viral Characteristics

SARS-CoV-2 is a zoonotic virus that belongs to the genus *betacoronarvirus* in the family *Coronaviridae*, which includes severe acute respiratory syndrome coronavirus (SARS-CoV) and Middle East respiratory syndrome coronavirus (MERS-CoV) which emerged in the earlier 21st century (Cool et al., 2022; J. Cui et al., 2019; B. Hu et al., 2021). SARS-CoV-2 is an enveloped, single-stranded, positive-sense RNA virus with a ~29.9 kB genome encoding 29 viral proteins (Yang & Rao, 2021). The genome is organized by the six major ORFs 5' to 3': replicase (ORF1a/b), spike (S), envelope (E), membrane (M), and nucleocapsid (N) with seven ORFs encoding accessory protein interspersed between the structural genes (B. Hu et al., 2021). The ORF1a/b gene encodes two overlapping polyproteins that are proteolytically cleaved into 16 nonstructural proteins involved in viral replication. The SARS-CoV-2 virion consists of the spike, envelope, membrane, and nucleocapsid proteins. The spike glycoprotein is responsible for binding the host cell receptor, angiotensin-converting enzyme 2 (ACE-2), and viral entry; making it the primary viral antigen for SARS-CoV-2 vaccines (Fernandes et al., 2022; Yang & Rao, 2021). The nucleocapsid protein and the spike protein are the two viral protein targets for either antigen or antibody detection assays (Fernandes et al., 2022). Mutations in the spike protein and across the viral genome have been shown to alter receptor binding affinity, infectivity, and immune escape (Harvey et al., 2021). This can result in the emergence of novel variants that challenge current diagnostics, vaccines, and public health.

1.3.2. Epidemiology

SARS-CoV-2 causative agent of COVID-19 was first identified in December 2019 in the city of Wuhan in the Hubei province of China. By January 2020, SARS-CoV-2 had spread across 33 provinces in China with cases reported in Thailand, Japan, South Korea, Malaysia, Singapore and the USA (Lu et al., 2020). Due to the accelerated international spread of SARS-COV-2 in late February and rapid spike in cases, the WHO declared COVID-19 a pandemic in March 2020 (Bostanghadiri et al., 2023; B. Hu et al., 2021). As the pandemic progressed, novel SARS-CoV-2 variants emerged that have been classified as variants of concern (VOCs) or variants of interest (VOIs) by the WHO based on mutations that affect transmissibility, virulence, immune evasion, and severity of disease (Carabelli et al., 2023; Tatsi et al., 2021; World Health Organization, 2023). The first VOC emerged in late 2020 in the United Kingdom designated alpha (B.1.1.7) variant, rapidly out competed the ancestral strain. The alpha variant would precede 4 VOCs which include beta (B.1.351), gamma (P.1), delta (B.1.617.2), and omicron (B1.1.529) variants. Each VOC would become the dominant variant out competing their predecessor either regionally or globally (Carabelli et al., 2023; Harvey et al., 2021). At least 8 SARS-CoV-2 variants had been designated as VOIs (Bostanghadiri et al., 2023). Currently, the JN.1 variant is the only VOI listed for SARS-CoV-2 (World Health Organization, 2025). These VOCs and VOIs present potential challenges for available diagnostics and vaccines perpetuating the threat to public health. The rapid development and deployment of vaccines and control measures would aid in bringing the COVID-19 pandemic to an end in May 2023 (Sarker et al., 2023; Steiner et al., 2024). However, SARS-CoV-2 remains endemic with the potential for novel variants to emerge.

Since 2019 SARS-CoV-2 has been demonstrated to have a broad host range through natural and experimental infections of numerous animal species that can serve as potential secondary reservoirs (Meekins et al., 2021; Prince et al., 2021). The World Organization of Animal Health (WOAH) has reported natural infections of SARS-CoV-2 in 29 animal species in 36 countries which include companion animals, farmed mink, zoo animals including large cats, otters, and gorillas (S. Cui et al., 2022; World Organization for Animal Health, 2023). Experimental infections of SARS-CoV-2 have demonstrated that 7 species are highly susceptible which include cats, ferrets, Syrian golden hamsters, non-human primates, white-tailed deer and others (Cool et al., 2022; Gaudreault, Trujillo, et al., 2020; Y. Il Kim et al., 2020; Meekins et al., 2021; J. Shi et al., 2020; Ulrich et al., 2022). One susceptible species that may serve as a significant wildlife reservoir is the white-tailed deer (*Odocoileus virginianus*), the most abundant wild ruminant species in the continental United States. White-tailed deer have been shown to be highly susceptible to SARS-CoV-2 through experimental infections (Cool et al., 2022; Palmer et al., 2021). Surveillance studies showed that 33-40% of free-ranging white-tailed deer across the midwestern United States had detectable levels of SARS-CoV-2 RNA or neutralizing antibodies (Chandler et al., 2021; Hale et al., 2022; Kuchipudi et al., 2022). The identification of SARS-CoV-2 alpha, gamma, delta, and omicron variants in free-ranging white-tailed deer months after declining in the human population, suggest multiple spillover events plus sustained deer to deer transmission. These studies also identified potential deer to human spillover events in North Carolina, Massachusetts, and Ontario, Canda (Feng et al., 2023; Pickering et al., 2022). It is critical to identify susceptible animal species both domestic and wild that could serve as secondary reservoirs, and which could lead to spillover and reverse-zoonosis events of emerging

or re-emerging variants. As SARS-CoV-2 continues to circulate in human and animal populations it is critical that surveillance efforts continue for the rapid identification and characterization of novel variants.

1.3.3. Clinical Disease

The severity of clinical disease associated with SARS-CoV-2 infection can vary with age and underlying co-morbidities. Younger populations generally develop mild respiratory disease or remain asymptomatic. Severe respiratory disease that requires hospitalization or death occur more commonly in older populations or people with co-morbidities (B. Hu et al., 2021). SARS-CoV-2 can be transmitted through direct and indirect routes and by respiratory droplets/aerosols (Harrison et al., 2020; Meyerowitz et al., 2020). The incubation period for SARS-CoV-2 can range from 1-14 days with clinical signs developing after an average of 5 days. Severe disease can develop after approximately 8 days following onset of symptoms (Z. Wu & McGoogan, 2020). Common clinical signs associated with SARS-CoV-2 include fever, fatigue and dry cough. Other clinical signs may include sore throat, headache, nausea, chills, loss of taste and smell (B. Hu et al., 2021). People with severe clinical disease requiring hospitalization may develop severe pneumonia and/or dyspnea that can lead to in respiratory failure, multiple organ failure, acute cardiac injury, and/or heart failure. SARS-CoV-2 infections and symptoms can persist for weeks to months prior to recovery (Pozzi et al., 2023).

The severity of disease associated with SARS-CoV-2 infections varies between animal species. SARS-CoV-2 infections can result in subclinical disease with minimal to no clinical signs developing which have been observed or demonstrated in white-tailed deer, cattle, sheep, domestic cats, domestic dogs and others (Cool et al., 2022; Gaudreault et al., 2022; Gaudreault,

Trujillo, et al., 2020; Meekins et al., 2021; Palmer et al., 2021). Syrian golden hamsters, ferrets, and mink, which are highly susceptible to SARS-CoV-2 infections, can develop clinical signs which may include weight loss, lethargy, anorexia, respiratory signs (nasal discharge and dyspnea), and/or mortality (mink and hamsters). Mild-to-severe postmortem lesions were observed in the respiratory tract of these highly susceptible species, consistent with respiratory disease (Meekins et al., 2021). Understanding the clinical presentation and manifestation of SARS-CoV-2 infections in susceptible hosts, both domestic and wild, is important for understanding the virus ecology and for developing experimental animal models for therapeutic and vaccine development.

1.3.4. Diagnostics

Diagnostic assays were rapidly developed following the emergence of SARS-CoV-2 that were crucial for detecting and monitoring the spread of SARS-CoV-2 during and after the pandemic. These assays include RT-qPCR, ELISAs for viral antigen and antibody detection. Targeted whole-genome sequencing protocols developed for SARS-CoV-2 were widely employed providing temporal phylogenetic characterization of SARS-CoV-2. The genetic information obtained from sequencing allowed for the rapid identification of emerging VOCs and VOIs both globally and regionally that would further aid in diagnostics, vaccines, and therapeutic development. These diagnostic assays are described in more detail below.

1.3.4.1. Detection of SARS-CoV-2 Genome

The detection of SARS-CoV-2 genome by RT-qPCR is considered the gold standard for diagnosis and surveillance of SARS-CoV-2 (Kevadiya et al., 2021; Pearson et al., 2021). These assays could be applied to a wide range of sample types to detect SARS-CoV-2 RNA such as

nasopharyngeal swabs, saliva, tissues, and wastewater (Ávila et al., 2022; Hale et al., 2022; Kata et al., 2023; Kevadiya et al., 2021). Various RT-qPCR assays have been developed to detect the RNA of different SARS-CoV-2 genes such as E, N, S, Orf1a, and RNA-dependent RNA polymerase (RdRp) independently (Lai & Lam, 2021; Yüce et al., 2021). As novel variants of SARS-CoV-2 emerged the chance of false negative results increased due to mutations at primer/probe binding sites; to address this, primer and probes were updated and diagnosis based on the detection of SARS-CoV-2 RNA requires two distinct gene targets (Davies et al., 2022; Yüce et al., 2021). Detection of SARS-CoV-2 by RT-qPCR has several drawbacks. False negatives can occur due to viral evolution, low quality RNA extractions arising from improper sampling or early viral infections (Kevadiya et al., 2021; Yüce et al., 2021). The other major drawback is the requirement for trained laboratory personnel, and expensive specialized equipment. Despite these drawbacks, RT-qPCR is a crucial diagnostic assay for the detection and surveillance of SARS-CoV-2 in both human and animal populations.

1.3.4.2. Targeted Whole Genome Sequencing SARS-CoV-2

Whole genome sequencing of SARS-CoV-2 has been extensively used throughout the pandemic to monitor the spread, transmission, and evolution around the world. International sequencing efforts of SARS-CoV-2 have resulted in the curation of >17 million genome sequences deposited in GISAID as of January 2025. The first and most widely used whole genome sequencing protocol is the ARTIC protocol (Itokawa et al., 2020; Koskela von Sydow et al., 2023; Quick, 2020). The ARTIC protocol is a targeted whole genome sequencing protocol that amplifies 400bp tiled amplicons spanning the SARS-CoV-2 genome with two independent reactions. The protocol can be used with Illumina, Oxford Nanopore, or PacBio sequencing

platforms. The Midnight protocol, a descendent of ARTIC, is another targeted whole genome sequencing protocol for SARS-CoV-2. This protocol generates tiled 1.2 kB amplicons across the SARS-CoV-2 genome and can be used with any sequencing platform. The protocol was also customized for long-read sequencing with the Oxford Nanopore platforms (Freed et al., 2020). This customization provided several advantages including real-time sequencing, portability, simple library preparation, and scalability (Koskela von Sydow et al., 2023). The availability and implementation of the ARTIC and Midnight protocols provided temporal evolutionary data of SARS-CoV-2 during the pandemic which was critical for the rapid identification and characterizations of emerging variants globally. As variants continue to emerge, mutations may occur in primer binding sites, resulting in amplicon drop-off and incomplete sequences, which is an inherent disadvantage for both protocols (Koskela von Sydow et al., 2023). For this reason, primer sets for either protocol must be updated to address this issue (Lambisia et al., 2022). The extensive use of whole genome sequencing for SARS-CoV-2 provided immense amount of genetic information vital for not only surveillance and evolution reasons but also diagnostic, vaccine, and therapeutic development.

1.3.4.3. Detection of SARS-CoV-2 Antigen and Antibodies

Antigen-based detection assays for diagnosing SARS-CoV-2 infections detect specific SARS-CoV-2 proteins such as the spike glycoprotein, matrix protein, or nucleocapsid protein (Yüce et al., 2021). SARS-CoV-2 antigen detection assays are available as in ELISA format for high throughput diagnostics in a laboratory setting or lateral flow format for rapid detection and point of care diagnostics. These assays have been validated for detecting viral antigen in nasopharyngeal swabs, and saliva. The nucleocapsid is one of the primary targets for antigen

detection lending to its high abundance (Lai & Lam, 2021). Both the ELISAs and lateral flow assays (LFA) sandwich style immunoassay like CSFV and ASFV antigen detection assays described above (Yüce et al., 2021). The point of care (LFA) provides a simple, cost effective, and rapid screening (15-30 minutes) system for detection SARS-CoV-2 infections (Lai & Lam, 2021; Yadegari et al., 2023). The major drawback to both the ELISA and point of care LFA compared to RT-qPCR is the reduced sensitivity of 70% (ELISA) and 56% (LFA) for clinical samples with low viral loads (Lai & Lam, 2021; Porte et al., 2020; Yadegari et al., 2023). The antigen-based diagnostics provide a cost-effective and rapid alternative to RT-qPCR for the diagnosis and screening SARS-CoV-2 in early stages of infection.

The detection of either viral RNA or viral antigens allows for the diagnosis of active SARS-CoV-2 infections but provides no information on previous infections or active immune responses to an infection. Several ELISAs and LFAs have been developed for the detection of SARS-CoV-2 specific IgM and IgG immunoglobulins in blood, serum, and plasma. These assays are designed to detect spike-, nucleocapsid-, or receptor-binding domain-specific immunoglobulins (Nerenz et al., 2022). Briefly, the antibody ELISA kits use microwell plates coated with recombinant antigen. Antigen-specific immunoglobulins present in the sample will bind the antigen followed by the addition of a conjugated-secondary antibody to detect bound immunoglobulins. These assays can be IgG or IgM specific (Nerenz et al., 2022). The LFA assays use gold nanoparticles coated with recombinant antigen; when a sample is added containing SARS-CoV-2 specific IgG or IgM an antibody-antigen complex is formed. These complexes flow across the membrane, bind to anti-IgG or anti-IgM antibodies located at the test line on the membrane, generating a band at their respective lines (Yüce et al., 2021). The other

serological test available is the virus neutralization assay for the detection of SARS-CoV-2 neutralizing antibodies from infection, vaccination, and for seroprevalence studies (Hale et al., 2022; Westhaus & Rabenau, 2022). However, this assay is time-consuming, requires trained personnel, and laboratories capable of working with live virus and cell culture. Serological assays provide the ability to detect SARS-CoV-2 antibodies arising from prior vaccination and SARS-CoV-2 infections.

1.3.5. Control Strategies

When SARS-CoV-2 emerged in late 2019 and rapidly spread around the globe resulting in the March 2020 pandemic no effective treatment or vaccine was available. Control measures to reduce community transmission included social distancing, face masks, and promoting hand hygiene (hand washing/disinfection) (Güner et al., 2020; Prather et al., 2020). The screening, diagnosis, and quarantine of infected individuals, either symptomatic or asymptomatic, further aided in controlling the spread of SARS-CoV-2. These control measures were critical to reduce the transmission and cases of SARS-CoV-2 until an effective vaccine or treatment was available. The international research efforts would lead to the development, manufacture, and deployment of SARS-CoV-2 vaccines in 12-15 months after SARS-CoV-2 emerged (Subbarao, 2021). Several vaccines were approved and available by the end of 2020 which included mRNA vaccines (Pfizer-BioNtech BNT162b2 and Moderna mRNA-1273), subunit vaccines (Novavax NVX-CoV2372), inactivated vaccine (Covaxin) and vector-based vaccines (Johnson & Johnson Ad26.COV2.S and Sputnik) (Logunov et al., 2021; Mistry et al., 2022; P et al., 2020; Patel et al., 2022; R et al., 2021). By the end of 2021 approximately 7 billion doses will be administered worldwide (Mistry et al., 2022). These vaccines remain effective, eliciting a protective immune

response to circulating SARS-CoV-2 variants (Harvey et al., 2021; Subbarao, 2021). By May 2023 with a significant portion of the global population vaccinated, and case numbers declining the WHO declared an end to COVID-19 pandemic (Sarker et al., 2023). While SARS-CoV-2 remains endemic, the availability of diagnostics, vaccines, and therapeutics will allow for a more rapid response in the future. However, it is critical that the surveillance of SARS-CoV-2 human and animal populations continues to identify emerging or re-emerging variants.

1.4. Nucleic Acid Sequencing: Technologies and Approaches

1.4.1. The Generations of Sequencing Technologies

1.4.1.1. First-Generation Sequencing

In 1977 a sequencing technique was developed that revolutionized the field of nucleic acid sequencing and laid the foundation that would usher in the era of next-generation sequencing; this technique is Sanger's 'chain-termination' or commonly known as Sanger sequencing (Sanger et al., 1977). The technique employs a chemical analog of deoxyribonucleotides (dNTPs) known as dideoxynucleotides (ddNTPs). These chemical analogs lack the 3' hydroxyl group required to form the phosphodiester bond with the 5' phosphate of the next dNTP in turn terminating DNA extension. These ddNTPs were radioactively labelled and mixed in four parallel DNA extension reactions, one for each nucleotide. The ddNTPs will be randomly incorporated in the DNA strands during extension resulting in a mixture of varying length DNA fragments. The reactions are resolved on a polyacrylamide gel and the sequence of the original template can be determined by the identification of radioactive bands in the corresponding lanes (Heather & Chain, 2016a; Sanger et al., 1977). Since the first iteration Sanger sequencing continued to evolve and improve. The radioactive labels were replaced with

fluorometric labels allowing the reaction to be completed in one tube. The detection was improved by replacing polyacrylamide gels with capillary electrophoresis. These two major improvements allowed for the development of the first DNA sequencers which were capable of sequencing DNA fragments less than one kilobase (kB) in length (Smith et al., 1986). For sequences greater than 1 kB, multiple overlapping fragments would be sequenced and assembled into contigs.

The field of sequencing began to rapidly advance with the development of polymerase chain reaction (PCR) and recombinant DNA technologies that allowed researchers to generate large amounts high purity DNA needed for sequencing (Heather & Chain, 2016a). These techniques allowed researchers to identify and characterize more efficient DNA polymerases that would lead to the development of new DNA sequencers that were capable of sequencing hundreds of samples simultaneously (Ansorge, 2009). Over the years numerous technological advances refined Sanger sequencing into the commonly used sequencing technique that we know today while establishing the foundation for the development of second-generation sequencers.

1.4.1.2. Second-Generation Sequencing

Around the time that the high throughput Sanger sequencing instruments were being developed a novel sequencing technique was developed by Pål Nyrén and colleagues termed pyrosequencing (Nyrén & Lundin, 1985). Comparable to Sanger sequencing, pyrosequencing is a sequencing by synthesis (SBS) technique but does not utilize ddNTPs in turn eliminating DNA extension termination. Pyrosequencing utilizes luminescence to measure the amount of pyrophosphate produced as nucleotides are washed across and incorporated to the DNA template affixed to a solid phase (Heather & Chain, 2016a). The system uses ATP sulfurylase which

converts pyrophosphate released following the addition of nucleotides during DNA extension into ATP, serving as substrate for luciferase. The luminescent intensity is proportional to the amount of pyrophosphate generated; lending to the technique's major drawback, accurately sequencing homopolymer regions (Nyrén & Lundin, 1985). This technique has several advantages, it does need chemically modified dNTPs and by utilizing luminescence it is capable of real time readouts. Eventually, the pyrosequencing license was acquired by 454 Life Sciences (acquired by Roche), later releasing the first second-generation sequencer.

The release of 454's pyrosequencing platform transformed the sequencing landscape, due to its ability to conduct mass parallel sequencing reactions, increasing the amount of DNA that can be sequenced in a single run (Margulies et al., 2005). The mass parallelization is achieved by generating sequencing libraries where DNA is attached to a bead coated with an adapter sequence. An emulsion PCR (emPCR) is performed that amplifies the DNA strand resulting in beads coated with clonal DNA fragments. The coated beads are washed across a picoliter reaction plate where each well contains a single coated bead. The DNA fragments are sequenced via pyrosequencing. The 454 platform was able to sequence fragments 400-500 bases in length across millions of wells drastically increase sequencing yields allowing researchers to sequence complex genomes, such as the human genome, with less effort and reduced cost (Heather & Chain, 2016a; Wheeler et al., 2008). The 454 pyrosequencing platforms would not be the only parallel sequencing technology to be developed in this generation.

One of the other major SBS technologies that arose during this generation was developed by Solexa which was later acquired by Illumina (Voelkerding et al., 2009). The Illumina sequencing platforms use flow cells coated with complementary oligonucleotides to an adapter

sequence that are attached to the 3' and 5' ends of DNA fragments during sequencing library preparation. Single-stranded DNA libraries are washed across the oligonucleotide field where the adapter containing DNA fragments anneal to the oligonucleotide surface. Following annealing, the complementary strand is synthesized which is covalently bonded to the flow cell, serving as the template for cluster generation (reverse strand). Clonal clusters are generated by solid phase bridge amplification PCR which generates a covalently bound complementary strand (forward strand) (Mercier & Slater, 2005). The double-strand bridge is denatured generating two single-stranded copies of tethered DNA. Several iterations of this process are completed generating millions of clusters, after which the reverse strand is cleaved. The forward strand is sequenced by fluorescently tagged nucleotides that are washed across the clusters and incorporated by a DNA polymerase. The fluorophores are excited by laser and imaged (Bentley et al., 2008; Illumina, 2010). The fluorophore is then cleaved, and the next cycle begins. The original Illumina sequencing technology had very limited read lengths of 35 bp, but with this technique, pair-end sequencing could be performed (Heather & Chain, 2016a). This in turn increased the accuracy by increasing the depth of coverage when mapping reads to reference sequence. Over the years, the read length and depth capabilities of Illumina platforms continued to increase as well as its popularity within the sequencing field.

The final SBS technology to contend with 454 pyrosequencing and Illumina sequencing was the Ion Torrent. Similar to the 454 platforms, Ion Torrent utilized beads coated in clonal DNA generated by emPCR. The beads are washed across a chip containing picowells large enough for one bead. The major difference between this system and the other two is that it does not use light emissions for detection of nucleotide incorporation. The system measures the

change in pH caused by the release of H^+ ions during polymerization using complementary metal-oxide semiconductor (CMOS) technology (Rothberg et al., 2011). The elimination of luminescence or fluorescence for detection allows decreased sequencing times. As with pyrosequencing this technology struggles with homopolymer regions (Loman et al., 2012).

The second generation of sequencing technologies made major leaps in the field of sequencing and has been described as the "genomic revolution" (Heather & Chain, 2016a). These technologies reduced the cost of DNA sequencing while at the same time increasing the ease of sequencing. The increases in output and accuracy with this generation has drastically changed the sequencing landscape. These platforms have played crucial roles in advancing the fields of infectious disease, cancer, diagnostics, and genetics (animal and plant) (Hernández-Neuta et al., 2023; Y.-C. C. Hou et al., 2022; Voelkerding et al., 2009).

1.4.1.3. Third-Generation Sequencing

As second-generation sequencing platforms continue to be extensively utilized in various scientific and medical fields, the next generation of sequencing is gaining momentum. Third-generation sequencing technologies can be characterized as single molecule sequencing in real time. These platforms do not require extensive clonal amplification prior to sequencing as seen with the second-generation (Heather & Chain, 2016a). One of the major defining features of this generation is the capability to sequence DNA fragments up to and greater than 10kB without fragmentation. There are two distinct third-generation sequencing platforms available, these are the PacBio platforms and Oxford Nanopore Technologies (ONT). The PacBio platforms use a technique called single molecule real-time (SMRT) sequencing. SMRT chips contain an array of nanopore structures called zero-mode waveguides (ZMWs) which filter light to a diameter

smaller than the wavelength, restricting illumination to the bottom of the well. This allows for visualization of single fluorescent molecules. At the bottom of ZMW wells is a single DNA polymerase (Schadt et al., 2010). DNA libraries and fluorescent dNTPs are washed across the array where the DNA polymerase incorporates fluorescent nucleotides that are detected in real time. Since sequencing occurs at the rate of polymerization, DNA fragments can be sequenced in a short period of time. The PacBio platforms can generate long reads with lengths up to and greater than 10kB (T. Hu et al., 2021; van Dijk et al., 2014).

Unlike PacBio, the ONT platforms do not utilize DNA polymerization and fluorescent dNTPs for sequencing, eliminating the need for fluorescent imaging systems. As the name implies, ONT platforms employ a nanopore based technology for sequencing. DNA libraries contain a sequencing tether and electrolytic solution are washed across an array of nanopores that are embedded in an electronically resistant polymer membrane. Each nanopore is connected to an electrode that is connected to a sensor chip. By applying a constant voltage an ionic current is generated across the nanopore that pulls the negatively charged DNA strands through the nanopore (Y. Wang et al., 2021). As translocation of DNA through the nanopore occurs it results in current fluctuations that correspond to nucleotide sequences that are present in the sensing region of the pore. The nucleotide sequence is determined using computational algorithms that decode the current fluctuations in real-time. The speed at which the DNA traverses the nanopore is controlled by a motor protein (phi29 DNA polymerase) that is attached to the nanopore. While controlling the speed of translocation the phi29 DNA polymerase has helicase activity allowing it to unwind double-stranded DNA as it ratchets the other strand through the nanopore (Y. Wang et al., 2021). One of the advantages of this technology is there is

no read length limitation as it does not rely on consumable reagents such as fluorescent dNTPs and polymerases. Since the release of the MinION, ONT flagship platform, in 2014 the maximum read length has increased from <800kB to 2.273Mb due to improvements in nanopore technology and library preparation (Y. Wang et al., 2021). The real time basecalling capabilities of nanopore sequencing enables researchers to perform real-time bioinformatical analysis which drastically reduces turnaround times when used in a diagnostic capacity (Stüder et al., 2021). Unlike any other sequencing platform ever developed, the ONT MinION platforms are the size of a cellphone battery pack, making it the only field deployable sequencing platform. Field applications of the MinION have been demonstrated with the sequencing of Ebola in Africa (Quick et al., 2016). Despite all these advantages nanopore sequencing generates lower quality reads and a high error rate compared to other sequencing technologies. However, improvements in accuracy and error rate have been made through optimization of nanopore technology, basecalling algorithms, and error corrections prior to downstream analysis (Y. Wang et al., 2021). ONT sequencing platforms have revolutionized sequencing by enabling decentralized sequencing and increasing the availability of sequencing.

Third-generation sequencing technologies have overcome the read length limitations that were seen with second-generation. The shift to single molecule sequencing has enabled amplification-free real-time sequencing which has drastically reduced sequencing times, making considerable impacts on the field of sequencing. Historically the third-generation sequencers have been known to have higher error rates compared to the second-generation sequencers with error rates of ~14% (PacBio) and 2-15% (ONT Nanopore) (T. Hu et al., 2021). These error rates continue to improve as these technologies are further modified and optimized. The other major

drawback of the PacBio platform over the ONT Nanopore is the cost, ~$525,000 (T. Hu et al., 2021). Every generation of sequencing technology has made significant far-reaching impacts in the scientific world. It will be very interesting to see what subsequent generations of sequencing technologies have in store.

1.4.2. Sequencing Approaches

There are two major sequencing approaches that are commonly used for whole genome sequencing of viral genomes; these are metagenomic sequencing and targeted sequencing. The method in which sequencing data is obtained does not differ between the methods. The differences are present in the steps prior to sequencing library preparation and sequencing, and in bioinformatical pipelines that are utilized during data analysis. Depending on the goal of sequencing one method may be more suitable. These methods are briefly described below.

1.4.2.1. Metagenomic Sequencing

Metagenomic sequencing, also known as shotgun sequencing, allows researchers to cast a wide net, since this approach sequences all the nucleic acids present in a sample. This approach can be used to detect infectious agents in diagnostic samples (Langelier et al., 2018), pathogen discovery (Wilson et al., 2017), or complex genomes (Spinard, O'Donnell, et al., 2023), while also being applied to a diverse range of sample types. One of the major limitations of metagenomic sequencing is the interference by host nucleic acids limiting detection of infectious agents at low concentrations which can result in partial genome sequences (Gu et al., 2024). Briefly, samples are prepared for metagenomic sequencing first by extracting nucleic acids. For DNA, the sample can proceed directly to sequencing library preparation. For RNA, a reverse transcription step using random hexamers is performed to generate cDNA followed by

sequencing library preparation (Hilt & Ferrieri, 2022). The abundance of host DNA can be reduced by completing enrichment steps which may include DNase treatment prior to extraction and/or depletion methylated genomic DNA (O'Donnell et al., 2020). Following sequencing, bioinformatic pipelines are used to identify or obtain the sequences of viral pathogens (Hilt & Ferrieri, 2022). Also, the reads can be mapped to a known reference genome. Metagenomic sequencing provides researchers with an unbiased sequencing technique with minimal sample preparation prior to sequencing but can require lengthy data analysis.

1.4.2.2. Targeted Sequencing

Targeted sequencing approaches as the name implies are used to sequence a specific organism or group of organisms. This approach is used for whole genome sequencing of numerous viruses (Höper et al., 2011; Quick, 2020; Töpfer et al., 2013), bacterial 16S ribosomal RNA sequencing for bacterial identification (Michael & L, 2007), and 28S ribosomal RNA sequencing for fungal identification (Hilt & Ferrieri, 2022; Wagner et al., 2018). The primary advantage of targeted sequencing of metagenomic sequencing is limited host DNA interference and higher sensitivity of detection in sample types with abundant host cells such as tissue. One disadvantage of targeted sequencing is sequences are limited to a specific organism or group of organisms (Hilt & Ferrieri, 2022). Targeted sequencing requires agent specific oligonucleotides or reference genomes to develop specific oligonucleotides; if these are not available, this will not be a suitable approach. The initial step of nucleic acid extraction is the same for both metagenomic and targeted sequencing for a sample of interest. Following nucleic acid extraction a PCR (DNA) or RT-PCR (RNA) is performed with oligonucleotides specific for the organism of interest. This serves to enrich and select for the organism of interest. The amplicons

generated during the PCR or RT-PCR are purified and sequencing library preparation is completed (Quick, 2020). Following sequencing, reads can be mapped to a reference genome to obtain a consensus sequence that can be used for phylogenetic characterization. Targeted sequencing provides higher depths of coverage compared to metagenomic sequencing which is beneficial for single nucleotide polymorphisms analysis.

These are two of the most common sequencing approaches. Metagenomic sequencing approaches cast a broad net that can discover novel pathogens while targeted sequencing approaches enable a deeper look at a specific pathogen or group of pathogens. Both sequencing approaches described above have advantages and disadvantages over one another, but both play significant roles in the field of sequencing.

1.5. Bioinformatic Analysis

Over the years with the increased volume of sequencing data generated by second- and third-generation sequencing platforms, numerous bioinformatic programs and pipelines have been developed to analyze these large data sets. Bioinformatic analysis for these large data sets can be computationally expensive and time consuming (Gu et al., 2024; Hilt & Ferrieri, 2022). As high-performance computational technologies continue to advance such as the development of cloud-based computing and machine learning, the time and cost to perform these analyses has been reduced (Dinhobl et al., 2024; Juul et al., 2015; Naccache et al., 2014; Wood & Salzberg, 2014). There are several preprocessing steps that are completed before any in depth bioinformatic analysis. Briefly, basecalling and filtering is completed which converts raw signals into sequencing reads and removes low quality reads. This process is completed by proprietary algorithms associated with specific sequencing platforms.

Following this process, sequencing reads can be loaded into a bioinformatic pipeline. These pipelines can begin with secondary read trimming and quality filter step to ensure that the highest quality reads are used for the next steps in the analysis pipeline. If these secondary read trimmings and quality filters are too stringent, pathogens in low abundance or low frequency single nucleotide variants may be excluded or overlooked in downstream analyses. After these preprocessing steps, there are two routes that the analysis can proceed which include *de novo* assembly or read alignment to the reference genome. The sequencing approach that was implemented will influence which bioinformatic analysis is performed, which is discussed below.

1.5.1. *De Novo* Assembly

De novo assembly is one of the bioinformatic analyses that is commonly used for metagenomic sequencing approaches. Briefly, this analysis uses algorithms to assemble sequencing reads into larger consensus sequences, termed contigs. Numerous contigs can be generated during *de novo* assemble with differing lengths and depths of coverage. Contigs with the highest depths of coverage can be considered to represent the most abundant sequences in the sample (Sohn & Nam, 2018). While these contigs represent the most abundant sequences, it does not identify the organisms that the sequences represent. This information is gained by screening contigs against databases of known sequences using BLAST, basic local alignment search tool, which identifies and ranks organisms based on sequence similarity (Altschul et al., 1990; McGinnis & Madden, 2004). Since metagenomic sequencing is an unbiased sequencing approach, by sequencing everything in a sample, this bioinformatic analysis is the most appropriate.

1.5.2. Read Alignment to Reference Genome (Read Mapping)

Bioinformatic analysis commonly combined with targeted sequencing approaches relies on aligning sequencing reads to a reference genome and can be referred to as read mapping. There are numerous alignment/mapping algorithms that can be used, but this section will focus on the mapping tool associated with CLC Genomic Workbench (Qiagen, 2024). Briefly, the optimal alignment of a read is determined by a cumulative score that is calculated using several cost parameters including match, mismatch, insertion, and deletions. The number of nucleotides in a read that match the reference are summed and multiplied by the match score. The number of mismatches, inserted, and deleted nucleotides are summed and multiplied by their respective cost scores. All these parameters are subtracted from the total matching score, resulting in the cumulative score for the read. The greater the read score indicates the greater/better optimal alignment. Prior to the read being mapped to the reference sequence and included in the output, a filtering process is applied to determine if the read is an appropriate match. The filtering process assesses the length and similarity fractions of the read. For example, if these parameters are set to 50% length and 80% similarity fractions; 50% of the aligned read must match the reference and half of the aligned read must have 80% similarity to the reference genome. By increasing these parameters, the aligned reads with highest alignment scores will be included in the output. The consensus sequence can be extracted from this mapping. Mutations that are present at greater than 50% of the mapped reads will be included in the consensus sequence. These read mappings can be used to determine genome coverage in both the depth and fraction of the reference (Qiagen, 2024). These mappings can be used for single nucleotide polymorphisms (SNPs or variants), which is discussed below.

1.5.3. Single Nucleotide Polymorphism Analysis: Variant Calling

Single Nucleotide Polymorphisms (SNPs) analysis can be performed to assess nucleotide mutations that can arise in viruses over time in the presence of selective pressures such as cell culture or during *in vivo* infections. SNP can be classified as synonymous and nonsynonymous which relates to the effect on the encoded amino acid sequence. Synonymous mutations are nucleotide substitutions that do not result in an amino acid substitution. Nonsynonymous mutations result in an amino acid substitution which can result in changes in receptor binding, replication efficiency, and host adaptations (Escalera et al., 2022; Halwe et al., 2024; Shastry, 2009; Zhou et al., 2021). As with read mapping there are numerous variant callers that can be used, but this section will focus on the low frequency SNP caller associated with CLC Genomic Workbench (Qiagen, 2024). Briefly, low frequency SNP analysis (variant calling) will determine all the SNPs at frequencies greater than a set threshold present in the read mapping. To increase the confidence of the SNPs called, coverage, read count, and quality thresholds can be added to the analysis. To evaluate nonsynonymous SNPs, the reference sequence must include annotation that indicates the coding sequence (CDS) of viral proteins (Qiagen, 2024). SNP analysis can be conducted for multiple samples and time points, providing information on SNP selection under differing selective pressures present during *in vivo* and *in vitro* viral infections (Z.-Z. Huang et al., 2024; Nogales & Dediego, 2019; Rozek et al., 2021). It is important to note that this analysis does not indicate the significances of these mutations unless previously described or evaluated *in vitro*. SNP analysis can provide insights into viral mutations that could impact viral fitness.

As sequencing technologies change and data sets increase, bioinformatic analysis continues to adapt to these changes. However, these changes can increase the complexity of

bioinformatic analysis which is the most time-consuming proportion within the field of sequencing (Gu et al., 2024; Hilt & Ferrieri, 2022). These timeframes are reducing with the implementation of real-time data analysis which can be used with ONT sequencing platforms and cloud based bioinformatic analysis (Juul et al., 2015; Naccache et al., 2014). The implementation of machine learning will have significant impacts on bioinformatic analysis in the future.

Chapter 2 - Experimental Infection of Domestic Pigs with African Swine Fever Virus Isolated in 2019 in Mongolia[1]

2.0. Abstract

African swine fever (ASF) is an infectious viral disease caused by African swine fever virus (ASFV), that causes high mortality in domestic swine and wild boar (Sus scrofa). Currently, outbreaks are mitigated through strict quarantine measures and the culling of affected herds, resulting in massive economic losses to the global pork industry. In 2019, an ASFV outbreak was reported in Mongolia, describing a rapidly progressing clinical disease and gross lesions consistent with the acute form of ASF; the virus was identified as a genotype II virus. Due to the limited information on clinical disease and viral dynamics within hosts available from field observations of the Mongolian isolates, we conducted the following study to further evaluate the progression of clinical disease, virulence, and pathology of an ASFV Mongolia/2019 field isolate (ASFV-MNG19), by the experimental infection of domestic pigs. Intramuscular inoculation of domestic pigs with ASFV-MNG19 resulted in clinical signs and viremia at 3 days post challenge (DPC). Clinical disease rapidly progressed, resulting in the humane euthanasia of all pigs by 7 DPC. ASFV-MNG19-infected pigs had viremic titers of 108 TCID50/mL and shed virus in oral secretions late in disease, as determined by infectious virus from oropharyngeal swabs. Whole-genome sequencing confirmed that the ASFV-MNG19 strain

[1] Reprinted with permission from McDowell, C.D.; et al. Experimental Infection of Domestic Pigs with African Swine Fever Virus Isolated in 2019 in Mongolia. Viruses. **2022**, 14, 2698. https://doi.org/10.3390/v14122698. Copyright 2022 by Chester D. McDowell.

used in this study was a genotype II strain highly similar to other regional strains. In conclusion, we demonstrate that ASFV-MNG19 is a virulent genotype II ASFV strain that causes acute ASF in domestic swine.

2.1. Introduction

African Swine Fever (ASF) is an infectious viral disease that causes high mortality in domestic swine and wild boar (*Sus scrofa*). Outbreaks of the disease have devastating economic impacts on affected regions and threaten swine health and the swine industry worldwide. No commercial vaccine or treatment is currently available, except for a live-attenuated vaccine called NAVET-ASFVAC that was recently (June 2022) licensed for restricted use only in Vietnam (Borca et al., 2021; X. H. Tran et al., 2022), however currently suspended by Vietnam's Minister of Agriculture and Rural Development (MARD) due to improper use that resulted in the death of vaccinated pigs. Therefore, the current control measures for ASF primarily rely on quarantine and biosecurity, animal movement restrictions, and the depopulation of infected/exposed animals (Sánchez-Cordón et al., 2018).

The causative agent of ASF is African Swine Fever virus (ASFV), which belongs to the *Asfarviridae* family, genus *Asfivirus* (Galindo & Alonso, 2017; Gaudreault, Madden, et al., 2020). The virus particle encapsulates a 170–192 kilobase (kB) double-stranded DNA genome encoding for more than 150 genes (Dixon et al., 2013, 2019; Vilem et al., 2020a; X. Wang et al., 2022a). Currently, 24 genotypes have been identified with varying virulence between and within genotypes (C. Gallardo et al., 2021; Sánchez-Cordón et al., 2019). Historically, ASFV was restricted to Sub-Saharan African countries until outbreaks emerged between the 1950s and 1980s in Europe, Russia and South America; by the 1990s, ASFV was confined to Africa and

Sardinia, where it remained endemic (Gaudreault, Madden, et al., 2020). In 2007, an outbreak in domestic pigs in the country of Georgia resulted in the spread of ASFV into eastern Europe and throughout Russia, where it became established in wild boar populations (Cwynar et al., 2019; Gogin et al., 2013; Sánchez-Vizcaíno et al., 2013). In 2018, China reported the first outbreak in Asia. By 2019, ASFV was reported in neighboring countries, including Cambodia, Laos, Mongolia, Myanmar, the Philippines, and Vietnam, as well as the Korean peninsula (H. J. Kim et al., 2020).

In January of 2019, the first case of ASFV was reported in a backyard herd consisting of 38 pigs in the Bulgan province of Mongolia (Heilmann et al., 2020). Following the index outbreak, subsequent outbreaks were confirmed in seven Mongolian provinces. Due to the rapid implementation of control measures, which included surveillance, movement restrictions in the affected districts, culling of the affected herds, and a temporary ban on the importation of pork products, the outbreak was declared over by April 2019 (Heilmann et al., 2020). The outbreak resulted in the loss of 2862 pigs, equivalent to 10% of the total Mongolian pig population (Ankhanbaatar et al., 2021; Heilmann et al., 2020). Initial molecular characterization of Mongolian field isolates determined that the circulating strain was a genotype II strain that was highly similar to other genotype II viruses found in China and Russia based on the major capsid protein (p72) and envelope protein (p54) sequences, as well as the central hypervariable region (CVR) of B602L (viral chaperone) (Ankhanbaatar et al., 2021).

Information on the clinical signs and progression of the ASFV Mongolia/2019 (ASFV-MNG19) strain is limited to observations from the field, describing clinical signs and gross pathological lesions that are consistent with an acute form of ASF (Ankhanbaatar et al., 2021). In

this study, we investigated the virulence and clinical progression of ASFV-MNG19 in a controlled experimental setting with domestic swine.

2.2. Materials and Methods

2.2.1. Cell Culture and Challenge Material Preparation

ASFV-MNG19 was isolated from the kidney of an infected pig from the Tov province of Mongolia during the 2019 outbreak. A tissue homogenate was prepared from the kidney and shipped to Kansas State University (KSU) via USDA-APHIS. All experiments involving ASFV-MNG19 were conducted in the BSL-3 laboratory at the Biosecurity Research Institute (BRI) at KSU in Manhattan, KS. ASFV-MNG2019 was propagated in T-75 cm2 flasks on near confluent primary swine pulmonary alveolar macrophages (PAM). Inoculated cell cultures were incubated at 37 °C in a humidified 5% CO2 incubator for 7 days. Virus-containing cell culture supernatants were aliquoted and stored at −80 °C. Virus titrations of the viral stock and clinical samples were performed on primary swine alveolar macrophages as previously described with minor modifications (WOAH: Manual of Diagnostic Tests and Vaccines for Terrestrial Animals, 2023a). PAM cells were seeded in 96-well plates one day before the experiment. A ten-fold dilution of viral stock or clinical samples were prepared in triplicates and transferred onto PAM cells. The presence of virus was visualized by hemadsorption, confirmed by immunofluorescence assay, and titers were calculated using the Spearman–Karber method. The limit of detection for virus isolation in EDTA blood by hemadsorption was 3.41×10^3 HAD_{50}/mL and by immunofluorescence 3.41×10^2 $TCID_{50}$/mL. The limit of detection for virus isolation in oropharyngeal (OP) swabs for both hemadsorption and immunofluorescence was 3.41×10^1 $TCID_{50}$ or HAD_{50}/mL. The challenge material was prepared by diluting PAM-

propagated ASFV-MNG19 viral stock to 360 HAD_{50}/mL in Dulbecco's Modified Eagle Medium (DMEM).

2.2.2. Next Generation Sequencing (NGS)

ASFV-MNG19 DNA extracted from the original virus stock and challenge inoculum were sequenced on the Illumina MiSeq sequencing platform (Illumina; San Diego, CA, USA). The Illumina Nextera XT Library Prep Kit (Illumina; San Diego, CA, USA) was used for the generation of sequencing libraries following the manufacturer's protocol. Libraries were paired-end sequenced using the Miseq v2 Reagent kit (300 cycles; Illumina; San Diego, CA, USA). Reads were parsed into individual FASTQ files and imported into CLC Genomics Workbench 20 (Qiagen; Carlsbad, CA, USA) for downstream analysis. Reads were trimmed and filtered for removal of the low-quality reads with a Q-score ≤ 25 and reads shorter than 50 nucleotides. The de novo assembly module within CLC Genomic Workbench was used to assemble one near full length contig of 173.5 kB (average coverage of 156.14×) and another of 14.3 kB (average coverage: 142.91×) for the original ASFV-MNG19 stock. The contigs were mapped to the Georgia/2007 reference genome a consensus sequence was generated. The ASFV-MNG19 reference genome was uploaded to GenBank under accession number: OP467597. The sequencing reads for the ASFV-MNG19 challenge material were mapped to the ASFV-MNG19 reference genome using CLC Genomics Workbench to assess any changes within the consensus sequence following passage on PAM cells. The sequence was uploaded to GenBank accession number: OP909713. BLAST (Morgulis et al., 2008; Z. Zhang et al., 2000) search using the NCBI nonredundant nucleotide database was completed to identify highest sequence similarity. The complete genomes of 31 ASFV strains including the ASFV-MNG19 original stock and

challenge material were aligned with CLC Genomics Workbench. Phylogenetic trees were constructed from the alignment using the maximum likelihood method with 1000 bootstrap replicates using MEGA11 (Tamura et al., 2021). Additionally, we compared our ASFV-MNG19 genomic consensus sequence to partial ASFV genome sequences related to genes p72 (MT851928 to MT851931), p54 (MT851924 to MT851927), B602L (MT851932 to MT851935), CD2v (MT851936 to MT851938), and intergenic region between I73R and I329L (MT852020 to MT852023), used by Ankhanbaatar et al. (Ankhanbaatar et al., 2021) for genotyping of the initial Mongolian isolates during the 2019 ASF outbreak. For this particular analysis we only considered the region between the primer loci used by Ankhanbaatar et al. (Ankhanbaatar et al., 2021) to prevent misidentification of mutations that reside within the primer loci.

2.2.3. Ethics Statement for Use of Animals

All animal studies and experiments were approved and performed under the KSU Institutional Biosafety Committee (IBC, Protocol #: 1314) and the Institutional Animal Care and Use Committee (IACUC, Protocol #: 4265) in compliance with the Animal Welfare Act. The research involving ASFV was conducted in BSL-3 and ABSL-3Ag facilities in the BRI at KSU in Manhattan, KS, USA.

2.2.4. Study Design

Clinical disease and progression of ASFV-MNG19 was assessed in six approximately 2-month-old crossbred male pigs (Figure 2.1). The animals were inoculated intramuscularly (IM) with 1 mL of ASFV-MNG19 (dose of 360 HAD_{50}/mL) in the right lateral cervical region cranial to the point of the shoulder. This dose and the IM inoculation route were chosen for consistency with our previous studies to allow for comparison of these data with pigs infected with different

ASFV strains. This study does not include other ASFV strains to avoid repetitiveness with our previous studies and reduce the unnecessary use of animals and resources. The IM route provides administration of a controlled dose and produces consistent disease progression. Following inoculation, daily body temperatures and clinical signs were recorded to assess disease progression. Daily health checks were performed every morning by team personnel, as well as in the evening when animals became febrile. Two animals were found dead and the remaining four were humanely euthanized using pentobarbital on 7 days post challenge (DPC) due to severe clinical signs. Necropsies were conducted on all animals, as described below.

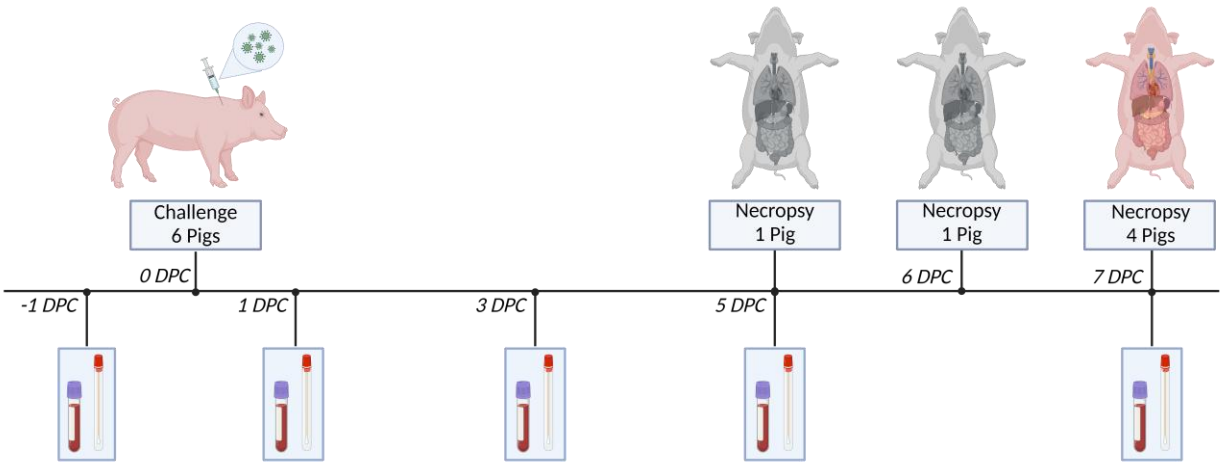

Figure 2.1. ASFV-MNG19 Challenge Study Schematic.

Six crossbred male pigs approximately 2-months-old were challenged with 360 HAD_{50} of ASFV-MNG19. Samples were collected on days −1, 1, 3, 5, and 7 DPC. Samples collected included whole blood (EDTA), OP swabs, and oral fluids collected from chewed ropes at the pen level. Body temperature and clinical scores were assessed daily. One pig (#307) was necropsied on 5 DPC as a result of complications following sample collection. Another pig (#306) was found dead on 6 DPC and subsequently necropsied. The remaining 4 pigs were humanely euthanized and necropsied at 7 DPC due to severe clinical signs.

2.2.5. Clinical Signs and Samples

Clinical scoring was completed daily and used to assess disease progression and to determine clinical endpoint for severely affected animals to eliminate suffering. The clinical score consisted of 8 criteria which included: liveliness (reluctance to stand or move), body shape (sunken flanks), respiration (tachypnea with abdominal component), neurological signs (ataxia to paralysis), skin (cyanosis and severity), digestive symptoms (diarrhea and vomiting with duration, presence of melena), ocular and nasal discharge, and pyrexia. Each of these criteria were scored from 0 to 3 dependent on severity, with the exception of pyrexia which was scored from 0 to 4; see Supplementary Table S1 for more details. An animal was considered at clinical endpoint when presenting either a cumulative score greater than 10 or severe clinical signs such as neurological signs (paralysis or convulsions), extensive dermal cyanosis, bloody diarrhea, or hypothermia which correspond to the highest score in the respective categories. On clinical sampling days behavior assessments were conducted, which included individual rope chewing, response to OP swabs, and general demeanor. Each pig received an individual score of 0–4 for each category with 0 being normal and 4 uninterested, as detailed in Supplementary Table S2.

Clinical samples were collected on −1, 1, 3, 5, and 7 DPC, consisting of EDTA blood, OP swabs, and oral fluids. The clinical samples were used to follow viremia and viral shedding in bodily fluids over the course of disease using both quantitative real-time PCR and viral titrations.

2.2.6. Quantitative Real-Time PCR Assay for ASFV DNA

ASFV specific DNA was detected and quantified in EDTA-collected blood and OP swabs of challenged pigs by quantitative real-time PCR (qPCR) assay as previously described

(Sunwoo et al., 2019a). Viral DNA from clinical samples was extracted and purified with the MagMax Pathogen RNA/DNA kit (ThermoFisher Scientific; Waltham, MA, USA) using the Kingfisher™ Duo Prime purification system, an automated magnetic bead extraction system, following manufacturer's protocol with minor modifications. EDTA blood or OP swab supernatant was mixed 1:1 with AL lysis buffer (Qiagen; Carlsbad, CA, USA) and heated at 70 °C for 10 min. Subsequently, 200 µL were mixed with 20 µL of bead mix (equal volume of nucleic acid binding beads and lysis enhancer). The mixture was gently mixed by pipetting and incubated for 2 min at room temperature. Phosphate-buffered saline (PBS, 100 µL) was added to the tube and the entire volume was added to the extraction plate well containing 400 µL lysis buffer, binding buffer and isopropyl alcohol. DNA bound to beads was washed twice with 300 µL of wash solution 1, a third wash was completed with 450 µL wash solution 2, and a final wash with 450 µL of 200 proof molecular grade ethanol. The DNA-bound beads were dried for 5 min prior to being eluted in 100 µL elution buffer. Negative (molecular grade water/PBS) and positive (ASFV p72 plasmid) controls were included with each extraction.

The ASFV DNA extracted from clinical samples was detected and quantified using the primers and probe for the detection of the p72 ASFV gene as previously described by Zsak et al. (Zsak et al., 2005), using a validated protocol performed with the PerfeCTa® FastMix® II (Quanta Biosciences; Gaithersburg, MD, USA) on the CFX96 Touch™ Real-Time PCR Detection System (Bio-Rad; Hercules, CA, USA) as previously described (Sunwoo et al., 2019a). Duplicate qPCR reactions were performed. Each PCR run included negative and positive controls, which consisted of nuclease-free molecular grade water and ASFV positive amplification control (p72 plasmid), respectively. Due to the analytical limits of the PCR assay,

the Ct cutoff was set to 38 for both replicate wells as positive; samples with a single replicate well of 38 or less were classified as suspect. A sample was considered negative if both replicate wells were between 38–45 Ct. The copy number (CN) of ASFV DNA was calculated using a standard curve generated using ten-fold serial dilutions of quantified ASFV p72 plasmid DNA.

2.2.7. Gross and Histological Pathology

Postmortem gross lesions were assessed and scored for all euthanized and found dead pigs. Lesions were scored following the standardization guidelines established by Galindo-Cardiel et al. (Galindo-Cardiel et al., 2013) with minor modifications as previously described (Sunwoo et al., 2019a). Briefly, gross evaluation was performed on the exterior carcass (dermis, body condition, and eyes), the thoracic cavity (heart and lungs), the abdominal cavity (stomach, liver, gall bladder, kidneys, small intestines, large intestines, and urinary bladder), as well as primary and secondary lymphoid organs including spleen, bone marrow, tonsils, and multiple lymph nodes (mandibular, cervical, tracheobronchial, gastrohepatic, mesenteric, and renal). Additional gross evaluation included oral cavity, trachea, thyroid glands, and the brain. The characterization and classification of gross lesions was performed for each organ. Gross lesions were classified as absent (0), mild (1), moderate (2), and severe (3) with an established numeric scoring system for each organ, see Supplementary Table S3.

Standardized histological evaluation was performed blindly on tonsil, and lymph nodes including submandibular, superficial cervical, perihepatic, mesenteric, and renal, as described by Galindo-Cardiel et al. (Galindo-Cardiel et al., 2013) with minor modifications (Sunwoo et al., 2019a). Additional tissues evaluated histologically included the lung, liver, spleen, kidney, heart, adrenal glands, skin and gastrointestinal tract. Lesion classification was established as absent (0)

or present at mild (1), moderate (2), severe (3) or marked (4) with the numerical score established for tonsils and lymph nodes. Lesion categories scored include: necrosis; cellular or tissue level, fibrin thrombi, deposition in tissue or fibrinoid degeneration of vessels, congestion and hemorrhage, inflammation; infiltrates of macrophages, eosinophils or neutrophils. Specific scoring results for each pig and organ are provided in Supplementary Table S4.

2.3. Results

2.3.1. Whole-Genome Sequencing of the ASFV-MNG19 Isolate

Whole-genome sequencing of the original ASFV-MNG19 isolated from the kidney of an infected pig in the Tov province of Mongolia was performed to confirm viral species and genotype. A near-full-length genome was obtained by de novo assembly. The BLAST search against the NCBI nonredundant nucleotide database show that ASFV-MNG19 is highly similar to other circulating genotype II strains in the region, which includes Chinese, Russian, and Korean strains (Table 2.1).

Table 2.1. The ten sequences with the highest similarity to ASFV-MNG19.

Accession	Name	Percent Identity
MK128995.1	China/2018/AnhuiXCGQ	99.99
MN172368.1	ASFV/pig/China/CAS19-01/2019	99.99
MK333180.1	Pig/HLJ/2018	99.99
ON075797.1	Korea/YC1/2019	99.98
MW306191.1	ASFV/Primorsky 19/WB-6723	99.99
MW396979.1	ASFV/Timor-Leste/2019/1	99.98
MN715134.1	ASFV_HU_2018	99.98
OL692744.1	IND/AR/SD-61/2020	99.98
OL692743.1	IND/AS/SD-02/2020	99.98
MW049116.1	ASFV Korea/pig/Yeoncheon1/2019	99.98

BLAST search results for the ten ASFV genomes with the highest sequence similarity to the ASFV-MNG19 full genome. First is NCBI accession number, followed by sequence name, and percent identity.

The challenge inoculum, ASFV-MNG19 propagated on PAM cells was sequenced and compared with the original ASFV-MNG19 stock prior to use in the described challenge experiment. We detected eight putative mutations in the inoculum compared with the stock (Supplementary Table S5), which could not be reliably confirmed due to the low coverage. Our direct sequencing approach lacks the minimum required depth needed for variant analysis. Targeted sequencing will be necessary to address this. The direct sequencing approach was sufficient for the identification and characterization of the original ASFV-MNG19 stock and challenge inoculum.

Phylogenetic analysis of the full-length sequences of ASFV-MNG19 isolates used in this study indicated that these viruses clustered with other genotype II isolates detected in Eastern Europe, Russia, and Southeastern Asia (Figure 2.2), which is in accordance with the global spread of the disease. The comparison of our ASFV-MNG19 isolates revealed a 100% nucleotide identity for the partial p72, full p54, partial B602L, partial CD2v and the intergenic region of I73R and I329L genes of the previously sequenced Mongolian isolates (Ankhanbaatar et al., 2021). The ASFV-MNG19 isolates contain the same CVR profile and display the major genotype II genetic features described by Ankhanbaatar et al. (Ankhanbaatar et al., 2021). We conclude that our ASFV-MNG19 isolate is a genotype II virus and displays the major genetic features described for the previously genotyped Mongolian isolates.

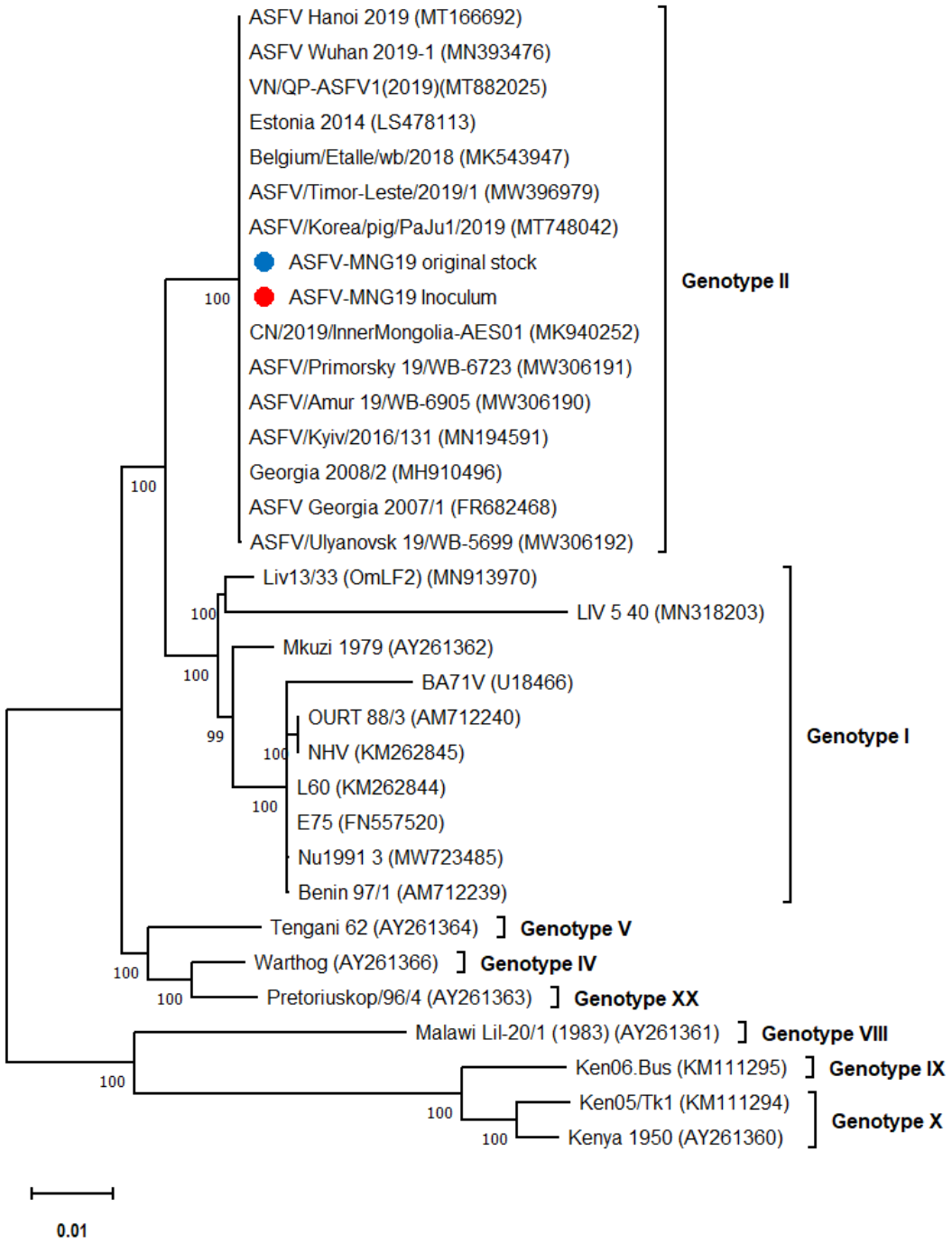

Figure 2.2. Phylogenetic tree of whole-genome sequences of ASFVs.

The phylogenetic tree was constructed using maximum likelihood approach with 1000 bootstrap replicates. The blue and red dots indicate the ASFV-MNG19 original stock and inoculum used in this challenge study, respectively.

2.3.2. Clinical Observations Following Challenge with ASFV-MNG19 Isolate

Following intramuscular inoculation of six pigs with 360 HAD_{50} of the ASFV-MNG19 isolate, the body temperatures were monitored daily or twice daily once temperatures became >40.5 °C (Figure 2.3A). All six pigs maintained normal temperatures for one or two days post challenge (DPC); by 3 DPC, three of the six pigs had temperatures greater than 40.5 °C. All pigs were febrile by 5 DPC with temperatures greater than 41 °C. The majority of the pigs maintained elevated temperatures until the animals were euthanized due to severe clinical signs or succumbed to ASF. Two animals (#306 and #307) died from an acute form of ASF. Following sample collection at 5 DPC, animal #307 went into respiratory distress followed by cardiovascular collapse; resuscitation was unsuccessful. Animal #306 was found dead at 6 DPC. The remaining four animals were euthanized on 7 DPC due to severe clinical signs (Figure 2.3B).

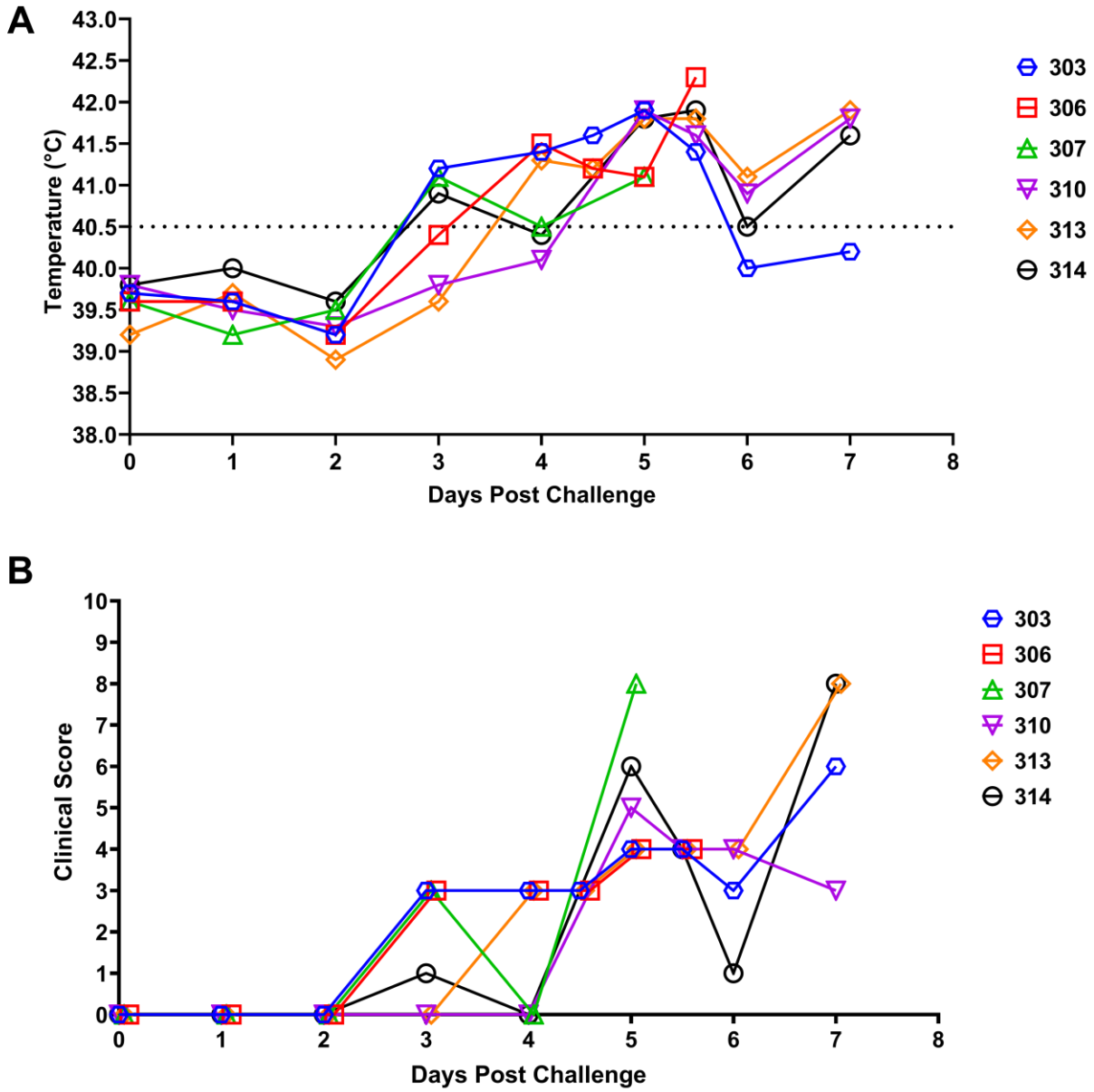

Figure 2.3. Clinical Observations of ASFV-MNG19 Infected Pigs.

Daily body temperatures (A) and cumulative clinical score (B) of the 6 pigs challenged IM with ASFV-MNG19 from 0 DPC to 7 DPC. Data indicates individual values (A) expressed as °C, (B) expressed as an integer value. Data for individual animals are shown. The dashed line in 3A indicates 40.5 °C which is considered a fever for this study.

Clinical scores were assessed daily along with body temperatures to assess severity of clinical symptoms. The scoring system consisted of eight criteria which included liveliness, body condition, respiration, neurological signs, skin, digestive symptoms, ocular/nasal discharge, and pyrexia. Total clinical scores greater than or equal to 10 were considered clinical endpoints. Daily clinical scores are shown in cumulative form in Figure 2.3B. Clinical signs following challenge with ASFV-MNG19 were observed starting by 3 DPC when animals became febrile and progressively worsened both in severity and ASF-specific clinical signs. As the pyrexia persisted, animals became lethargic and anorexic, exhibiting reduced interest in rope chewing and normal activities. Two of the animals had respiratory signs consisting of open mouth breathing with an abdominal component following sample collection on 3 DPC; these included #306 which recovered, and #307 which died at 5 DPC as described above. Later in the study, two animals had sunken flanks suggestive of an empty stomach. The remaining four pigs on 7 DPC were displaying mild neurological signs which included stumbling and swaying gaits, and were euthanized on that day. By the end of the study on 7 DPC the major clinical symptoms observed were severe pyrexia, lethargy, and mild neurological and digestive signs. The respiratory signs described were noted following sample collection which could have been exacerbated by excitation from manipulation.

2.3.3. Detection and Quantitation of ASFV DNA by qPCR

Quantitative real-time PCR for detection of ASFV p72 (B646L gene) DNA was performed on viral DNA extracted from EDTA whole blood collected at −1, 1, 3, 5, 6, and 7 DPC; the one blood sample from 6 DPC was collected from pig #306 which was found dead. At 3 DPC, pigs infected with the ASFV-MNG19 isolate had on average 2.49×10^6 CN/mL (Ct =

24.85) of viral DNA present in their blood. Viral loads increased by a $\log_{10}$ at 5 DPC and plateaued by 7 DPC (Figure 4A). The increasing viral loads correlated with the prolonged, severe pyrexia and increased clinical scores. Viral DNA was detected in OP swabs at 5 DPC from all animals, except pig #310, which had detectable viral DNA at 3 DPC but not at 5 DPC as a result of transient shedding or sampling technique (Figure 4B). The remaining animals that were euthanized on 7 DPC had detectable ASFV DNA in their OP swabs. This is indicative of virus shedding in saliva and is corroborated further by detectable viral DNA in oral fluids collected at the pen level on 5 DPC (Figure 4C), where 3/6 pigs were observed chewing the ropes but with reduced enthusiasm, see Supplementary Table S6.

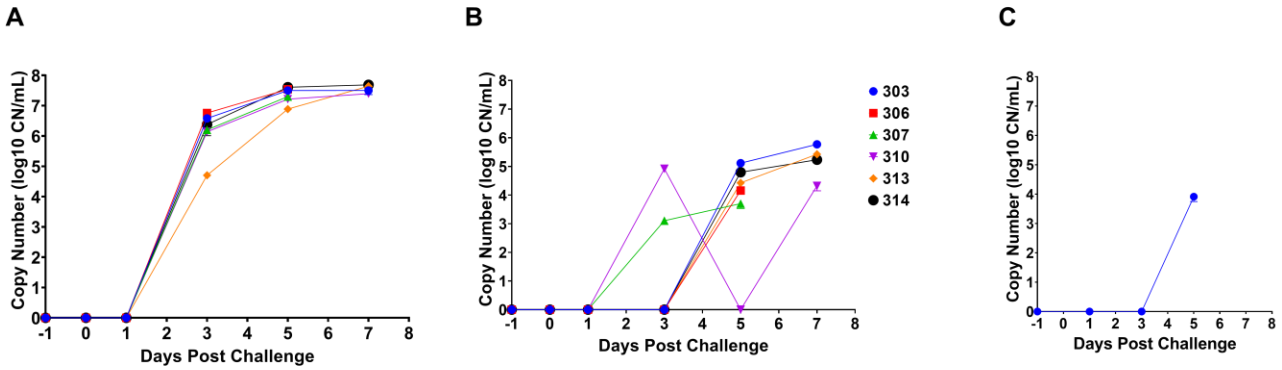

Figure 2.4. Quantitative real-time PCR for ASFV DNA detected in blood, OP swabs, and oral fluids.

(A) The calculated copy number (CN) of ASFV DNA extracted from EDTA blood collected on −1, 1, 3, 5, and 7 DPC using a ten-point standard curve. Datapoints for individual pigs are represented. The single data point at 6 DPC represents blood collected from pig #306, which was found dead. (B) The calculated copy number of ASFV DNA extracted from OP swabs collected on −1, 1, 3, 5, and 7 DPC using a ten-point standard curve. Datapoints for individual pigs are represented. (C) The calculated copy number of ASFV DNA extracted from oral fluids (rope chewing) collected on −1, 1, 3, and 5 DPC using a ten-point standard curve. Datapoints represent the pen level.

2.3.4. Viral Titrations in Blood and OP Swabs

Virus titrations were performed on the EDTA blood and OP swabs collected at −1 to 7 DPC for all animals. The presence of infectious virus was determined by hemadsorption and confirmed by immunofluorescence assay. As expected, there was no detectable virus at −1 DPC in blood or swabs. All animals had detectable infectious virus in the blood by 3 DPC with titers ranging from 10^4–10^6 $TCID_{50}$/mL. As disease progressed, virus titers in the blood increased to 10^7–10^8 $TCID_{50}$/mL (Figure 2.5.A). The viral titers obtained from blood samples were consistent with the viral DNA loads determined by qPCR (see Figure 2.4.A). No infectious virus was detected in the OP swabs until 7 DPC; only low levels (7.34×10^1 $TCID_{50}$/mL) were detected from 2/6 pigs (Figure 2.5.B). However, qPCR detected viral DNA at 5 DPC from 5/6 pigs.

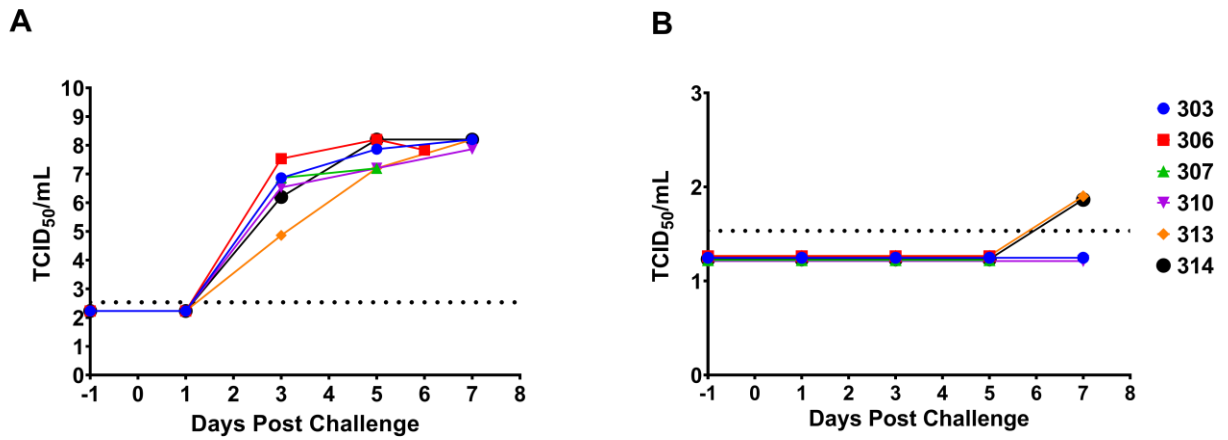

Figure 2.5. Viral titers in blood and OP swabs.

(A) The log transformed viral titers ($TCID_{50}$/mL) of ASFV-MNG19 in EDTA blood collected on −1, 1, 3, 5, and 7 DPC. All samples were run in triplicate. The datapoints represent the calculated titers using the Spearman–Karber method. The dashed line represents the limit of detection for the assay. Datapoints for individual pigs are represented. The single data point at 6 DPC represents samples collected from pig #306 that was found dead. (B) The log transformed viral titers ($TCID_{50}$/mL) of ASFV-MNG19 in OP swabs collected on −1, 1, 3, 5, and 7 DPC. All samples were run in triplicate. The datapoints represent the calculated titers using the Spearman–

Karber method. The dashed line represents the limit of detection for the assay. Datapoints for individual pigs are represented.

2.3.5. Gross Pathologic Lesions

All pigs found dead or euthanized due to ASF were necropsied to evaluate gross pathologic lesions as described in Supplementary Table S3. All pigs displayed loss in body condition with mild to moderate cutaneous hyperemia of the skin at the ear tips, ventral abdomen and distal limbs. Moderate to severe gross lesions consistent with acute ASF included splenomegaly, hemorrhagic lymph nodes, and pulmonary congestion and edema. Splenic congestion and necrosis were consistently observed (Figure 2.6.A). Lymph nodes were moderately enlarged with ranging severity of edema (mandibular and prescapular lymph nodes) or hemorrhages. Severe hemorrhagic lymphadenopathy was observed in the cranial mediastinal, renal, and gastrohepatic lymph nodes in 4/6 pigs (Figure 2.6.B). All pigs had moderate to moderate-to-severe pulmonary congestion and edema, and two of the pigs had multifocal pulmonary hemorrhage with consolidation (Figure 2.6.C). Mild-to-moderate renal corticomedullary congestion was noted in 4/6 pigs, renal cortical thrombosis was observed in 3/6 pigs. One pig had marked retroperitoneal effusion with a viscous serous fluid filling, expanding to the connective tissue of the caudal dorsal abdomen and surrounding the kidneys (Figure 2.6.D). Gross lesions observed for the cardiovascular system consisted of perivascular hemorrhages at venipuncture site for 2/6 pigs reflective of ASF induced coagulopathy. Thrombi were observed in the interventricular branch of the right coronary artery and the right ventricle of the heart of one pig, further supporting the ASF-associated coagulopathy. Moderate locally extensive hyperemia of the epicardium was observed in the auricles of the right and left atria in 3/6 pigs. Other ASF associated lesions observed were severe diffuse subarachnoid hemorrhagic

meningitis (5/6 pigs), moderate hyperemic gastritis (5/6), and mild to moderate hemorrhagic colitis (5/6). The average gross score for all six pigs was 41.33 ± 11.89 which is considered moderate acute ASF; detailed lesion scoring for each system are described in Supplementary Tables S7 and S8.

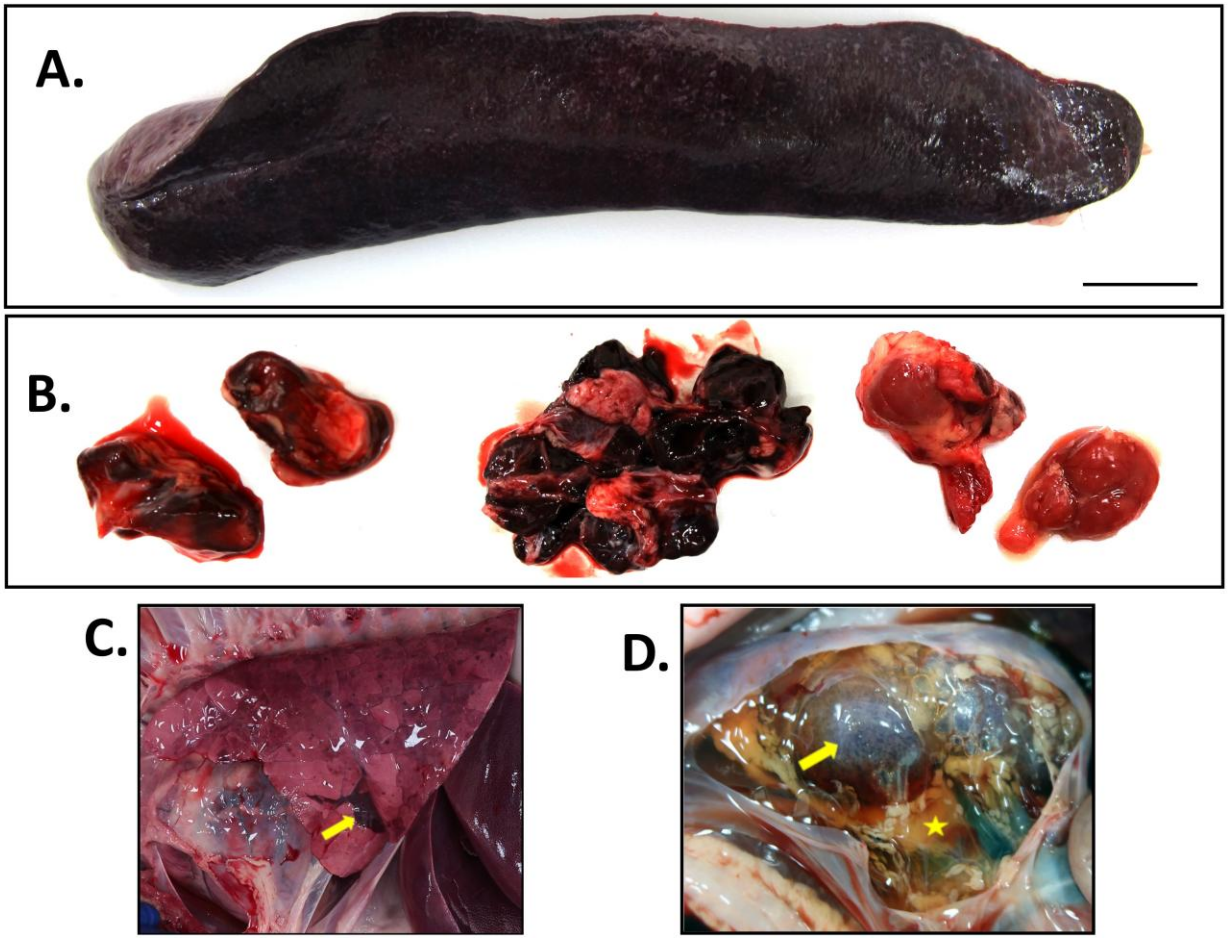

Figure 2.6. Gross pathology lesions following ASFV-MNG19 infection.

(A) Spleen: severe splenomegaly; (B) Lymph nodes: hemorrhage (from left to right: renal lymph node, gastrohepatic lymph node, and cranial mediastinal lymph node); (C) Lungs: pulmonary edema with congestion, consolidation (yellow arrow), and ecchymosis; (D) Kidney: retroperitoneal serous effusion indicated by the yellow star, petechial hemorrhages of renal cortex indicated by the yellow arrow.

2.3.6. Histopathological Lesions

Histological analysis was performed on liver, lung, kidney, spleen, and tonsil, as well as mesenteric, mandibular, renal, gastrohepatic, prescapular, ileocecal and inguinal lymph nodes. Figure 2.7 contains representative images of histopathological changes seen in the spleen (Figure 2.7.A), lymph node (Figure 2.7.B), lung (Figure 2.7.C), and kidney (Figure 2.7.D) from pigs infected with ASFV-MNG19. Changes in the spleen and lymph nodes consisted of marked lympholysis with collapse and loss of periarterial sheaths/follicles, accompanied by fibrin clots in the marginal zone of the spleen and sinuses of the lymph nodes. Fibrinoid degeneration and vasculitis is prominent in many lymph nodes and is frequently accompanied by subcapsular and sinusoidal hemorrhage (Figure 2.7.B). Within the lungs there was moderate to severe congestion of alveolar capillaries which commonly contained fibrin thrombi, cellular debris and large foamy macrophages. Edema, fibrin and macrophages commonly filled alveolar spaces and were occasionally accompanied by hemorrhage (Figure 2.7.C). Figure 2.7.D depicts renal lesions seen in two pigs with marked systemic intravascular coagulation. There were large fibrin thrombi filling interstitial capillaries, which were multifocal throughout the cortex resulting in coagulation necrosis and dystrophic mineralization of tubules. Fibrin thrombi occurred in glomeruli. Multifocal areas of hemorrhage occurred in the cortex and interstitium, frequently occurring around large vessels. Supplementary Table S4 contains the scoring of individual lymph nodes for all infected pigs and ranking of the lesions for each lymph node. Overall, two pigs in the group had severe lymphoid lesions, while three were classified with moderate lymphoid lesions and one with mild lymphoid lesions. The gastrohepatic and the renal lymph nodes were most severely affected followed by the ileocecal, mandibular and cranial mediastinal

lymph nodes, see Supplementary Table S4.

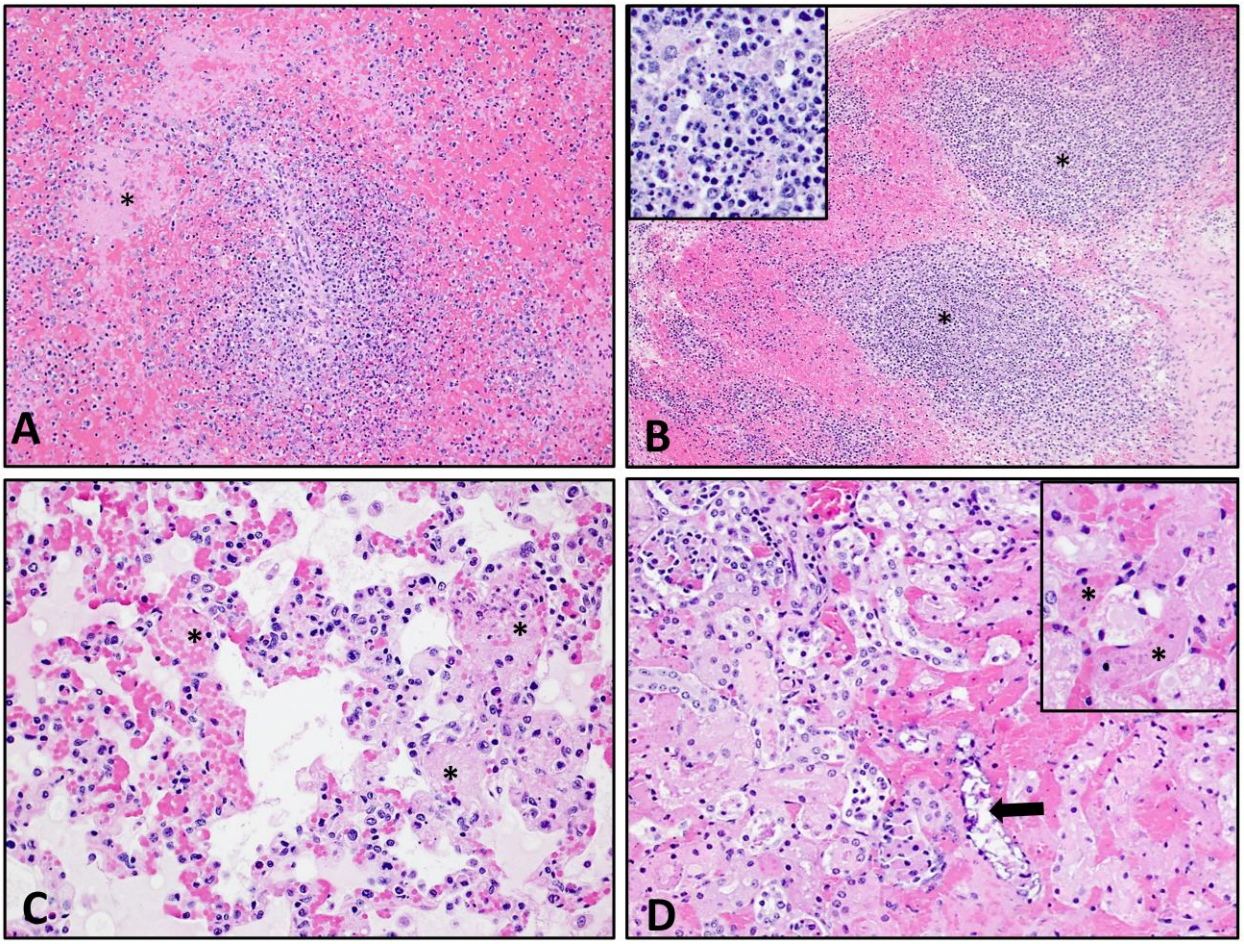

Figure 2.7. Histological lesions following ASFV-MNG19 infection.

(A) Spleen: Marked lympholysis and collapse of periarterial sheaths and fibrin thrombi (asterisk) in marginal zone (100×). (B) Renal lymph node: Marked lympholysis and necrosis (asterisk and insert) with loss of cortical and sinusoidal lymphocytes accompanied by marked filling and expansion of the subcapsular and medullary sinuses with hemorrhage and fibrin (100× and 400× insert). (C) Lung: Marked expansion of the alveolar spaces by congestion, fibrin thrombi (asterisk) and necrotic cellular debris, eosinophilic proteinaceous material; edema, fibrin and occasional macrophages fill the alveolar spaces (200×). (D) Kidney: Multifocal congestion and fibrin thrombosis (insert-asterisk) of the interstitial capillaries accompanied by hemorrhage and coagulative necrosis and dystrophic mineralization (arrow) of tubules (200×, 400×-insert).

2.4. Discussion

The results in this study show that the ASFV strain isolated from naturally infected pigs during the 2019 outbreak in Mongolia is a genotype II ASFV strain with high similarity to regional genotype II ASFV strains identified in 2018 and 2019 from China, Korea, and Russia. Following passage of ASFV-MNG19 on PAM cells several putative mutations were identified in the consensus sequence, which could not be reliably validated due to low coverage in these regions. A targeted whole-genome sequencing approach is required to determine if these mutations are adaptations arising from passage on primary cell lines or sequencing artifacts. The sequence of the ASFV-MNG19 strain was compared with the available partial sequences from an isolate collected in the Bulgan province of Mongolia during the 2019 outbreak and found to be identical to these partial sequences. Since only partial sequences are available for the Bulgan isolate, we cannot confidently determine that these two isolates are the same strain. Further studies are needed to infer the relationship between these two isolates and others, which include whole-genome sequencing of the Bulgan isolate and other isolates collected during the 2019 outbreak.

The intramuscular inoculation of pigs with a 360 HAD_{50} dose of ASFV-MNG19 resulted in rapid, fatal disease, with all animals dying or having to be euthanized due to severe clinical disease by 7 DPC. Clinical signs consisting of lethargy and pyrexia were observed by 3 DPC, which continued to progress, and by 5 DPC all animals developed high grade fevers (≥41 °C) with progressively worsening clinical signs. Viremia with virus titers of 10^6 $TCID_{50}$/mL by 3 DPC, which rose to 10^8 $TCID_{50}$/mL by 5 or 7 DPC, correlated with presentation of clinical signs. Two of the animals died suddenly on 5 and 6 DPC, respectively, within 2 days of developing

clinical signs. The ASFV-MNG19 strain efficiently replicates and disseminates systemically in domestic pigs, resulting in severe disease within days after clinical signs are noted. Gross lesions observed at necropsy were consistent with acute ASF such as splenomegaly, enlarged hemorrhagic lymph nodes, and pulmonary edema. Similar to what was seen with other Eurasian ASFV genotype II strains in domestic pigs, the most severely affected lymph nodes with gross and histological lesions were the gastrohepatic and the renal lymph nodes followed by the ileocecal, mandibular and cranial mediastinal lymph nodes (Guinat et al., 2014; Salguero, 2020). The clinical signs, gross lesions, and sudden death observed shortly after development of clinical symptoms were in line with what has been described for field infections with Mongolia isolates (Ankhanbaatar et al., 2021). Based on these findings we have found no evidence that the virulence of ASFV-MNG19 was altered following propagation on primary porcine cells.

As demonstrated previously with other ASFV strains, the ASFV-MNG19 strain most likely can be transmitted through oral secretions (Guinat et al., 2014; Lee et al., 2021; Ramirez-Medina et al., 2022; D. Zhao et al., 2019). In the current study, infectious virus was detected in the OP swabs of two pigs at 7 DPC. We were unable to determine if the animals continued to shed virus since all were euthanized at 7 DPC. The detection of infectious virus in OP swabs suggests the virus could be shed and potentially transmitted through oral secretions. However, one of the limitations of this study is the lack of naïve contact control pigs to study transmission.

The data from this study provides information on the genetics, virulence and virus–host infection dynamics of the genotype II ASFV-MNG19 field isolate. The present study confirms that the ASFV-MNG19 strain is a virulent genotype II virus that causes similar clinical disease presentation and progression as other historic and regionally circulating genotype II ASFV

isolates. Infection of pigs with the ASFV-MNG19 isolate resulted in rapid progression of clinical disease resulting in death from acute ASF. The incubation period of 3–5 days and clinical disease progression are similar to other genotype II strains, which include regional strains such as a 2018 Chinese isolate (D. Zhao et al., 2019) and a 2019 Vietnamese isolate (Lee et al., 2021) as well as the historic genotype II Georgia2007/1 (Guinat et al., 2014) and Armenia 2008 (Gabriel et al., 2011) isolates, which all cause acute ASF after IM inoculation.

The global ASF status has drastically changed over the past 15 years beginning with the 2007 outbreak in the country of Georgia allowing ASFV to spread across eastern Europe and Russia with outbreaks reported between 2008 and 2017 in domestic pig and wild boar populations (Bosch et al., 2017; Cwynar et al., 2019; Gogin et al., 2013; Sánchez-Vizcaíno et al., 2013, 2015). By 2018, ASFV had reached China causing a devastating outbreak that resulted in the loss of 1.2 million pigs and massive economic losses (K. Wu et al., 2020). Afterwards, ASFV continued to spread to neighboring countries and regions (H. J. Kim et al., 2020) as well as globally with outbreaks in India (Rajukumar et al., 2021) and Germany in 2020 (Sauter-Louis et al., 2021), and in the Dominican Republic in 2021 (Gonzales et al., 2021; Ramirez-Medina et al., 2022). Some of these outbreaks were resolved through strict mitigation strategies that included quarantine, restrictions on animal movement, and depopulation of affected herds and/or wild boar. All of these outbreaks are the result of infections with virulent genotype II ASFV strains (Ankhanbaatar et al., 2021; H. J. Kim et al., 2020; Lee et al., 2021; Ramirez-Medina et al., 2022). It is important that controlled experimental studies are conducted to evaluate the genetics, virulence and clinical progression of emerging ASFV strains described in the field, and to aid in

the development and validation of diagnostic tools used by regulatory agencies for the rapid detection and implementation of mitigation strategies.

Chapter 3 - Targeted Whole Genome Sequencing of African Swine Fever Virus and Classical Swine Fever Virus on the MinION Portable Sequencing Platform

3.0. Abstract

African swine fever virus (ASFV) and classical swine fever virus (CSFV) are important transboundary animal diseases (TADs) affecting swine. ASFV is a large DNA virus with a genome size of 170-190 kilobases (kB) belonging to the family *Asfarviridae*, genus *Asfivirus*. CSFV is a single-stranded RNA virus with genome size of approximately 12 kB belonging to the family *Flaviviridae*, genus *Pestivirus*. Outbreaks involving either one of these viruses result in significant economic impacts from death due to the disease or culling for control measures and imposed export restrictions of pork products in affected countries. Current detection methods during an outbreak provide minimal genetic information on the circulating virus strains/genotypes. Due to the increasing availability and reduced cost of next-generation sequencing (NGS), it is vital to have NGS protocols in place for the rapid identification and complete genetic characterization of such viruses for outbreak investigations and understanding viral evolution for the development of novel and effective control measures. In this study, panels of primers spanning the genomes of ASFV and CSFV were independently developed to generate approximately 10kB and 6kB amplicons, respectively. The primer panels consisted of 19 primer pairs for ASFV and 2 primer pairs for CSFV, therefore providing whole genome amplification of each pathogen; these primer pools were further optimized for batch pooling and thermocycling conditions. Following the optimization of primer pools, a total of 5 primer pools/reactions were

used for ASFV and 2 primer pairs/reactions for CSFV. The ASFV primer panel was tested on viral DNA extracted from blood collected from pigs experimentally infected with ASFV genotype I and genotype II viruses. The CSFV primer panel was tested on 11 different strains of CSFV representing the 3 known CSFV genotypes, as well as 21 samples collected from pigs experimentally infected with 2 different genotype 1 viruses. ASFV and CSFV amplicons from optimized PCR reactions were subsequently sequenced on the Oxford Nanopore MinION platform. The targeted protocols for these viruses resulted in an average coverage greater than 1000X for ASFV with 99% of the genome covered, and 10,000X-20,000X for CSFV with 97% to 99% of the genomes covered. The ASFV targeted whole genome sequencing protocol has been optimized for genotype II ASF viruses which have been involved in the most recent outbreaks. The CSFV targeted whole genome sequencing protocol has universal applications for the detection of all CSFV genotypes. These protocols will be important tools to assist in the early pathogen detection and genetic characterization of these high consequence swine viruses in outbreak and surveillance situations globally and within the United States, should an outbreak occur.

3.1. Introduction

Transboundary animal diseases (TADs) are of great concern to the global agricultural market. TADs can easily traverse national and international borders resulting in devasting economic impacts due to death from the disease or culling as part of mitigation strategies, and imposed trade restrictions. This study focuses on two TADs that have had significant impacts on the global pork industry. One of these TADs currently in the spotlight is African swine fever virus (ASFV) which is the causative agent of African swine fever a contagious viral disease of

domestic swine and wild boar (*Sus Scrofa*) that can cause high mortality in affected swine populations. ASFV belongs to the *Asfarviridae* family, genus *Asfivirus* (Galindo & Alonso, 2017; Gaudreault, Madden, et al., 2020). The virus particle of ASFV encapsulates a 170-192kB double stranded DNA genome encoding more than 150 genes (Dixon et al., 2013, 2019; Vilem et al., 2020b; X. Wang et al., 2022b). Historically, there were 24 genotypes of ASFV with varying virulence between and within genotypes; recent retrospective studies of ASFV sequences suggest that there are only 6 to 7 genotypes including the genotype I/II virus recombinant virus isolated in China (Spinard, Dinhobl, et al., 2023; D. Zhao et al., 2023b). Since the 2007 outbreak in Georgia, ASFV's global presence has expanded to Asia, Southeast Asia, India, the Caribbean, and several European countries (L. Wang et al., 2024). Another important TAD in this study is classical swine fever virus (CSFV) the causative agent of classical swine fever or historically termed "hog cholera"(H.-J. Thiel et al., 1991). CSFV belongs to the *Flaviviridae* family, genus *Pestivirus*; the enveloped virus particle contains a non-segmented single-stranded positive sense RNA genome of approximately 12 kB encoding 13 viral proteins (Blome, Staubach, et al., 2017; Chander et al., 2014). Currently there are three known genotypes with over 13 subgenotypes (Y. Liu et al., n.d.). CSFV was first described in the United States and has since been eradicated from the swine population. However, CSFV remains endemic in countries around the world. The risk of introduction and reintroduction into currently CSFV-free countries remains high. Until these two TADs are eradicated, they will continue to threaten the global pork industry. Currently, rapid detection and implementation of mitigations strategies is the most effective way of impeding global spread.

Currently, the WOAH recommends the use of qPCR or RT-qPCR for the detection of ASFV and CSFV, respectively (WOAH: Manual of Diagnostic Tests and Vaccines for Terrestrial Animals, 2023a, 2023b). These methods have high specificity and sensitivity with reduced time compared to the other molecular techniques such as ELISA and virus isolation. However, these techniques are unable to provide genotypic information circulating viral strain in an outbreak. Traditionally, this information is obtained by sequencing specific genes or regions that are conserved within genotypes. In the case of ASFV, genotyping is based on the partial sequencing of the C-terminal variable region of the B646L gene that encodes the major capsid protein, p72 (478 bp) (Bastos et al., 2003; Mulumba-Mfumu et al., 2017). ASFV strains are further characterized by sequencing of the envelope protein (p54), the central hypervariable region (CVR) of B602L (vial chaperone), and CD2v C-type lectin (C. Gallardo et al., 2009). Genotyping of CSFV is achieved by sequencing the 5'-NTRs, partial or full E2 gene, partial NS5B, or whole genome (Postel et al., 2012; WOAH: Manual of Diagnostic Tests and Vaccines for Terrestrial Animals, 2023b). Due to the size of the ASFV genome and cost of sequencing at the time the partial sequencing of these two agents was sufficient for genetically characterizing circulating or outbreak strains. However, these techniques provide limited genetic information which is beneficial for developing novel diagnostics and therapeutics. The limited genetic information has the potential for erroneous characterization of viral strains and limit researchers' ability to fully understand the viral evolution of these pathogens (Spinard, Dinhobl, et al., 2023). Recent studies by Forth *et al.* investigating the phylogenetic landscape of ASFV strains circulating Germany found that there are multiple variants that have diverged from the original outbreak strain (Forth et al., 2023).

The rapid advances in sequencing technologies have greatly reduced the costs and time needed to obtain whole genome sequences of these agents and other viral agents. The development of the Oxford Nanopore MinION a portable sequencing platform has drastically changed the landscape of sequencing. The MinION platform uses a pore-based sequencing technology that has eliminated read length restrictions observed with previous sequencing technologies. This advancement has allowed for the development of targeted long read amplicon-based sequencing protocols. The MinION platform is relatively inexpensive compared to the bench top sequencing platforms, increasing the availability of sequencing technology (Heather & Chain, 2016b).

In this study we aimed to develop targeted whole genome sequencing protocols using the MinION sequencing platform for the complete genetic characterization of ASFV and CSFV. The protocols are designed to rapidly obtain whole genome sequences of these two viral agents from samples within 36 to 48 hours. These protocols will aid in increasing the availability of whole genome sequences of ASFV and CSFV which will provide lacking genetic information to understand viral evolution and aid in the development of novel diagnostics and effective vaccines.

3.2 Material/Methods

3.2.1 Samples/Source of samples

All experiments involving African swine fever virus (ASFV) and classical swine fever virus (CSFV) were conducted in the BSL-3 laboratory at the Biosecurity Research Institute (BRI) at Kansas State University (KSU) in Manhattan, KS. The ASFV and CSFV samples used

in this study were collected from experimentally infected pigs at KSU-BRI and cell culture derived virus stocks, as detailed below.

3.2.2 Ethics Statement for Use of Animals

All animal studies and experiments were approved and performed under the KSU Institutional Biosafety Committee (IBC, Protocol #s:1314 and 1397) and the Institutional Animal Care and Use Committee (IACUC, Protocol #s: 4265, 5005) in compliance with the Animal Welfare Act. The research involving ASFV and CSFV was conducted in BSL-3 and ABSL-3Ag facilities in the Biosecurity Research Institute (BRI) at KSU in Manhattan, KS, USA.

3.2.3 Nucleic acid Extraction and Quantitative Real-time PCR

3.2.3.1 ASFV DNA Extraction and Quantitation

ASFV specific DNA was detected and quantified in EDTA blood and spleens from pigs experimentally infected with ASFV strains Armenia/2007, Mongolia/2019 (McDowell et al., 2022b), or E70 by quantitative real-time PCR (qPCR) assay as previously described (McDowell et al., 2022b; Sunwoo et al., 2019b). Viral DNA was extracted and purified with the MagMax Pathogen RNA/DNA kit (ThermoFisher Scientific, Waltham, MA, USA) using the Kingfisher™ Duo Prime purification system, an automated magnetic bead extraction system, following manufacturer's protocol with minor modifications. EDTA blood supernatant was mixed 1:1 with AL lysis buffer (Qiagen; Carlsbad, CA, USA) and heated at 70 °C for 10 min. Subsequently, 200 µL was mixed with 20 µL of bead mix (equal volume of nucleic acid binding beads and lysis enhancer). The mixture was gently mixed by pipetting and incubated for 2 min at room temperature. Phosphate-buffered saline (PBS, 100 µL) was added to the tube and the entire volume was added to the extraction plate well containing 400 µL lysis buffer, binding buffer and

isopropyl alcohol. DNA bound to beads was washed twice with 300 µL of wash solution 1, a third wash was completed with 450 µL wash solution 2, and a final wash with 450 µL of 200 proof molecular grade ethanol. The DNA bound beads were dried for 5 min prior to being eluted in 100 µL elution buffer. Negative (molecular grade water/PBS) and positive (ASFV p72 plasmid) controls were included with each extraction.

The ASFV DNA extracted from EDTA blood and spleens was detected and quantified using the primers and probe for the detection of the p72 ASFV gene as previously described by Zsak et al. (Zsak et al., 2005), using a validated protocol performed with the PerfeCTa® FastMix® II (Quanta Biosciences, Gaithersburg, MD, USA) on the CFX96 Touch™ Real-Time PCR Detection System (Bio-Rad, Hercules, CA, USA) as previously described (Sunwoo et al., 2019a). Duplicate qPCR reactions were performed. Each PCR run included negative and positive controls which consisted of nuclease-free molecular grade water and ASFV positive amplification control (p72 plasmid), respectively. Due to the analytical limits of the PCR assay, the Ct cutoff was set to 38 for both replicate wells as positive; samples with a single replicate well of 38 or less were classified as suspect. A sample was considered negative if both replicate wells were between 38–45 Ct. The copy number (CN) of ASFV DNA was calculated using a standard curve generated using ten-fold serial dilutions of quantified ASFV p72 plasmid DNA.

3.2.3.2 CSFV RNA Extraction and Quantitation

Specific CSFV RNA was detected and quantified from the serum and tonsils of pigs experimentally infected with either Brescia or Bavaro strains of CSFV and from cell culture supernatant of 11 CSFV viral stocks by quantitative real time reverse transcriptase PCR (RT-qPCR) described by *Eberling et. al* (Eberling et al., 2011). Viral RNA was extracted using the

GeneReach Taco extraction system (GeneReach Biotechnology Corp., Taichung, Tiawan). Cell culture supernatant or serum was mixed at 1:1 ratio with RLT lysis buffer. 200 µl of cell supernatant and RLT mixture were added to extraction plate well containing 50µl of magnetic, 500µl lysis buffer, binding buffer, 100µl phosphate buffered saline (PBS) and 200µl isopropyl alcohol. RNA bound to beads was washed twice with 750µl of wash buffer A, a third wash was completed with 750µl wash buffer B, and a final wash with 750µl of 200 proof molecular grade ethanol. The RNA bound beads were dried for 5 minutes prior to being eluted in 100µl elution buffer. Negative (molecular grade water/PBS) and CSFV positive extraction controls (provided by USDA-APHIS FADDL) controls were included with each extraction.

The CSFV RNA extracted from cell supernatant was detected and quantified using the primers and probe for detection of CSFV described by Eberling *et.al.* using a validated protocol performed with qScript XLT 1-step RT-qPCR ToughMix (Quanta Biosciences, Gaithersburg, MD, USA) on the CFX96 Touch^{TM} Real-Time PCR Detection System (Bio-Rad, Hercules, CA, USA). Briefly, the final reaction mixture consisted of 2.5 µl of viral RNA combined with 17.5 µl master mix including 0.2 µM forward primer, 0.4 µM reverse primer, and 0.2 µM probe. Thermocycling conditions were as follows 50ºC for 20 min, 95ºC for 5 min, followed by 45 cycles at 95ºC for 10 sec and 60ºC 1 min. Duplicate qPCR reactions were performed. Each PCR run included negative and positive controls which consisted of nuclease-free molecular grade water and CSFV positive amplification control (supplied by USDA-APHIS FADDL), respectively. Samples were positive for Ct values <40.

3.2.4 Primer Design

3.2.4.1 African Swine Fever Virus

A panel of 19 ASFV primer pairs (Table 3.1 and Figure 3.1) were designed based on the ASFV genotype II Georgia 2007 genome using Snapgene (GSL Biotech LLC, Boston, MA, USA) and CLC Genomic Workbench 23.0.1 (Qiagen; Carlsbad, CA, USA). The tiled primers were designed to generate approximately 10 kB amplicons with 150-200 base pair (bp) overlaps at the 3' and 5' ends. All primers were designed with similar melting temperatures allowing for the use of one set of thermocycling conditions for all 19 reactions and primer pooling applications.

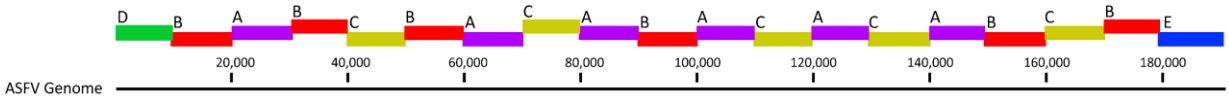

Figure 3.1. Genome map of the ASFV genome displaying nineteen 10kB amplicons.

The colored bars represent the 5 primer pools: A: purple, B: red, C: yellow, D: green, E: blue.

Table 3.1. ASFV primers and associated pools

Primer	Sequence	Primer Pool
ASFV-1-F	GCGTTCATTTCACAAGATGCG	D
ASFV-1-R	TGGGATTTGTACCAGCAGGG	D
ASFV-2-F	GGGCTTTGGGTCAGAACAGT	B
ASFV-2-R	ACAAGCTATACACGGCTCTCAG	B
ASFV-3-F	TGCATTCCGATATCTCATCATCTGT	A
ASFV-3-R	TACGGCGTTAGTGAAGGCTG	A
ASFV-4-F	CTTGGCACCTAGCTCTCGAC	B
ASFV-4-R	ACGATTTAGCACAACCATGCG	B
ASFV-5-F	GCCAATTCCTGAACCTGATGC	C
ASFV-5-R	AAACGTGTTGTCCCTCAGCA	C
ASFV-6-F	GAAACGACTGCACGAATGGG	B
ASFV-6-R	TGTCGTGCTTGTTTGGTACG	B
ASFV-7-F	TGAAACAATACCCCGGCCTC	A
ASFV-7-R	CATTGAACGCCCGCAACATC	A
ASFV-8-F	TTACCTCCTGCCGACCATTG	C
ASFV-8-R	TCCCTGTGTTTCTTGAGCGG	C
ASFV-9-F	AGACCAAACAGCAAAACGCA	A
ASFV-9-R	CAGTTGGTAGGGCTTGTGGT	A
ASFV-10-F	AGGATCCCTACAGCACGATG	B
ASFV-10-R	TTTTCCCGTCAAAGCAACCG	B
ASFV-11-F	GGGAAGCGGCACTGTACTAT	A
ASFV-11-R	AAGCAACTCAACCCGCAAAC	A
ASFV-12-F	GAAAGAAGGGTGTAGTCAAA	C
ASFV-12-R	ACACAAATGTCCAACTAGCTC	C
ASFV-13-F	GTCTCCTAGGGGCATAAGCG	A
ASFV-13-R	AGGCAGGGCTTAATGCAAGA	A
ASFV-14-F	GCGAGGAACAGAGCCCATAA	C
ASFV-14-R	AAAGCCTATTGACTGAACCCGT	C
ASFV-15-F	ATGAAAATACTCCCCGTGGCA	A
ASFV-15-R	GTATCAGCGGGGTAAGCAGT	A
ASFV-16-F	GCGAGCAAAGCTGAGATACG	B
ASFV-16-R	AACCTTTTCCGGGTACGTGA	B
ASFV-17-F	GCCGCTTTGCCTCATTTACG	C
ASFV-17-R	ACGTCCATCGTTCAAGGAGT	C
ASFV-18-F	ATTGCGTTGCGATCCAGTTC	B
ASFV-18-R	ACCCGAGAACGCTTCACAA	B
ASFV-19-F	AACAAGGGAACGATGGGAAG	E
ASFV-19-R	CTGCTGTAGGTGTCAAAGAT	E

3.2.4.2 Classical Swine Fever Virus

A panel of 2 CSFV primer pairs (Table 3.2) were designed using CLC genomics workbench 23.0.1 (Qiagen; Carlsbad, CA, USA) to generate approximately 6 kB fragments with a 380 bp overlap (Figure 3.2). The primer design module within the CLC genomic workbench 23.0.1 (Qiagen; Carlsbad, CA, USA) was used to identify candidate primers. The candidate primer sequences were compared to an alignment of multiple CSFV genome sequences to confirm binding sites were in conserved or low diversity regions within the CSFV genome. Degenerate nucleotides were added to primer sequences in regions of diversity for amplification of different CSFV genotypes. All primers were designed to have similar melting temperatures so thermocycling conditions were consistent for the 2 primer pairs.

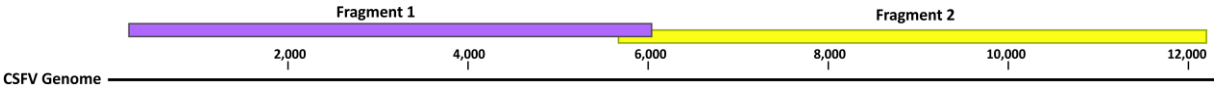

Figure 3.2. Genome map of CSFV genome displaying the two ~6 kB amplicons generated from the two primer pairs.

Table 3.2. CSFV Primers

Primer	Sequence
CSFV-1-F	AWGCCCAAGACRCACCTTAAYC
CSFV-1-R	GGTTGYGDCATCTGRCARAAGT
CSFV-2-F	ATAGGDGAGATGAAGGARGG
CSFV-2-R	TAGTGTGGTAACWYGAGGTAG

3.2.5 Whole Genome Amplification

3.2.5.1 African Swine Fever Virus

PCR reactions for all 19 primer pairs were tested individually for specificity and optimization of thermocycling condition using ASFV viral DNA isolated from experimentally infected pigs. Individual primer sets were tested in 20 µl PCR reactions consisted of 10 µl Platinum Superfi II Green PCR MasterMix (ThermoFisher Scientific, Waltham, MA, USA), 1 µl of primer pools (20 µM), 2 µl of viral DNA, and molecular grade water; with the following thermocycling conditions: 98^{o}C for 30 seconds, followed by 35 cycles at 98^{o}C for 10 seconds, 60^{o}C for 10 seconds, 68^{o}C for 5 minutes, followed by a final extension step of 72^{o}C for 5 minutes. Correct amplicon sizes were confirmed by gel electrophoresis. Once thermocycling conditions were optimized, 5 primer pools (A-E) were optimized to reduce the number of reactions needed for whole genome amplification (Figure 3.1), primer sequences and associated primer pools are available in Table 3.1. ASFV amplicons were generated using the 5 primer pools using the following 40 µl PCR reactions consisted of 20 µl Platinum Superfi II Green PCR MasterMix (ThermoFisher Scientific, Waltham, MA, USA), 4 µl of primer pools (20 µM), 4 µl of viral DNA, and molecular grade water; with the following thermocycling conditions: 98^{o}C for 30 seconds, followed by 35 cycles at 98^{o}C for 10 seconds, 60^{o}C for 10 seconds, 68^{o}C for 5 minutes, followed by a final extension step of 72C for 5 minutes. Amplicon pools were individually purified using Beckman Coulter AMPure XP beads (Beckman Coulter, Indianapolis, IN, USA) following the manufacturers protocol. Following the PCR clean-up with AMPure beads, the DNA concentration for each amplicon pool was quantified using the Invitrogen Qubit 4 Fluorometer (ThermoFisher Scientific, Waltham, MA, USA) with the broad range dsDNA

quantification kit. Amplicon pools A-E were combined into one tube at a 1:1:1:1:1 ratio. The final pool was used for sequencing library preparation.

3.2.5.2 Classical Swine Fever Virus

A two-step RT-PCR was used to amplify the two 6 kB amplicons. Firstly, viral cDNA was generated for each fragment individually using the LunaScript RT Master Mix kit (primer-free) (New England Biolabs, Ipswich, MA, USA) using a 20 µl reaction consisting of 4 µl of LunaScript RT Master mix, 1 µl of CSFV reverse primer (10 µM), 5 µl of viral RNA, and molecular grade water. The reaction was completed using the following thermocycling conditions: 55ºC for 10 minutes followed by 95ºC for 1 minute. Following cDNA synthesis 5 µl of viral cDNA was added to a 45 µl PCR master mix consisting of 25 µl of Q5 High-Fidelity 2X Master Mix (New England Biolabs, Ipswich, MA, USA), 5 µl of primer pools (10 µM), and molecular grade water. The reaction was completed using the following thermocycling conditions: 98ºC for 1 minute, followed by 35 cycles at 98ºC for 10 seconds, 60ºC for 30 seconds, 72C for 5 minutes, followed by a final extension step of 72ºC for 5 minutes and hold at 4ºC. Amplicon size was confirmed by gel electrophoresis. Amplicons were individually purified using Beckman Coulter AMPure XP beads (Beckman Coulter, Indianapolis, IN, USA) following the manufacturers protocol. Following the PCR clean-up with AMPure beads, the DNA concentration for each amplicon was quantified using the Invitrogen Qubit 4 Fluorometer (ThermoFisher Scientific, Waltham, MA, USA) with the broad range dsDNA quantification kit. Amplicons were combined into one tube at a 1:1 ratio. The final pool was used for sequencing library preparation.

3.2.6 Sequencing Library Preparation and MinION Sequencing

Sequencing libraries for both ASFV and CSFV were prepared using the Oxford Nanopore Rapid Barcoding Kit 96 (Oxford Nanopore Technologies, OX4 4DQ, UK) following manufacturer's protocol. For ASFV, sequencing libraries consisting of 6 barcoded samples were prepared. For CSFV, sequencing libraries consisting of up to 24 barcoded samples were prepared. Barcoded libraries were loaded onto the Oxford Nanopore MinION R9 flowcell (Oxford Nanopore Technologies, OX4 4DQ, UK) following manufacturer's protocol. The MinION was run for 16 hours with a read length inclusion of greater than 1 kB. Following completion of the run, base calling and demultiplexing was completed using the Oxford Nanopore MinKNOW software (Oxford Nanopore Technologies, OX4 4DQ, UK). Parsed reads were imported into CLC genomics workbench 23.0.1 (Qiagen; Carlsbad, CA, USA). Reads were mapped to their respective reference genomes for coverage graph generation and mapping statistics. In the case of CSFV with limited availability of whole genome sequences *de novo* assembly was completed and contigs were BLAST'd to determine most similar available CSFV genome. These genomes served as the reference for subsequent read mappings for coverage graph generation and calculating mapping statistics.

3.3 Results

3.3.1 ASFV AmpliSeq Results

Thermocycling conditions were optimized for all 19 individual ASFV primer pairs. The amplicons size was confirmed on gel electrophoresis with the presences of a single band at approximately 10kB, no partial or unspecific bands were observed. The 19 primer pairs were pooled into 5 primer pools in a manner to avoid overlapping segments, shown in Table 3.1 and Figure 3.1. Gel electrophoresis of the 5 primer pools show single amplicons at approximately

10kB, since all primer pairs amplify a 10kB fragment, a single band on the agarose gels was expected. The amplicon pools were sequenced on the MinION platform to confirm amplification and the presence of all amplicons. Figure 3.3 shows the coverage graphs of four samples sequenced using this protocol. These samples include a blood and spleen sample from a pig experimentally infected with ASFV Armenia/2007 and another pig experimentally infected with ASFV Mongolia/2019 isolate. All amplicons in the primer pools were successfully amplified and sequenced. Sequencing bias was observed for pools D and E, most likely because these pools generated a single amplicon, whereas pools A, B, and C amplified multiple amplicons.

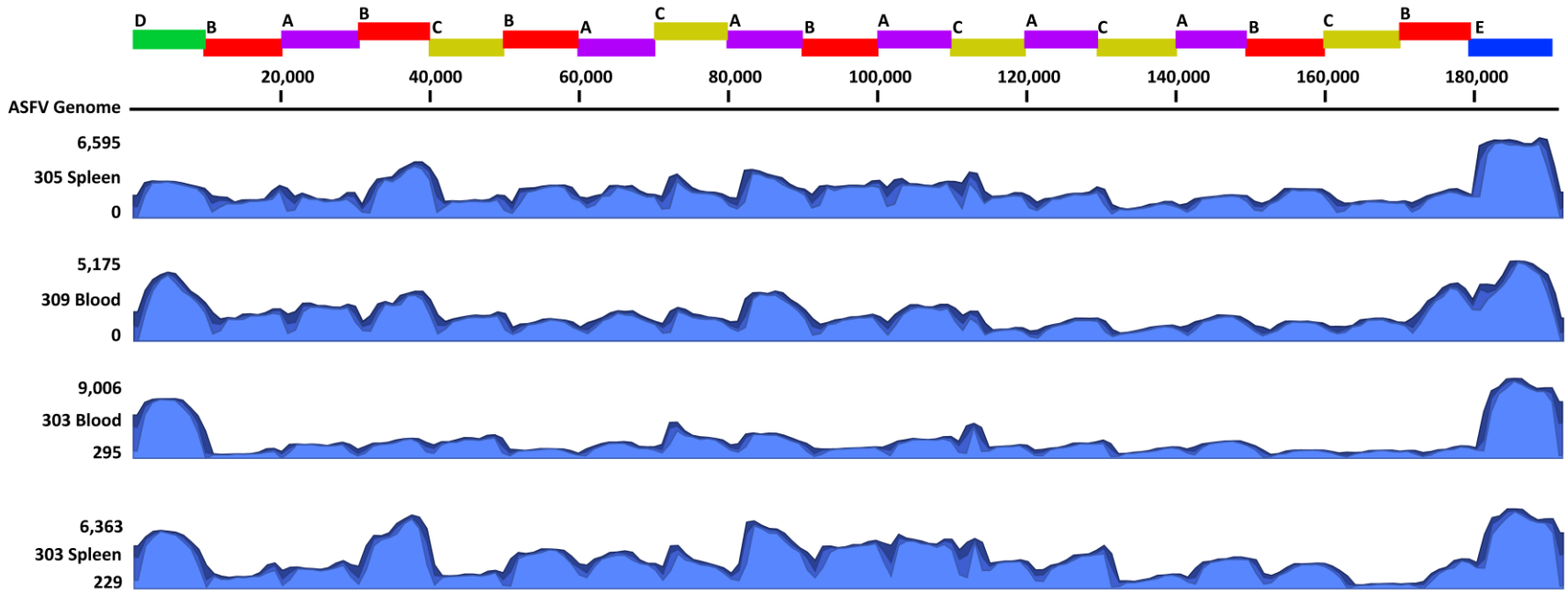

Figure 3.3. Coverage graphs of reads mapped to the ASFV genome.

The primer schematic is displayed on top indicating the 19 amplicons and the associated pools such as A-E. The graphs shown are a subset of samples tested using the ASFV AmpliSeq protocol. These samples include a blood and spleen sample from a pig experimentally infected with ASFV Armenia/2007 (#305 and #309) or ASFV Mongolia/2019 (#303).

The protocol was tested on 20 different ASFV samples; the samples included 19 clinical samples collected from pigs experimentally infected with ASFV genotype I E70 virus, ASFV genotype II Armenia/2007 and Mongolia/2019 viruses, and Armenia/2007 propagated in cell culture (Table 3.3). The selected ASFV samples had Ct values for the ASFV p72 gene ranging from 14-33; samples with a Ct of less than 25 were diluted 1:10 to prevent inhibition of the PCR reaction. Sequencing reads for genotype II samples were mapped to their respective ASFV genomes, Armenia/2007 or Mongolia/2019, Figure 3.3. Sequencing reads for the ASFV genotype I E70 sample were mapped to a similar genotype I virus E75. On average 220,00 sequencing reads were obtained following a 16-hour sequencing run with approximately 72% of the reads mapping the respective ASFV genomes, with read lengths averaging 2.5kB, Table 3.3. The average coverage of read mapping was greater than 1,000X, covering 99% of the ASFV genome except for samples from animals #304, 190, and 79. Animal #304 had a high Ct value which may have contributed to the drop in coverage. Furthermore, the sample DNAs may have been degraded from freeze thaws necessary to perform other assays. Overall, following the 16-hour MinION runs with 6 samples per run, an average read length of 2.5kB was obtained with 72% of reads mapping to the reference genome. For the genotype II viruses ASFV Armenia 2007 and Mongolia 2019, 99% of the reference genome was covered with an average coverage of 1,764X. For ASFV genotype I E70 strain, ~59,000 reads mapped 85% of the genome was covered with an average coverage of 1,081X; this would be sufficient for genotypic identification. The regions that were not amplified and sequenced ranged in size from 8,000-20,000 bp with the largest regions at the 3’ end which is a region that encodes numerous multiple gene families (MGFs). These regions may not have been amplified due to sequence differences

at the primer binding sites. There is sufficient coverage of the genome for genotypic characterization. The ASFV AmpliSeq is an excellent protocol for obtaining the near full-length genome of genotype II viruses with 99% coverage and ~1000X coverage. This protocol has an average error rate of 1.5% compared to a metagenomic approach with a 6.5% error rate when mapping reads to reference genome. This protocol will allow researchers to investigate the evolution of genotype II viruses which have resulted in the most recent ASFV global outbreaks. This protocol will provide sufficient genetic information for identifying recombinant ASFV viruses which have recently been characterized.

Table 3.3. Sequencing data for ASFV samples tested with ASFV AmpliSeq

Animal ID	DPC	Type	Strain	Genotype	Ct	Reference Length	Mapped Reads	Total Reads	% Reads Mapped	Average Coverage	% Reference Covered	Average Read Length
Arm07 Cos-1	P3	Cell culture	Arm07	II	27	190,584	51,134	65,081	78.57	1,017.61	0.99	3,749
63	7	Blood	Arm07	II	16	190,584	127,541	158,104	80.67	2,138.01	0.99	3,157
67	9	Blood	Arm07	II	19	190,584	149,958	184,043	81.48	2,323.76	0.99	2,928
87	7	Blood	E70	I	25	181,187	59,820	91,435	97.37	1,081.24	0.85	3,357
190	7	Blood	Arm07	II	15	190,584	60,571	80,273	75.46	864	0.99	2,681
192	7	Blood	Arm07	II	16	190,584	85,585	112,479	76.09	1,226.02	0.99	2,694
303	7	Blood	MNG-19	II	19	187,868	120,141	166,122	72.32	2,124.92	0.99	3,306
303	7	Spleen	MNG-19	II	19	187,868	155,498	207,421	74.97	2,511.41	0.99	3,020
304	7	Blood	Arm07	II	25	190,584	64,340	308,436	20.86	440.05	0.96	1,242
305	7	Blood	Arm07	II	21	190,584	136,574	173,381	78.77	2,193.54	0.99	3,035
306	6	Blood	MNG-19	II	22	187,868	423,361	575,567	73.56	2,313.04	0.99	1,019
307	3	Blood	MNG-19	II	22	187,868	264,992	390,731	67.82	1,465.03	0.99	1,029
308	7	Blood	Arm07	II	21	190,584	310,219	426,981	72.65	1,842.86	0.99	1,117
309	7	Blood	Arm07	II	19	190,584	96,240	123,894	77.68	1,726.88	0.99	3,378
310	7	Blood	MNG-19	II	19	187,868	66,069	88,936	74.29	1,079.36	0.99	3,047
311	7	Blood	Arm07	II	19	190,584	98,755	129,042	76.53	1,676.69	0.99	3,187
312	7	Blood	Arm07	II	20	190,584	131,299	173,421	75.71	2,299.50	0.99	3,297
314	7	Blood	MNG-19	II	22	187,868	307,810	421,638	73	1,714.75	0.99	1,037
511	7	Blood	Arm07	II	20	190,584	121,736	152,400	79.88	1,912.97	0.99	2,970
635	7	Blood	Arm07	II	14	190,584	165,992	215,116	77.16	2,654.20	0.99	3,022

DPC: Days post challenge; Arm07-Cos-1: ASFV Armenia 2007 passaged on Cos-1 cells; P3: Passage 3; Arm07: ASFV Armenia 2007; MNG-19: ASFV Mongolia 2019; E70: ASFV E70

3.3.2 CSFV AmpliSeq Results

Two primer sets were designed to amplify approximately 6 kB fragments of all known CSFV genotypes. The primers were tested against 5 CSFV strains isolated from cell culture which included genotype 1 (Brescia, Bavaro, Guatemala), genotype 2 (Germany 99), and genotype 3 (Congenital Tremor) viruses for optimizing thermal cycling conditions and suitability to amplify viruses representing the three known genotypes. Both primer sets amplified the correct size amplicons for all test strains which were confirmed by gel electrophoresis. Smaller amplicons were observed after RT-PCR for fragment 2, likely due to partial or non-specific amplification; these smaller amplicons were excluded during the sequencing run using appropriate built-in bioinformatics filters. The efficiency of amplification for genotype 3 viruses was reduced, as observed by reduced concentrations of fragment 2 following RT-PCR. Following sequencing of the amplicons derived using the two primer sets, the average coverage ranged from 10,770X -20,356X (Figure 3.4 and Table 3.4). The large spike in coverage observed in the coverage graphs is a result of the overlapping segment between the two primer pairs. We observed a significant reduction in coverage for fragment 2 of the Congenital Tremor strain with the depth of coverage reducing to 500-1,000 (Figure 3.4 and Table 3.4). We speculate that this could be related to primer mismatches and/or higher sample Ct value. The CSFV AmpliSeq was also tested on six additional CSFV cell derived virus stocks: Alfort, PAV250, Paderborn, Parma98, Germany-95, and Kanagawa (Table 3.4). For the 11 strains tested there was an average coverage of 12,278X with an average read length of 1.6kB covering 97%-99% of the genome (see Table 3.4). Like the Congenital Tremor strain, the other genotype 3 strain Kanagawa also had reduced amplification of fragment 2 with a reduction in coverage depth to

2,000. The reduced depth of coverage of fragment 2 for both genotype 3 strains could be related to primer mismatches and/or higher Ct values. Despite the reduction in depth of coverage for fragment 2; the depth is sufficient for obtaining the near full-length genomes of genotype 3 viruses.

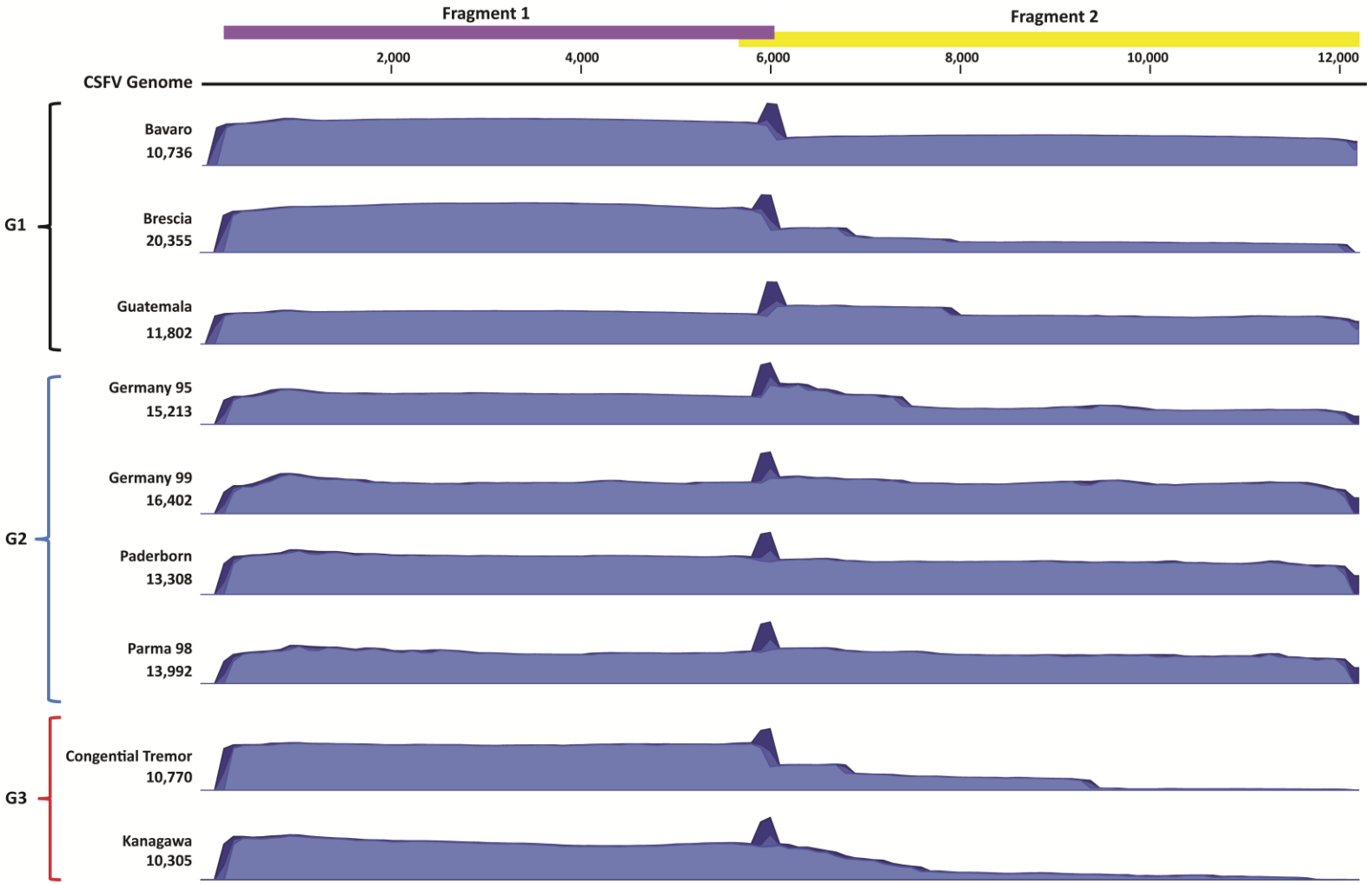

Figure 3.4. Coverage graphs of reads mapped to the CSFV genome.

The primer schematic is displayed on top indicating the 2 amplicons. The graphs shown are a subset of viral stocks tested using the CSFV AmpliSeq protocol. These samples represent the known genotypes of CSFV. Genotype 1 (G1): Bavaro, Brescia, Guatemala. Genotype 2 (G2): Germany 95, Germany 99, Paderborn, and Parma 98. Genotype 3 (G3): Congenital Tremor and Kanagawa.

Table 3.4. Sequencing data for 11 CSFV strains tested with CSFV AmpliSeq

Strain	Genotype	Ct	Reference Length	Mapped Reads	Total Reads	% Reads Mapped	Average Coverage	% Reference Covered	Average Read Length
Alfort	1.1	33	12,298	85,869	128,711	66.7	8,643.29	0.97	1,235
Brescia	1.2	17	12,283	147,575	191,259	77.2	20,355.95	0.98	1,683
Bavaro	1.3	23	11,955	61,093	80,719	75.7	10,736.37	0.99	2,112
PAV250	1.2	32	12,283	57,373	120,788	47.5	6,275.58	0.97	1,337
Guatemala	1.3	26	11,955	75,909	85,462	88.8	11,802.41	0.99	1,868
Paderborn	2.1	30	12,296	102,050	147,935	68.9	13,308.74	0.97	1,599
Parma 98	2.2	31	12,296	128,430	173,185	74.2	13,992.47	0.97	1,333
Germany 1995	2.3	32	12,296	112,426	151,928	73.9	15,213.59	0.97	1,659
Germany 1999	2.3	29	12,296	123,679	142,929	86.5	16,402.40	0.97	1,627
Congenital Tremor	3.1	32	12,298	75,708	103,765	72.9	10,770.79	0.97	1,750
Kanagawa	3.4	34	12,298	87,635	146,523	59.8	10,305.39	0.97	1,447

To evaluate the use of this protocol for field application, we tested the protocol on clinical samples collected from pigs experimentally infected with two different genotype 1 CSFV strains, Bavaro strain or Brescia strain (see Table 3.5). The Ct values for these samples ranged from 16 to 29. The clinical samples tested included serum collected on 5 and 7 DPC, tonsils collected at 11 DPC and one mandibular lymph node collected on 5 DPC. The average coverage for the clinical samples was 15,496X with an average read length of 1.7 kB covering 98%-99% of the genome. The coverage of the clinical samples was consistent with the cell culture derived virus stocks. The CSFV AmpliSeq protocol can be used to obtain the near full length CSFV genomes from clinical samples and cell derived virus stocks representing the three currently known genotypes. While a reduction of coverage of fragment 2 was observed for genotype 3 viruses and samples with Ct values greater than 30, the depth of coverage is sufficient for phylogenetic characterization.

Table 3.5. Sequencing data for clinical CSFV samples tested with CSFV AmpliSeq

Animal ID	DPC	Sample Type	Strain	Genotype	Ct	Reference Length	Mapped Reads	Total Reads	% Reads Mapped	Average Coverage	% Reference Covered	Average Read Length
169	5	Serum	Brescia	1.2	24.84	12,283	133,564	165,617	80.6	19,738.50	0.98	1,802
226	5	Serum	Brescia	1.2	23.63	12,283	121,651	148,444	81.9	19,799.28	0.98	1,984
226	5	Mandibular LN	Brescia	1.2	22.7	12,283	88,935	138,679	64.1	13,850.58	0.97	1,901
287	5	Serum	Brescia	1.2	20.89	12,283	109,336	142,280	76.8	17,646.33	0.98	1,970
348	5	Serum	Bavaro	1.3	28.83	11,955	98,559	106,690	92.4	15,503.91	0.99	1,888
353	5	Serum	Brescia	1.2	20.09	12,283	107,481	133,827	80.3	15,333.07	0.98	1,739
354	5	Serum	Brescia	1.2	21.26	12,283	112,049	143,418	78.1	15,997.95	0.98	1,742
358	5	Serum	Bavaro	1.3	27.3	11,955	184,126	203,348	90.5	30,853.70	0.99	2,007
374	5	Serum	Bavaro	1.3	29.15	11,955	88,296	106,370	83	11,465.05	0.99	1,563
3246	5	Serum	Bavaro	1.3	26.43	11,955	118,471	131,482	90.1	18,171.38	0.99	1,841
3248	5	Serum	Bavaro	1.3	29.36	11,955	89,295	100,880	88.5	10,791.20	0.99	1,445
169	7	Serum	Brescia	1.2	16.1	12,283	75,350	94,675	79.6	10,040.89	0.98	1,625
287	7	Serum	Brescia	1.2	16.9	12,283	132,993	167,506	79.4	17,255.71	0.98	1,582
348	7	Serum	Bavaro	1.3	25.5	11,955	92,379	104,221	88.6	12,824.24	0.99	1,664
358	7	Serum	Bavaro	1.3	26.1	11,955	88,799	103,837	85.5	13,585.76	0.99	1,833
374	7	Serum	Bavaro	1.3	27.03	11,955	57,973	66,023	87.8	7,522.64	0.99	1,553
3246	7	Serum	Bavaro	1.3	19.98	11,955	108,501	117,808	92.1	16,394.22	0.99	1,809
3248	7	Serum	Bavaro	1.3	29.25	11,955	100,504	110,978	90.6	13,020.98	0.99	1,548
169	11	Tonsil	Brescia	1.2	17	12,283	147,575	191,259	77.2	20,355.95	0.98	1,683
348	11	Tonsil	Bavaro	1.3	23	11,955	61,093	80,719	75.7	10,736.37	0.99	2,112
3246	11	Tonsil	Bavaro	1.3	25	11,955	88,948	103,779	85.8	14,534.34	0.99	1,955

DPC: Days post challenge, LN: Lymph Node

3.4 Discussion

Historically, ASFV and CSFV were genetically characterized and phylogenetically grouped based on partial genetic sequences due to limited sequencing capabilities. For ASFV, the community relied heavily on the partial sequencing of the major capsid protein (p72) for genotyping (Bastos et al., 2003; Mulumba-Mfumu et al., 2017). Sequencing of p54, variable region of B602L, and CD2v and C-type lectin (C. Gallardo et al., 2009; Malogolovkin et al., 2015) combined with p72 allows for further discrimination of ASFV strains. These methods provide vital information for identification and outbreak investigations but only provide minimal genetic information on this large viral genome. Recent advances in sequencing technologies allowed researchers to obtain full genome sequences of ASFV through direct sequencing approaches (Spinard, O'Donnell, et al., 2023). This is a resource expensive method resulting in low coverage of the genome and sequencing of host genome. Due to the large genome of ASFV amplicon-based sequencing has been difficult due to the need of numerous PCR reactions. The protocol developed in this study uses an amplicon-based targeted sequencing method. We reduced the number of reactions needed to amplify the ASFV genome by generating long amplicons of approximately 10kB, these reactions were further reduced by generating primer pools allowing for the amplification of multiple 10kB amplicons in one reaction. The resulting protocol allows for whole genome amplification of ASFV in 5 reactions in 4 to 4.5 hours. Amplicon pools were sequenced with the Oxford Nanopore MinION platform. With this protocol, we can obtain full length genotype II ASFV genomes in 36-48 hours with average coverages of 1,000X at approximately $70 per sample. Along with the increased depths of coverage, this protocol provides an average error rate of 1.5% compared to 6.5% error rate with a metagenomic approach for mapping reads to a reference genome. The protocol was tested on

genotype I virus with approximately 85% of the genome covered. This protocol will allow researchers and investigators to assemble near full-length genome sequences of this large DNA virus to study viral evolution and perform detailed phylogenetic inference.

Genetic characterization and phylogenetic analysis of CSFV historically relied on partial sequencing of the E2 gene, 5'-NTR, or NS5 gene (Postel et al., 2012; WOAH: Manual of Diagnostic Tests and Vaccines for Terrestrial Animals, 2023b). However, with advances in sequencing technology and continuing reduction in cost for sequencing the WOAH recommends full length sequencing of the E2 gene or whole genome sequencing. Protocols are available for amplification of full-length E2 gene and whole CSFV genome that can be applied for sequencing (Leifer et al., 2010; Nguyen et al., 2021). The protocol described by Leifer *et al.* for amplification of the whole CSFV genome requires multiple RT-PCR due to the average amplicon size being ~1kB. The protocol described in this study generates two ~6kB amplicons which serve to amplify the whole CSFV genome in two RT-PCR reactions. The pooled amplicons were sequenced on the Oxford Nanopore MinION platform. With this protocol, we obtained the near full-length genomes of viruses representing three currently known CSFV genotypes isolated from cell culture with average coverage greater than 10,000X in 36-48 hours at cost of approximately $30 per sample. The protocol was tested on clinical samples from pigs experimentally infected with two different genotype 1 viruses. This protocol will reduce the cost and amount of sample required to obtain the whole genome sequences of CSFV, allowing for more in depth understanding of the genetic evolution of CSFV while providing the necessary genetic information required for phylogenetic characterization of CSFV.

3.5 Conclusions

The targeted whole genome sequencing protocols described in this study will provide vital tools for diagnostics and research of these two high consequence swine pathogens that have far reaching impacts in both the global economy and food supply. These protocols will enable researchers to rapidly obtain the near full-length genome of ASFV and CSFV, providing more complete genetic information for phylogenetic analysis and viral evolution studies of these pathogens. Further development is needed for obtaining the complete genomes of all ASFV genotypes, but we show that this can detect the genotypes have emerged and continue to spread outside of Africa. While this study focuses on utilizing the MinION sequencing platform, these protocols would also be compatible with other sequencing platforms such as PacBio and Illumina. The reduced cost and timeframe of these protocols will be important tools to assist in early pathogen detection and genetic characterization of these high consequence swine viruses in outbreak and surveillance situations globally and within the United States, should an outbreak occur.

Chapter 4 - Assessment of SARS-CoV-2 Strain Competition in Co-Infected Adult White-tailed Deer by Targeted Whole Genome Sequencing[2]

4.0. Abstract

The zoonotic *betacoronavirus* SARS-CoV-2 has spread rapidly around the world resulting in a global public health crisis. Early in the pandemic, the genetic lineage A of SARS-CoV-2 dominated. However, as the virus continues to circulate, variants of concern (VOCs), characterized by increased fitness and transmissibility, have emerged. The lineage B alpha VOC, (B.1.1.7 or UK variant) emerged in the fall of 2020, and rapidly became a dominant variant. Additional beta, gamma, and delta VOCs emerged in mid to late 2020 in South Africa, Brazil, and India, respectively. A thorough understanding of potential wildlife reservoirs is needed for developing effective control strategies for SARS-CoV-2. White-tailed deer (*Odocoileus virginianus)* fawns have been shown to be susceptible to SARS-CoV-2. To investigate the role of an emerging VOC in this host, we conducted a competition experiment whereby adult white-tailed deer (WTD) were co-infected with lineage A (USA-WA1/2020) and lineage B alpha variant (B.1.1.7-like; USA/CA_CDC_5545/2020) SARS-CoV-2 isolates. Nasal swabs and respiratory tissues from adult WTD, which were co-infected intranasally and orally, were evaluated using next generation sequencing (NGS) and BLAST-based analysis, and the percentages of the individual lineage A and B viruses were determined at multiple time points

[2] This chapter contains data that has been previously published. Reprinted with permission from Cool, K., McDowell, C.D.; et al. Infection and transmission of ancestral SARS-CoV-2 and its alpha variant in pregnant white-tailed deer. *Emerging Microbes & Infections*, *11*(1), 95–112. https://doi.org/10.1080/22221751.2021.2012528. Copyright 2021 by Chester D. McDowell.

post-infection. To confirm NGS results, lineage A and B-specific RT-qPCR assays were developed targeting a non-conserved region within the spike gene. The SARS-CoV-2 lineage B alpha variant had improved fitness compared to the lineage A virus in adult WTD, with the lineage A strain only recovered at early time points in small quantities. Here we demonstrated that the strain specific RT-qPCR assays are capable of differentiating both SARS-CoV-2 lineages. The RT-qPCR assays could potentially be used in epidemiological surveillance for VOCs in human and animal populations.

4.1. Introduction

In 2019 a novel zoonotic *betacoronarvirus* emerged, SARS-CoV-2, resulting in one of the largest global pandemics. SARS-CoV-2 virus belongs to the family *Coronaviridae* which includes four genera *Alpha-, Beta-, Delta-,* and *Gamma-coronaviruses* (Cool et al., 2022). These viruses are enveloped, single-stranded, positive-sense RNA viruses with genomes of 27-32kB (De Wit et al., 2016). As SARS-CoV-2 continued to circulate, variants of concern (VOCs), characterized by increased fitness and transmissibility, emerged and continue to emerge (Choi & Smith, 2021; Zhou et al., 2021). The lineage B alpha variant, B.1.1.7, emerged in the United Kingdom in late 2020 and rapidly out competed the ancestral lineage A strain. Additional VOCs have emerged which include beta (B.1.351), gamma (P.1), delta (B.1.617.2), omicron (B.1.1.529), and others (Flores-Vega et al., 2022; Tao et al., 2021). As SARS-CoV-2 continues to evolve it is important to identify susceptible species that can serve as potential secondary reservoirs that could give rise to novel variants of concern and reverse-zoonosis events.

Since 2023, the World Organization of Animal Health (WOAH) has reported natural infections of SARS-CoV-2 in 29 species in 36 countries (World Organization for Animal Health, 2023). Experimental infections of SARS-CoV-2 have demonstrated that 7 species are highly

susceptible which include cats, ferrets, Syrian golden hamsters, non-human primates, and others (Y. Il Kim et al., 2020; Meekins et al., 2021; J. Shi et al., 2020). A thorough understanding of potential wildlife reservoirs of SARS-CoV-2 is needed for developing effective control strategies. White-tailed deer are the most abundant wild ruminant species in the continental United States. Surveillance studies have shown that 33-40% of free-ranging white-tailed deer (*Odocoileus virginianus*) across the midwestern United States had detectable levels of SARS-CoV-2 RNA or neutralizing antibodies (Chandler et al., 2021; Hale et al., 2022; Kuchipudi et al., 2022). Publications have described the susceptibility of white-tailed deer through experimental infections (Cool et al., 2022; Palmer et al., 2021). Identification and surveillance of animal populations which could act as secondary reservoirs for SARS-CoV-2 is critical for identifying novel variants of concern as well as potential avenues for reverse-zoonosis events.

To investigate the role of an emerging VOC in this host, we conducted a competition experiment whereby adult white-tailed deer (WTD) were co-infected with lineage A (USA-WA1/2020) and lineage B alpha variant (B.1.1.7-like; USA/CA_CDC_5545/2020) SARS-CoV-2 isolates (Cool et al., 2022). The percent composition of lineage A and lineage B viruses in nasal/oropharyngeal swabs and respiratory tissues were assessed at multiple points post-infection via BLAST-based next-generation sequencing (NGS) analysis. The NGS results were confirmed by strain specific RT-qPCRs. The lineage B alpha variant rapidly outcompeted lineage A virus in co-infected adult WTDs. The results showed that the SARS-CoV-2 lineage B alpha variant had improved fitness compared to the lineage A virus in adult WTD.

4.2. Material Methods

4.2.1. Samples Tested

Viral RNA was extracted from viral stocks of lineage A (USA-WA1/2020) and lineage B alpha variant of concern (B.1.1.7-like; USA/CA_CDC_5545/2020) propagated in cell culture. Clinical samples were collected from experimentally infected adult WTDs that were co-infected with lineage A (USA-WA1/2020) and lineage B alpha variant (B.1.1.7-like; USA/CA_CDC_5545/2020) SARS-CoV-2 isolates. Viral RNA was extracted from nasal swabs, collected at 1-, 3-, 5-, and 7-days post challenge (DPC), and respiratory tissues collected at 4 DPC. Viral RNA was extracted following the method described by Cool *et. al* (Cool et al., 2022).

4.2.2. Next-Generation Sequencing[3]

RNA extracted from cell culture supernatant (virus stocks), clinical swab/tissue homogenates, and clinical samples were sequenced by next generation sequencing (NGS) using an Illumina NextSeq platform (Illumina Inc.; San Diego, CA, USA) to determine the genetic composition (% lineage) of viral RNA in each sample. SARS-CoV-2 viral RNA was amplified using the ARTIC-V3 RT-PCR protocol [Josh Quick 2020. nCoV-2019 sequencing protocol v2 (GunIt). Protocols.io https://gx.doi.org/10.17504/protocols.io.bdp7i5rn] (Quick, 2020). Library preparation of amplified SARS-CoV-2 DNA for sequencing was performed using a Nextera XT library prep kit (Illumina Inc.; San Diego, CA, USA) following the manufacturer's protocol. The libraries were sequenced on the Illumina NextSeq using 150 bp paired end reads with a mid-output kit. Reads were demultiplexed and parsed into individual sample files that were imported into CLC Workbench version 7.5 (Qiagen; Carlsbad, CA, USA) for analysis. Reads were

[3] Reprinted with permission from Cool, K., McDowell, C.D.; et al. Infection and transmission of ancestral SARS-CoV-2 and its alpha variant in pregnant white-tailed deer. *Emerging Microbes & Infections*, *11*(1), 95–112. https://doi.org/10.1080/22221751.2021.2012528. Copyright 2021 by Chester D. McDowell.

trimmed to remove ambiguous nucleotides at the 5’ terminus and filtered to remove short and low-quality reads. The consensus sequences of viral stocks used for challenge material preparation were found to be homologous to the original strains obtained from BEI GISAID accession numbers: EPI_ISL_404895 (WA-CDC-WA1/2020) and EPI_ISL_751801 (CA_CDC_5574/2020). To determine an accurate relative percentage of each SARS-CoV-2 lineage in each sample, BLAST databases were first generated from individual trimmed and filtered sample reads. Subsequently, two 40-nucleotide (nt) long sequences were generated for each strain at locations that include the following gene mutations: Spike (S) A570D, S D614G, S H1118H, S ΔH69V70, S N501Y, S P681H, S 982A, S T716I, S ΔY145, Membrane (M) V70, Nucleocapsid protein (N) D3L, N R203KG204R, N 235F, and non-structural NS3 T223I, NS8 Q27stop, NS8 R52I, NS8 Y73C, NSP3 A890D, NSP3 I1412T, NSP3 T183I, NSP6 ΔS106G107F108, NSP12 P323L, NSP13 A454V and NSP13 K460R. A word size of 40 was used for the BLAST analysis to exclude reads where the target mutation fell at the end of a read or reads that partially covered the target sequence. The two sequences for each of the locations listed above, corresponding to either lineage A (USA-WA1/2020) or alpha VOC B.1.1.7 (USA/CA_CDC_5574/2020), were subjected to BLAST mapping analysis against individual sample read databases to determine the relative amount of each strain in the samples. The relative amount of each strain present was determined by calculating the percent of reads that hit each of the twenty-three target mutations. The percentages for all mutations were averaged to determine the relative amount of each strain in the sample.

4.2.3. Strain Specific RT-qPCR for Strain Differentiation

Strain specific primers and probes were designed to target a region in the spike gene (152-256 nt). The targeted region contains a 6-nucleotide deletion present in the lineage B alpha

VOC (USA/CA_CDC_5574/2020) resulting in the deletion of two amino acids (H69 and V70), otherwise present in lineage A (USA-WA1/2020). Lineage A (USA-WA1/2020) RNA was detected and quantified by a Taqman probe with a FAM fluorophore, figure 4.1 (bottom). Lineage B (USA/CA_CDC_5574/2020) RNA was detected and quantified by a locked nucleic acid (LNA) probe, that spanned the deletion site, with a Cy5 fluorophore, figure 4.1 (top). The locked nucleic acid probe was used to increase the specificity of the probe to the target strain and binding site.

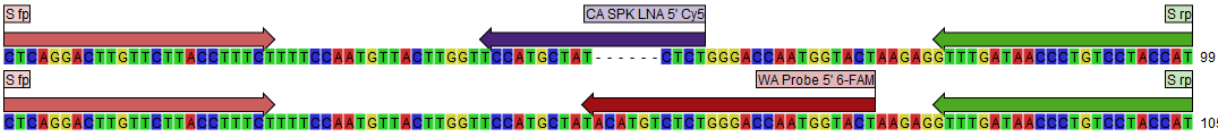

Figure 4.1. Strain specific RT-qPCR primer and probe schematic.

The sequence on the top illustrates the sequence and position of the LNA probe (purple arrow) for detection of lineage B strain. The 6-nucleotide deletion is position within the probe. The bottom sequence illustrates the sequence and position of the Taqman probe (dark red arrow) for detection of lineage A strain. Both RT-qPCRs use the same forward (light red arrow) and reverse (green arrow) primers.

Individual RT-qPCR reactions were setup for each strain using the following mixture: 2X qScript XLT One-Step RT-qPCR ToughMix (Quanta Biosciences, Galthersburg, MD), primers (400nM), lineage specific probes (200nM), 2.5 µl viral RNA, and nuclease-free water up to 20 µl. The Bio-Rad CFX was used to carry out the RT-qPCR reactions. Following optimization, strain specific viral RNA (10^6 copies/µl) was ten-fold serially diluted and used to generate standard curves for copy number determination, figure 4.2 panel A and B. The copy number of viral RNA for each strain was calculated using the line of best fit for viral RNA standard curves for WA1 (y=-1.401ln(x) + 43.371), figure 4.2 panel C, and B.1.1.7 (y=-1.498ln(x) + 44.717), figure 4.2 panel D.

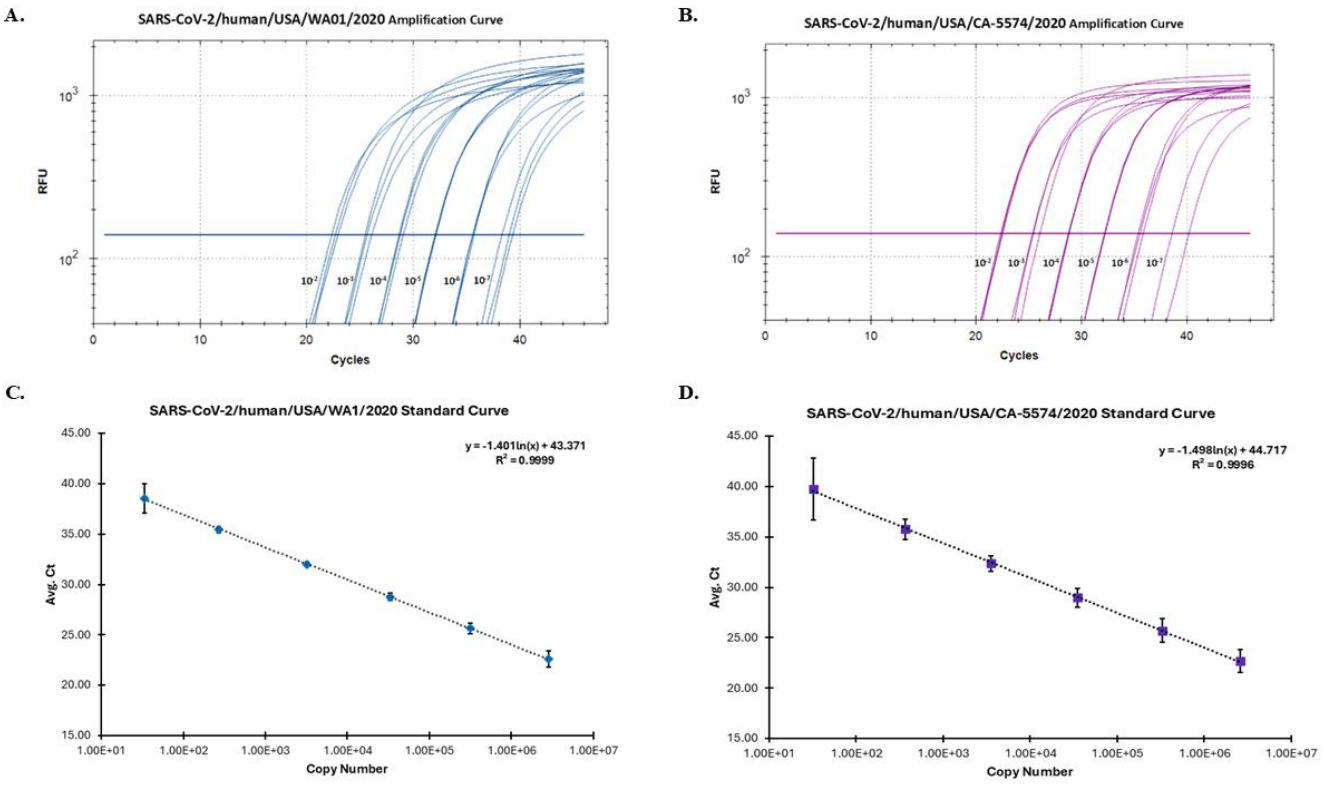

Figure 4.2. SARS-CoV-2 strain specific spike RT-qPCR.

A) RT-qPCR amplification curves of lineage A strain (WA1; SARS-CoV-2/human/USA/WA01/2020) RNA serial dilutions. The assay has a limit of detection of 10-100 RNA copies/µl. B) RT-qPCR amplification curves of lineage B alpha VOC (B.1.1.7; SARS-CoV-2/human/USA/CA-5574/2020) RNA serial dilution. The assay has a limit of detection 10-100 RNA copies/ µl. C) Standard curve of Ancestral Strain (WA1; SARS-CoV-2/human/USA/WA01/2020) RNA used for calculating viral RNA copy number. D) Standard curve of alpha VOC (B.1.1.7; SARS-CoV-2/human/USA/CA-5574/2020) RNA used for calculating viral RNA copy number.

Following standard curve generation, viral RNA from lineage A (USA-WA1/2020) and lineage B (B.1.1.7; USA/CA_CDC_5574/2020) were combined to generate known viral RNA populations. The series of known viral RNA populations were generated by maintaining lineage B RNA at a constant concentration while lineage A was diluted by 2- and 10-folds, figure 4.3. The predicted strain composition was calculated using the best fit lines from the standard curves, table 4.1. The strain specific RT-qPCR reactions were performed on each mixture with four

replicates. The actual percent strain composition was calculated using the best fit lines for the respective strains.

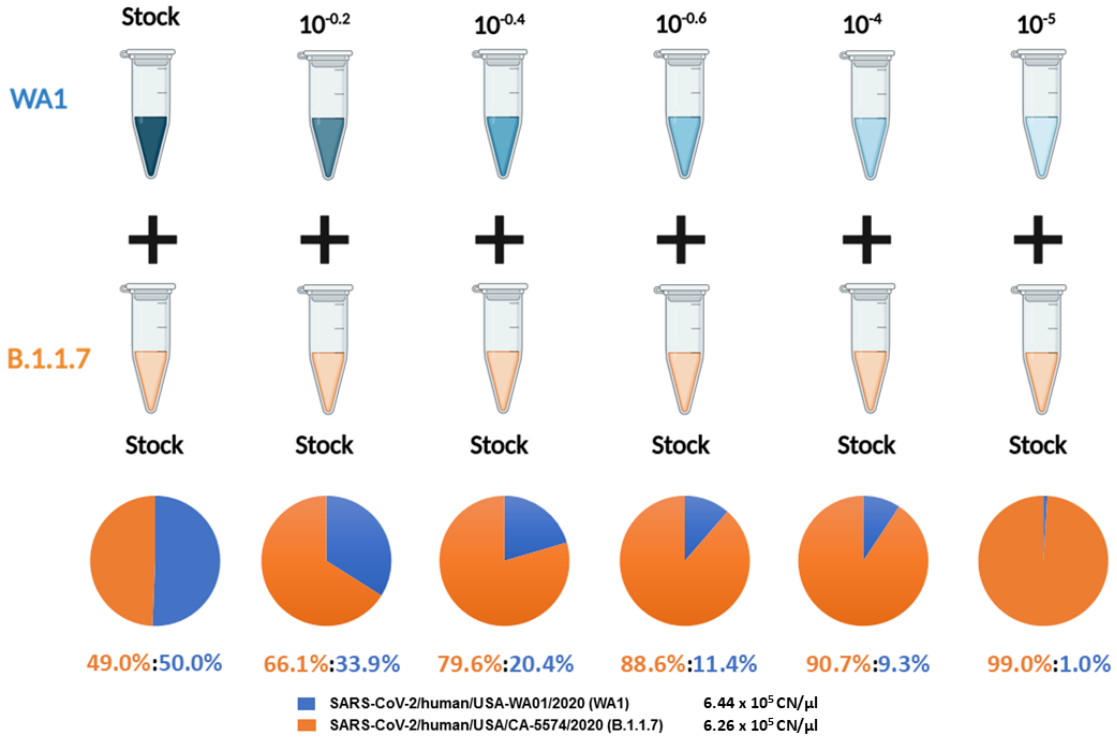

Figure 4.3. Schematic for the generation of known viral RNA populations.

Lineage A (WA1) was diluted 2- and 10-fold and combined with lineage B (B.1.1.7) that was held at a constant concentration. The pie charts show the predicted percent composition of each strain.

4.3 Results

4.3.1. SARS-CoV-2 Strain Competition Analysis by Sequencing

The *in vivo* competition of a SARS-CoV-2 lineage A and lineage B (alpha VOC) strain was assessed by sequencing SARS-CoV-2 cDNA that was amplified from viral RNA extracted from the inoculum used for experimental challenge, nasal swabs, and respiratory tissue homogenates collected from experimentally infected adult white-tailed deer (WTD). The inoculum used for the experimental infection of WTD consisted of an intended 1:1 mixture of

the two strains. The sequencing analysis of the inoculum demonstrated a 60.4% lineage B alpha VOC and 39.6% lineage a WA1 (Cool et al., 2022). The strain composition of the nasal swabs collected at 1 DPC showed a 0.7-40% lineage A and 60-99.3% lineage B detected by sequencing in the principally infected animals, figure 4.4. By 3 DPC, only the lineage B strain was detected in nasal swabs, rapidly out competing the lineage A strain, figure 4.4. The lineage A strain was not detected in nasal swabs after 3 DPC. Lineage B sequences were detected in one sentinel animal at 7 DPC suggesting that the lineage B virus was transmissible between animals. The strain composition of the respiratory tissues collected at 4 DPC from two principally infected WTDs was also evaluated by sequencing. These tissues included the nasal conchae, proximal trachea, and right cranial lung lobe (R. Cr. Lung Lobe). All respiratory tissues from both animals had a 100% lineage B with no detectable lineage A sequences, figure 4.5. The sequencing analysis to assess strain competition suggests that the lineage B virus out competed lineage A as well as to transmitting to sentinel animals. To confirm these results, we developed and optimized a strain specific RT-qPCR.

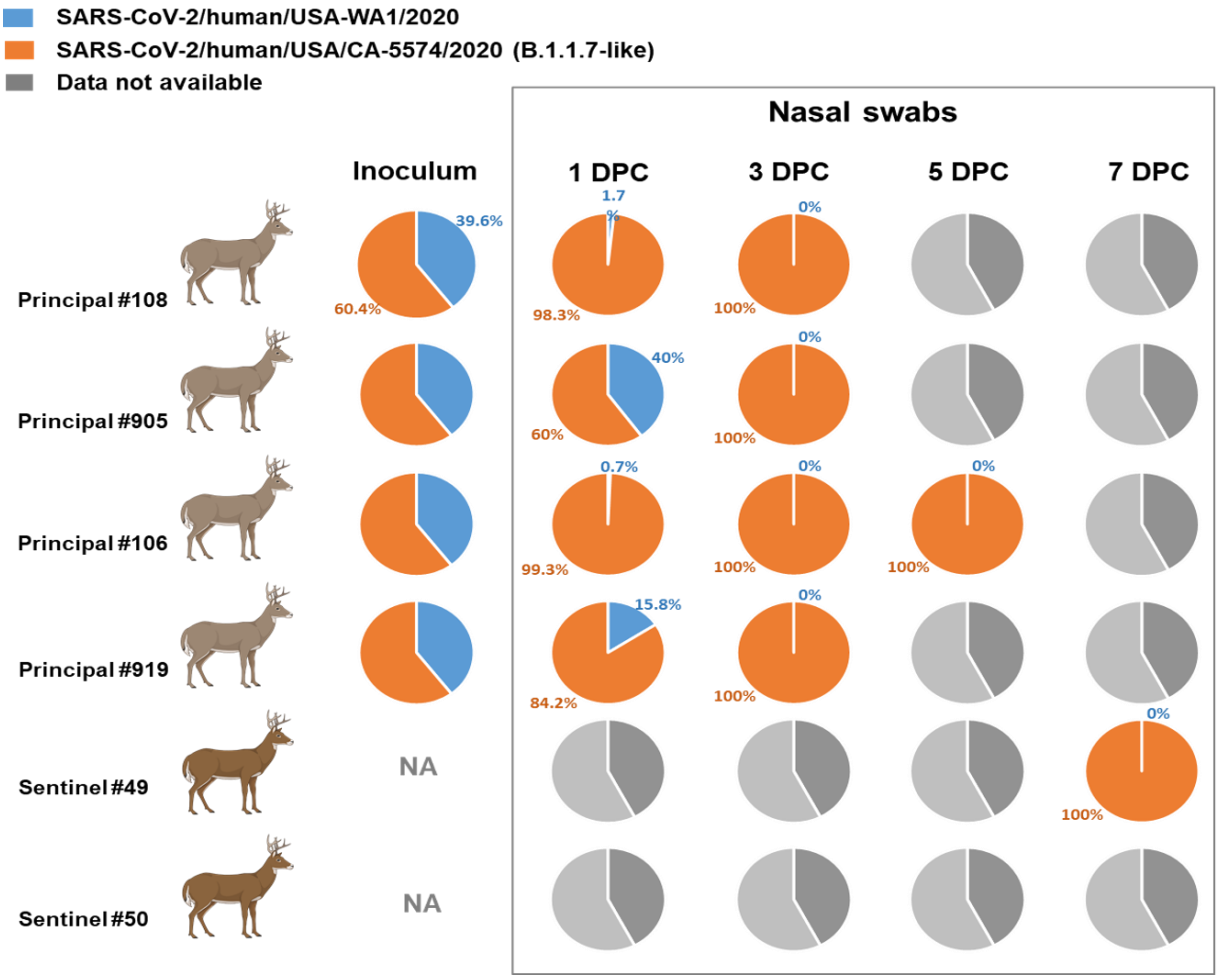

Figure 4.4. NGS results of nasal swabs collected from adult WTD co-infected with SARS-CoV-2 ancestral strain (WA1) and alpha VOC (B.1.1.7).

The gray pie charts represent samples that did not have detectable SARS-CoV-2 RNA for sequencing, or the sample was unavailable.

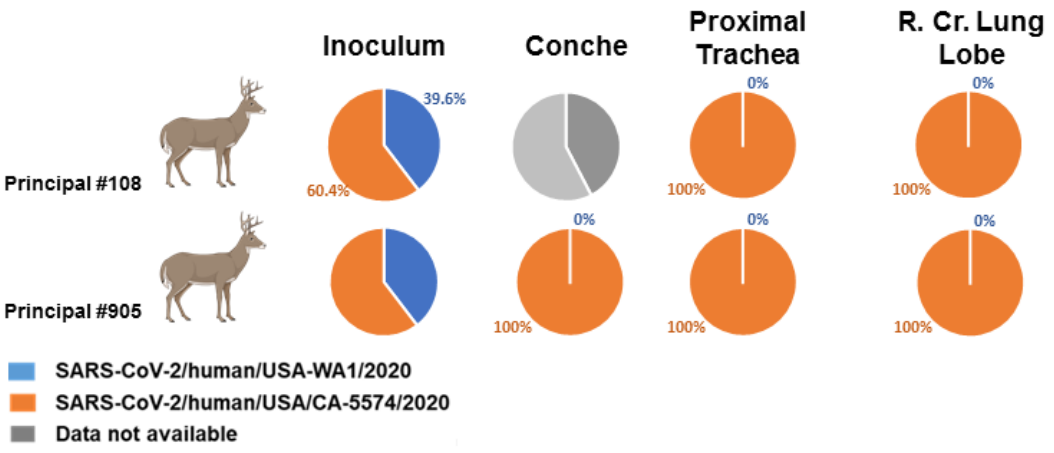

Figure 4.5. NGS of respiratory tissues collected at 4 DPC from WTD co-infected with SARS-CoV-2 ancestral strain (WA1) and alpha VOC (B.1.1.7).

4.3.2. Strain Specific RT-qPCR

To confirm the strain composition results of the inoculum, nasal swabs, and respiratory tissues determined by our sequencing analysis, two strain specific RT-qPCRs were developed and optimized to detect and quantify lineage A and lineage B viral RNA. Standard curves were generated to determine the sensitivity and for determination of viral RNA copy number of each assay shown in figure 4.2. The limit of detection for both the lineage A and lineage B RT-qPCR assays was 10-100 RNA copies/µL. There was no cross reactivity between the assays. The results show these assays are both sensitive and specific for their respective viral strains, demonstrating the feasibility for lineage differentiation.

Following optimization, a series of known viral RNA populations were screened to assess the ability of the RT-qPCRs to differentiate between lineages. These viral RNA populations consisted of a mixture of lineage A (WA1) and Lineage B alpha VOC (B.1.1.7) at known percentages based on viral RNA copy number, figure 4.3. The RT-qPCRs assays demonstrated

the capability to detect and quantify strain specific viral RNA in a mixed population, figure 4.6. There was 5-6% difference between the predicted and actual composition of the known mixtures, which may be attributed to mixing and dilution errors. Despite these differences, these RT-qPCRs were able to differentiate and quantify the respective strain specific viral RNA.

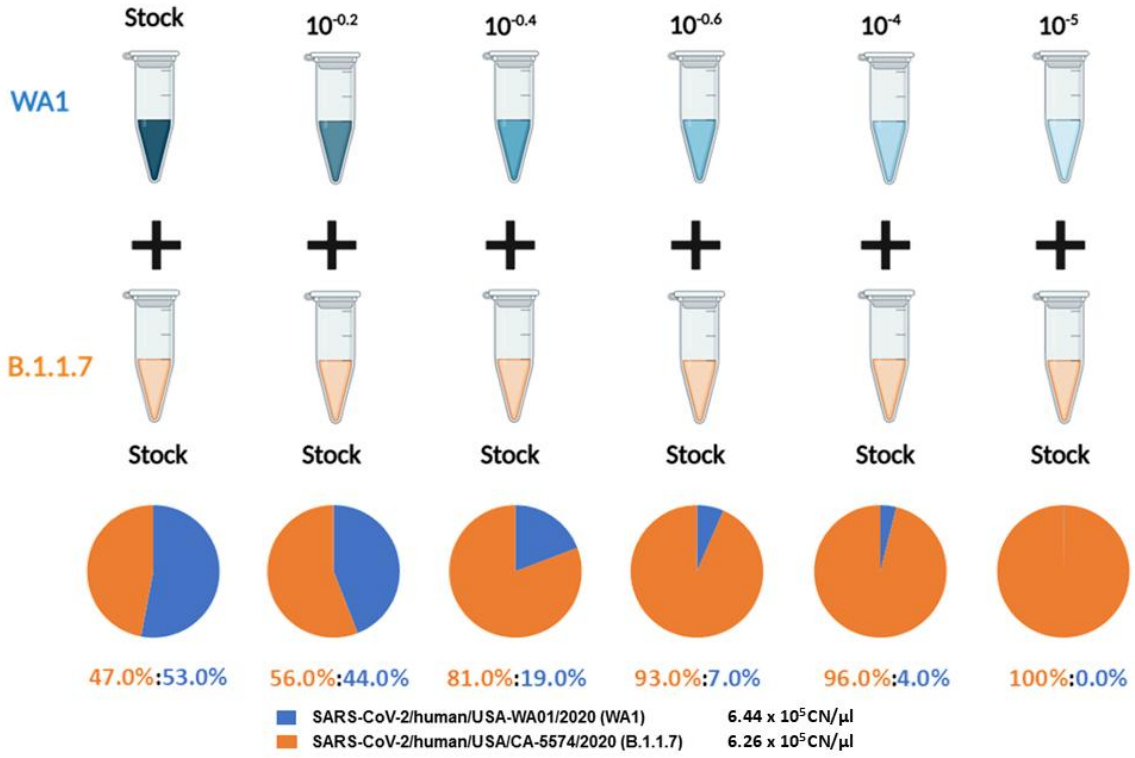

Figure 4.6. Quantification of WA1 and B.1.1.7 within a known viral RNA population.

B.1.1.7 was held at a constant concentration while the concentration of WA1 was diluted 2-fold and 10-fold to represent a distribution of strain compositions.

4.3.3. Strain Specific RT-qPCR for Clinical Samples

The strain composition of inoculum, clinical samples (nasal swabs and respiratory tissues) determined by sequencing were confirmed using the strain specific RT-qPCRs. The RT-qPCR of inoculum demonstrated a strain composition of 60% lineage B (B.1.1.7) and 40% lineage A (WA1), a difference of less than 1.0% from the sequencing results. The strain composition of clinical samples (nasal swabs and respiratory tissues) evaluated by RT-qPCR

versus NGS were within a 7% range, table 4.2 and 4.3. These results further validate the strain composition results obtained through our NGS analysis.

Table 4.1. Strain composition of clinical swabs analyzed by RT-qPCR.

	Nasal Swabs							
	1 DPC		3 DPC		5 DPC		7 DPC	
Animal ID	**%WA1**	**%B.1.1.7**	**%WA1**	**%B.1.1.7**	**%WA1**	**%B.1.1.7**	**%WA1**	**%B.1.1.7**
Principal #108	**0.0%**	**100.0%**	**0.0%**	**100.0%**	NS	NS	NS	NS
Principal #905	**33.0%**	**67.0%**	**0.0%**	**100.0%**	NS	NS	NS	NS
Principal #106	**0.0%**	**100.0%**	**0.0%**	**100.0%**	**0.0%**	**100.0%**	ND	ND
Principal #919	ND	ND	**0.0%**	**100.0%**	ND	ND	ND	ND
Sentinel #49	ND	ND	NT	NT	ND	ND	**0.0%**	**100.0%**
Sentinel #50	ND	ND	NT	NT	ND	ND	ND	ND
ND = not detected; NT = not tested; NS = no sample								

Table 4.2. Strain composition of respiratory tissue analyzed by RT-qPCR.

	4 DPC			
	#108		#905	
Sample	**%WA1**	**%B.1.1.7**	**%WA1**	**%B.1.1.7**
Conchae	**0.0%**	**100.0%**	ND	ND
Proximal Trachea	**0.0%**	**100.0%**	**0.0%**	**100.0%**
R. Cr. Lung Lobe	**0.0%**	**100.0%**	**0.0%**	**100.0%**
ND = not detected				

4.4 Discussion

Since the emergence of SARS-CoV-2 in 2019 variants of concern (VOC) have emerged and continue to emerge as the virus continues to evolve and adapt. In this study while investigating the susceptibility of WTDs to SARS-CoV-2, we also evaluated the *in vivo* competition between an ancestral isolate (WA1) and an alpha VOC isolate (B.1.1.7). The alpha VOC was the first variant that emerged during the global pandemic, rapidly becoming the

dominate circulating strain of SARS-CoV-2 in the human population (Choi & Smith, 2021). To assess the competition between these two SARS-CoV-2 strains we evaluated the strain composition present in clinical samples collected from experimentally co-infected adult WTD by NGS analysis and strain specific RT-qPCRs.

The NGS analysis demonstrated that the alpha VOC rapidly outcompeted ancestral strain of SARS-CoV-2 in clinical swabs and respiratory tissues collected from co-infected WTD. Following challenge, the alpha VOC became the dominate strain by 3 DPC and the only strain to be detected in tissues at 4 DPC. Strain specific RT-qPCRs were used to evaluate the strain composition as a means to confirm sequencing results. The strain compositions from RT-qPCR were within 7% range of the NGS analysis. Both sequencing and RT-qPCR strain composition analysis of clinical samples suggest that the lineage B alpha VOC isolate has a competitive advantage over the ancestral lineage A isolate in co-infected adult WTD. This competitive advantage was reported *in vivo* in ferrets, hamsters, and transgenic hACE2 mice models (Cool et al., 2022; Y. J. Hou et al., n.d.; Zhou et al., 2021).

The strain specific RT-qPCR assays that were developed in this study are sensitive and specific demonstrating the feasibility of these assays to differentiate between lineages in clinical samples. These assays were able to detect and quantify strain specific viral RNA in known viral populations. The RT-qPCR assays described in this study were employed to confirm the composition of strain specific viral RNA determined by NGS analysis. These assays also have potential applications in epidemiological surveillance for VOCs in human and animal populations. However, as SARS-CoV-2 continues to evolve, novel variants will continue to emerge, which will require constant redesign and validation of variant specific RT-qPCR assays. To overcome this hurdle the combination of targeted whole genome sequencing protocols and

bioinformatic programs, such as VirStrain (Liao et al., 2022), will provide a means to quickly evaluate viral strain compositions within a mixed population. During the global pandemic next-generation sequencing has played and will continue to play a crucial role in the surveillance and identification of emerging VOCs.

Chapter 5 - Concluding Remarks

The advances in sequencing technologies have increased the availability and feasibility for implementation into numerous scientific fields such as molecular diagnostics of infectious diseases and virology to name a few. Sequencing and bioinformatics have and will continue to play crucial roles in the studies of infectious diseases. Metagenomic sequencing allows for the detection and discovery of novel pathogens. Targeted sequencing allows researchers to obtain the sequences of a known viral pathogen for phylogenetic analysis and single nucleotide polymorphisms (SNPs) analysis. Targeted sequencing methodologies have been used for decades prior to for genotyping viral pathogens such as African Swine Fever virus (ASFV) and classical swine fever virus (CSFV) (Bastos et al., 2003; Mulumba-Mfumu et al., 2017; Postel et al., 2012). However, due to the limitations in sequencing technologies at the time of their induction in the field of diagnostics or genome size (i.e., ASFV), these methods were limited to targeting conserved regions and genes of these pathogens. These methods provided a means to genotype these pathogens and provide minimal phylogenetic information. Further phylogenetic inference is made by sequencing multiple regions, which can be used in tracing the origin of ASFV outbreaks.

The advances in sequencing and molecular biology technology have allowed for the amplification and sequencing of longer amplicons enabling the development of targeted whole genome sequencing protocols for larger viral genomes. These protocols provide a more complete set of phylogenetic information in turn increasing the accuracy of phylogenetic characterization. For example, during the SARS-CoV-2 pandemic, targeted whole genome sequencing protocols were used extensively serving to identify emerging variants and a temporal view of viral evolution as it continued to circulate (Lv et al., 2024; Markov et al., 2023; Olivero

et al., 2022). It is critical that whole genome sequencing protocols are available for characterizing and studying emerging and high consequence viral pathogens such as SARS-CoV-2, ASFV and CSFV. The recent identification of a genotype I/II recombinant strain of ASFV is another example of how this technology and these protocols are essential (D. Zhao et al., 2023a). These targeted whole genome protocols enable researchers to rapidly obtain the complete genetic characterization of ASFV and CSFV, providing more information on the viral evolution of these pathogens.

Since, the 2018 outbreak of ASFV in China rapidly spread to neighboring and regional countries. In 2019, Mongolia reported the first outbreak of ASFV, field reports described clinical signs, disease progression, and postmortems lesions consistent with acute ASF caused by a virulent strain and identified as a genotype II virus. In order to have a clear understanding of clinical disease and progression, pigs were experimental infected with the Mongolian strain (ASFV-MNG19). This study confirmed that the ASFV-MNG19 strain is a virulent genotype II virus that causes similar clinical disease presentation and progression as other historic and regionally circulating genotype II ASFV isolates. Infection of pigs with the ASFV-MNG19 isolate resulted in rapid progression of clinical disease resulting in death from acute ASF. The incubation period of 3–5 days and clinical disease progression are similar to other genotype II strains, which include regional strains such as a 2018 Chinese isolate (D. Zhao et al., 2019) and a 2019 Vietnamese isolate (Lee et al., 2021) as well as the historic genotype II Georgia2007/1 (Guinat et al., 2014) and Armenia 2008 (Gabriel et al., 2011) isolates, which all cause acute ASF after IM inoculation (McDowell et al., 2022a). Controlled experimental studies like this one, are important to evaluate the genetics, virulence and clinical progression of emerging viruses and different variants/strains described in the field, and to aid in the development and validation of

diagnostic tools used by regulatory agencies for the rapid detection and implementation of mitigation strategies.

By utilizing cell-derived viral stocks and clinical samples collected from swine experimentally infected with ASFV and CSFV, we developed a targeted whole genome protocol for each virus. For ASFV, we used a tiled targeted whole genome approach comparable to the ARTIC and Midnight protocols for SARS-CoV-2 (Freed et al., 2021; Quick, 2020). The protocol consists of 5 primer pools amplifying multiple 10kB amplicons in one reaction. It allows for whole genome amplification of ASFV in 4 to 4.5 hours. Combined with the long-read sequencing technology of Oxford Nanopore MinION platform, we can obtain full length genotype II ASFV genomes in 36-48 hours with average coverages of 1,000X at approximately $70 per sample. The protocol was tested on genotype I virus with approximately 85% of the genome covered. For CSFV, the protocol generates two ~6kB amplicons amplifying the whole CSFV genome with two RT-PCR reactions. The amplicons were sequenced on the Oxford Nanopore MinION platform. With this protocol, we obtained the near full-length genomes of virus strains representing the three currently known CSFV genotypes isolated from cell culture with average coverage greater than 10,000X in 36-48 hours at cost of approximately $30 per sample. While these protocols focused on the MinION sequencing platform, these protocols would also be compatible with other sequencing platforms such as PacBio and Illumina. Further, studies are needed to validate these protocols on other sequencing platforms. The reduced cost and timeframe of these protocols will be important tools to assist in early pathogen detection and genetic characterization of these high consequence swine viruses in outbreak and surveillance situations globally and within the United States, should an outbreak occur.

Targeted whole genome sequencing protocols such as ones developed in this study and others (i.e., SARS-CoV-2) can be utilized to evaluate SNVs and competition between viral strains during co-infection. In the study described in chapter 4, the ARTIC targeted whole genome sequencing protocol of SARS-CoV-2 was used to evaluate the strain composition of adult white-tailed deer that were co-infected with the ancestral lineage A strain (WA01-like) and lineage B alpha VOC (B.1.1.7-like). The strain composition was assessed using a BLAST-based analysis on the sequencing data obtained from nasal swabs and respiratory tissues. The NGS analysis demonstrated that the alpha VOC rapidly outcompeted the ancestral strain becoming the dominate strain identified in nasal swabs by 3 DPC and 4 DPC in respiratory tissue. Strain specific RT-qPCR assays were developed to confirm the sequencing results. The sequencing and RT-qPCR results of the strain composition were within 7% of one another. The results from both the sequencing and RT-qPCR strain composition analysis of clinical samples suggest that the lineage B alpha VOC isolate has a competitive advantage over the ancestral lineage A isolate in co-infected adult WTD. This study demonstrates that NGS data and bioinformatic pipelines can be used to evaluate strain composition in the presence of a co-infection. The targeted whole genome sequencing protocols developed for ASFV and CSFV could be applied to similar co-infection studies or evaluate viral quasispecies populations and SNV arising during infection, providing more information on the evolution of these high consequence pathogens.

The potential applications of the targeted whole genome protocols for ASFV and CSFV have yet to be explored. Future studies testing these protocols on field samples collected for surveillance and during outbreaks will be important to demonstrate real world application while obtaining full genome sequences of circulating ASFV and CSFV strains. For the ASFV protocol, further development is needed to provide a universal whole genome sequencing

protocol for all ASFV genotypes. Another direction could be to evaluate quasispecies population and SNVs that arise during infection. These protocols could serve to evaluate strain composition and/or potential recombination events in co-infection studies. The development of targeted whole genome sequencing protocols for these two high consequence swine pathogens provides researchers with a means to rapidly obtain the whole genomes of these two pathogens as well as the ability to study their viral evolution at the genetic level.

References

Aebischer, A., Müller, M., & Hofmann, M. A. (2013). Two newly developed Erns-based ELISAs allow the differentiation of Classical Swine Fever virus-infected from marker-vaccinated animals and the discrimination of pestivirus antibodies. *Veterinary Microbiology*, *161*(3), 274–285. https://doi.org/https://doi.org/10.1016/j.vetmic.2012.07.046

Agüero, M., Fernández, J., Romero, L., C, S. M., Arias, M., & Sánchez-Vizcaíno, J. M. (2003). Highly Sensitive PCR Assay for Routine Diagnosis of African Swine Fever Virus in Clinical Samples. *Journal of Clinical Microbiology*, *41*(9), 4431–4434. https://doi.org/10.1128/jcm.41.9.4431-4434.2003

Altschul, S. F., Gish, W., Miller, W., Myers, E. W., & Lipman, D. J. (1990). Basic local alignment search tool. *Journal of Molecular Biology*, *215*(3), 403–410. https://doi.org/https://doi.org/10.1016/S0022-2836(05)80360-2

Ankhanbaatar, U., Auer, A., Ulziibat, G., Settypalli, T. B. K., Gombo-Ochir, D., Basan, G., Takemura, T., Tseren-Ochir, E. O., Ouled Ahmed, H., Meki, I. K., Datta, S., Soumare, B., Metlin, A., Cattoli, G., & Lamien, C. E. (2023). Comparison of the Whole-Genome Sequence of the African Swine Fever Virus from a Mongolian Wild Boar with Genotype II Viruses from Asia and Europe. *Pathogens*, *12*(9). https://doi.org/10.3390/pathogens12091143

Ankhanbaatar, U., Sainnokhoi, T., Khanui, B., Ulziibat, G., Jargalsaikhan, T., Purevtseren, D., Settypalli, T. B. K., Flannery, J., Dundon, W. G., Basan, G., Batten, C., Cattoli, G., & Lamien, C. E. (2021). African swine fever virus genotype II in Mongolia, 2019. *Transboundary and Emerging Diseases*, *68*(5), 2787–2794. https://doi.org/10.1111/tbed.14095

Ansorge, W. J. (2009). Next-generation DNA sequencing techniques. *New Biotechnology*, *25*(4), 195–203. https://doi.org/10.1016/J.NBT.2008.12.009

Arce, H. D. de, Pérez, L. J., Frías, M. T., Rosell, R., Tarradas, J., Núñez, J. I., & Ganges, L. (2009). A multiplex RT-PCR assay for the rapid and differential diagnosis of classical swine fever and other pestivirus infections. *Veterinary Microbiology*, *139*(3–4), 245–252. https://doi.org/10.1016/j.vetmic.2009.06.004

Arias, M., Jurado, C., Gallardo, C., Fernández-Pinero, J., & Sánchez-Vizcaíno, J. M. (2018). Gaps in African swine fever: Analysis and priorities. *Transboundary and Emerging Diseases*, *65*, 235–247. https://doi.org/10.1111/tbed.12695

Asadi, R., & Mollasalehi, H. (2021). The mechanism and improvements to the isothermal amplification of nucleic acids, at a glance. *Analytical Biochemistry*, *631*, 114260. https://doi.org/https://doi.org/10.1016/j.ab.2021.114260

Ávila, L. M. S., Galvis, M. L. D., Campos, M. A. J., Lozano-Parra, A., Villamizar, L. A. R., Arenas, M. O., Martínez-Vega, R. A., Cala, L. M. V., & Bautista, L. E. (2022). Validation of RT-qPCR test for SARS-CoV-2 in saliva specimens. *Journal of Infection and Public Health*, *15*(12), 1403–1408. https://doi.org/https://doi.org/10.1016/j.jiph.2022.10.028

Bastos, A. D. S., Penrith, M. L., Crucière, C., Edrich, J. L., Hutchings, G., Roger, F., Couacy-Hymann, E., & Thomson, G. R. (2003). Genotyping field strains of African swine fever virus by partial p72 gene characterisation. *Archives of Virology*, *148*(4), 693–706. https://doi.org/10.1007/s00705-002-0946-8

Beer, M., Goller, K. V, Staubach, C., & Blome, S. (2015). Genetic variability and distribution of Classical swine fever virus. *Animal Health Research Reviews*, *16*(1), 33–39. https://doi.org/DOI: 10.1017/S1466252315000109

Bentley, D. R., Balasubramanian, S., Swerdlow, H. P., Smith, G. P., Milton, J., Brown, C. G., Hall, K. P., Evers, D. J., Barnes, C. L., Bignell, H. R., Boutell, J. M., Bryant, J., Carter, R. J., Keira Cheetham, R., Cox, A. J., Ellis, D. J., Flatbush, M. R., Gormley, N. A., Humphray, S. J., … Smith, A. J. (2008). Accurate whole human genome sequencing using reversible terminator chemistry. *Nature*, *456*(7218), 53–59. https://doi.org/10.1038/nature07517

Birch, R. R. (1922). *Hog Cholera: Its Nature and Control*. Macmillan.

Blome, S., Gabriel, C., Schmeiser, S., Meyer, D., Meindl-Böhmer, A., Koenen, F., & Beer, M. (2014). Efficacy of marker vaccine candidate CP7_E2alf against challenge with classical swine fever virus isolates of different genotypes. *Veterinary Microbiology*, *169*(1), 8–17. https://doi.org/https://doi.org/10.1016/j.vetmic.2013.12.002

Blome, S., Moß, C., Reimann, I., König, P., & Beer, M. (2017). Classical swine fever vaccines—State-of-the-art. *Veterinary Microbiology*, *206*, 10–20. https://doi.org/10.1016/j.vetmic.2017.01.001

Blome, S., Staubach, C., Henke, J., Carlson, J., & Beer, M. (2017). Classical swine fever—an updated review. In *Viruses* (Vol. 9, Issue 4, pp. 1–24). MDPI AG. https://doi.org/10.3390/v9040086

Blome, S., Wernike, K., Reimann, I., König, P., Moß, C., & Beer, M. (2017). A decade of research into classical swine fever marker vaccine CP7-E2alf (Suvaxyn® CSF Marker): A review of vaccine properties. In *Veterinary Research* (Vol. 48, Issue 1). BioMed Central Ltd. https://doi.org/10.1186/s13567-017-0457-y

Bohorquez, J. A., Lanka, S., Rosell, R., Pérez-Simó, M., Alberch, M., Rodriguez, F., Ganges, L., & Maddox, C. W. (2023). Efficient detection of African Swine Fever Virus using minimal equipment through a LAMP PCR method. *Frontiers in Cellular and Infection Microbiology*, *13*. https://doi.org/10.3389/fcimb.2023.1114772

Bohórquez, J. A., Muñoz-Aguilera, A., Lanka, S., Coronado, L., Rosell, R., Alberch, M., Maddox, C. W., & Ganges, L. (2024). Development of a new loop-mediated isothermal amplification test for the sensitive, rapid, and economic detection of different genotypes of Classical swine fever virus. *Frontiers in Cellular and Infection Microbiology*, *14*. https://doi.org/10.3389/fcimb.2024.1372166

Bohórquez, J. A., Muñoz-González, S., Pérez-Simó, M., Muñoz, I., Rosell, R., Coronado, L., Domingo, M., & Ganges, L. (2020). Foetal immune response activation and high replication rate during generation of classical swine fever congenital infection. *Pathogens*, *9*(4). https://doi.org/10.3390/pathogens9040285

Bool, P. H., Ordas, A., & Botija, C. S. (1969). *Diagnosis of African swine fever by immunofluorescence*.

Borca, M. v., Ramirez-Medina, E., Silva, E., Vuono, E., Rai, A., Pruitt, S., Espinoza, N., Velazquez-Salinas, L., Gay, C. G., & Gladue, D. P. (2021). Asfv-g-Δi177l as an effective oral nasal vaccine against the eurasia strain of africa swine fever. *Viruses*, *13*(5). https://doi.org/10.3390/v13050765

Bosch, J., Rodríguez, A., Iglesias, I., Muñoz, M. J., Jurado, C., Sánchez-Vizcaíno, J. M., & de la Torre, A. (2017). Update on the Risk of Introduction of African Swine Fever by Wild Boar into Disease-Free European Union Countries. *Transboundary and Emerging Diseases*, *64*(5), 1424–1432. https://doi.org/10.1111/tbed.12527

Bostanghadiri, N., Ziaeefar, P., Mofrad, M. G., Yousefzadeh, P., Hashemi, A., & Darban-Sarokhalil, D. (2023). COVID-19: An Overview of SARS-CoV-2 Variants—The Current Vaccines and Drug Development. *BioMed Research International*, *2023*(1), 1879554. https://doi.org/https://doi.org/10.1155/2023/1879554

Brellou, G. D., Tassis, P. D., Apostolopoulou, E. P., Fortomaris, P. D., Leontides, L. S., Papadopoulos, G. A., & Tzika, E. D. (2021). Report on the first african swine fever case in Greece. *Veterinary Sciences*, *8*(8). https://doi.org/10.3390/vetsci8080163

Caixia, W., Songyin, Q., Ying, X., Haoyang, Y., Haoxuan, L., Shaoqiang, W., Chunyan, F., & Xiangmei, L. (2022). Development of a Blocking ELISA Kit for Detection of ASFV Antibody Based on a Monoclonal Antibody Against Full-Length p72. *Journal of AOAC INTERNATIONAL*, *105*(5), 1428–1436. https://doi.org/10.1093/jaoacint/qsac050

Cao, Y., Han, D., Zhang, Y., Zhang, K., Du, N., Tong, W., Li, G., Zheng, H., Liu, C., Gao, F., & Tong, G. (2021). Identification of one novel epitope targeting p54 protein of African swine fever virus using monoclonal antibody and development of a capable ELISA. *Research in Veterinary Science*, *141*, 19–25. https://doi.org/https://doi.org/10.1016/j.rvsc.2021.10.008

Carabelli, A. M., Peacock, T. P., Thorne, L. G., Harvey, W. T., Hughes, J., de Silva, T. I., Peacock, S. J., Barclay, W. S., de Silva, T. I., Towers, G. J., Robertson, D. L., & Consortium, C.-19 G. U. K. (2023). SARS-CoV-2 variant biology: immune escape, transmission and fitness. *Nature Reviews Microbiology*, *21*(3), 162–177. https://doi.org/10.1038/s41579-022-00841-7

Chander, V., Nandi, S., Ravishankar, C., Upmanyu, V., & Verma, R. (2014). Classical swine fever in pigs: Recent developments and future perspectives. In *Animal Health Research Reviews* (Vol. 15, Issue 1, pp. 87–101). Cambridge University Press. https://doi.org/10.1017/S1466252314000024

Chandler, J. C., Bevins, S. N., Ellis, J. W., Linder, T. J., Tell, R. M., Jenkins-Moore, M., Root, J. J., Lenoch, J. B., Robbe-Austerman, S., Deliberto, T. J., Gidlewski, T., Kim Torchetti, M., & Shriner, S. A. (2021). SARS-CoV-2 exposure in wild white-tailed deer (Odocoileus virginianus). *PNAS*, *118*(47). https://doi.org/10.1073/pnas.2114828118/-/DCSupplemental

Chapman, D. A. G., Tcherepanov, V., Upton, C., & Dixon, L. K. (2008). Comparison of the genome sequences of non-pathogenic and pathogenic African swine fever virus isolates. *Journal of General Virology*, *89*(2), 397–408. https://doi.org/10.1099/vir.0.83343-0

Choi, J. Y., & Smith, D. M. (2021). SARS-CoV-2 variants of concern. In *Yonsei Medical Journal* (Vol. 62, Issue 11, pp. 961–968). Yonsei University College of Medicine. https://doi.org/10.3349/ymj.2021.62.11.961

Cole, C. G., Henley, R. R., Dale, C. N., Mott, L. O., Torrey, J. P., & Zinober, N. R. (1884). Part I. Early history and research work. *HISTORY OF HOG CHOLERA RESEARCH in the US DEPARTMENT OF AGRICULTURE, 1960*, 60.

Cool, K., Gaudreault, N. N., Morozov, I., Trujillo, J. D., Meekins, D. A., McDowell, C., Carossino, M., Bold, D., Mitzel, D., Kwon, T., Balaraman, V., Madden, D. W., Artiaga, B. L., Pogranichniy, R. M., Roman-Sosa, G., Henningson, J., Wilson, W. C., Balasuriya, U. B. R., García-Sastre, A., & Richt, J. A. (2022). Infection and transmission of ancestral SARS-CoV-2 and its alpha variant in pregnant white-tailed deer. *Emerging Microbes and Infections*, *11*(1). https://doi.org/10.1080/22221751.2021.2012528

Costard, S., Mur, L., Lubroth, J., Sanchez-Vizcaino, J. M., & Pfeiffer, D. U. (2013). Epidemiology of African swine fever virus. *Virus Research*, *173*(1), 191–197. https://doi.org/https://doi.org/10.1016/j.virusres.2012.10.030

Cui, J., Li, F., & Shi, Z.-L. (2019). Origin and evolution of pathogenic coronaviruses. *Nature Reviews Microbiology*, *17*(3), 181–192. https://doi.org/10.1038/s41579-018-0118-9

Cui, S., Liu, Y., Zhao, J., Peng, X., Lu, G., Shi, W., Pan, Y., Zhang, D., Yang, P., & Wang, Q. (2022). An Updated Review on SARS-CoV-2 Infection in Animals. In *Viruses* (Vol. 14, Issue 7). MDPI. https://doi.org/10.3390/v14071527

Cwynar, P., Stojkov, J., & Wlazlak, K. (2019). African swine fever status in europe. In *Viruses* (Vol. 11, Issue 4). MDPI AG. https://doi.org/10.3390/v11040310

Daigle, J., Onyilagha, C., Truong, T., Le, V. P., Nga, B. T. T., Nguyen, T. L., Clavijo, A., & Ambagala, A. (2021). Rapid and highly sensitive portable detection of African swine fever virus. *Transboundary and Emerging Diseases*, *68*(2), 952–959. https://doi.org/https://doi.org/10.1111/tbed.13770

Davies, E., Farooq, H. Z., Brown, B., Tilston, P., McEwan, A., Birtles, A., O'Hara, R. W., Ahmad, S., Machin, N., Hesketh, L., & Guiver, M. (2022). An Overview of SARS-CoV-2 Molecular Diagnostics in Europe. *Clinics in Laboratory Medicine*, *42*(2), 161–191. https://doi.org/https://doi.org/10.1016/j.cll.2022.02.005

De León, P., Bustos, M. J., & Carrascosa, A. L. (2013). Laboratory methods to study African swine fever virus. In *Virus Research* (Vol. 173, Issue 1, pp. 168–179). https://doi.org/10.1016/j.virusres.2012.09.013

De Wit, E., Van Doremalen, N., Falzarano, D., & Munster, V. J. (2016). SARS and MERS: Recent insights into emerging coronaviruses. In *Nature Reviews Microbiology* (Vol. 14, Issue 8, pp. 523–534). Nature Publishing Group. https://doi.org/10.1038/nrmicro.2016.81

Diaz, A., Netherton, C., Dixon, L., & Wilson, A. (2012). African Swine Fever Virus Strain Georgia 2007/1 in Ornithodoros erraticus Ticks. *Emerging Infectious Disease Journal*, *18*(6), 1026. https://doi.org/10.3201/eid1806.111728

Dinhobl, M., Spinard, E., Tesler, N., Birtley, H., Signore, A., Ambagala, A., Masembe, C., Borca, M. V., & Gladue, D. P. (2024). Reclassification of ASFV into 7 Biotypes Using Unsupervised Machine Learning. *Viruses*, *16*(1). https://doi.org/10.3390/v16010067

Dixon, L. K., Chapman, D. A. G., Netherton, C. L., & Upton, C. (2013). African swine fever virus replication and genomics. In *Virus Research* (Vol. 173, Issue 1, pp. 3–14). https://doi.org/10.1016/j.virusres.2012.10.020

Dixon, L. K., Stahl, K., Jori, F., Vial, L., & Pfeiffer, D. U. (2020). African Swine Fever Epidemiology and Control. *Annu. Rev. Anim. Biosci*, *8*, 221–267. https://doi.org/10.1146/annurev-animal-021419

Dixon, L. K., Sun, H., & Roberts, H. (2019). African swine fever. In *Antiviral Research* (Vol. 165, pp. 34–41). Elsevier B.V. https://doi.org/10.1016/j.antiviral.2019.02.018

Eberling, A. J., Bieker-Stefanelli, J., Reising, M. M., Siev, D., Martin, B. M., McIntosh, M. T., & Beckham, T. R. (2011). Development, optimization, and validation of a Classical swine fever virus real-time reverse transcription polymerase chain reaction assay. *Journal of Veterinary Diagnostic Investigation*, *23*(5), 994–998. https://doi.org/10.1177/1040638711416970

Edwards, S., Fukusho, A., Lefèvre, P.-C., Lipowski, A., Pejsak, Z., Roehe, P., & Westergaard, J. (2000). Classical swine fever: the global situation. *Veterinary Microbiology*, *73*(2), 103–119. https://doi.org/https://doi.org/10.1016/S0378-1135(00)00138-3

Escalera, A., Gonzalez-Reiche, A. S., Aslam, S., Mena, I., Laporte, M., Pearl, R. L., Fossati, A., Rathnasinghe, R., Alshammary, H., van de Guchte, A., Farrugia, K., Qin, Y., Bouhaddou, M., Kehrer, T., Zuliani-Alvarez, L., Meekins, D. A., Balaraman, V., McDowell, C., Richt, J.

A., … Aydillo, T. (2022). Mutations in SARS-CoV-2 variants of concern link to increased spike cleavage and virus transmission. *Cell Host & Microbe*, *30*(3), 373-387.e7. https://doi.org/https://doi.org/10.1016/j.chom.2022.01.006

Eustace Montgomery, R. (1921). On A Form of Swine Fever Occurring in British East Africa (Kenya Colony). *Journal of Comparative Pathology and Therapeutics*, *34*, 159–191. https://doi.org/10.1016/S0368-1742(21)80031-4

Feng, A., Bevins, S., Chandler, J., DeLiberto, T. J., Ghai, R., Lantz, K., Lenoch, J., Retchless, A., Shriner, S., Tang, C. Y., Tong, S. S., Torchetti, M., Uehara, A., & Wan, X.-F. (2023). Transmission of SARS-CoV-2 in free-ranging white-tailed deer in the United States. *Nature Communications*, *14*(1), 4078. https://doi.org/10.1038/s41467-023-39782-x

Fernandes, Q., Inchakalody, V. P., Merhi, M., Mestiri, S., Taib, N., Moustafa Abo El-Ella, D., Bedhiafi, T., Raza, A., Al-Zaidan, L., Mohsen, M. O., Yousuf Al-Nesf, M. A., Hssain, A. A., Yassine, H. M., Bachmann, M. F., Uddin, S., & Dermime, S. (2022). Emerging COVID-19 variants and their impact on SARS-CoV-2 diagnosis, therapeutics and vaccines. *Annals of Medicine*, *54*(1), 524–540. https://doi.org/10.1080/07853890.2022.2031274

Floegel-Niesmann, G. (2001). Classical swine fever (CSF) marker vaccine: Trial III. Evaluation of discriminatory ELISAs. *Veterinary Microbiology*, *83*(2), 121–136. https://doi.org/https://doi.org/10.1016/S0378-1135(01)00411-4

Flores-Vega, V. R., Monroy-Molina, J. V., Jiménez-Hernández, L. E., Torres, A. G., Santos-Preciado, J. I., & Rosales-Reyes, R. (2022). SARS-CoV-2: Evolution and Emergence of New Viral Variants. In *Viruses* (Vol. 14, Issue 4). MDPI. https://doi.org/10.3390/v14040653

Forth, J. H., Calvelage, S., Fischer, M., Hellert, J., Sehl-Ewert, J., Roszyk, H., Deutschmann, P., Reichold, A., Lange, M., Thulke, H. H., Sauter-Louis, C., Höper, D., Mandyhra, S., Sapachova, M., Beer, M., & Blome, S. (2023). African swine fever virus–variants on the rise. *Emerging Microbes and Infections*, *12*(1). https://doi.org/10.1080/22221751.2022.2146537

Freed, N. E., Vlková, M., Faisal, M. B., & Silander, O. K. (2021). Rapid and inexpensive whole-genome sequencing of SARS-CoV-2 using 1200 bp tiled amplicons and Oxford Nanopore Rapid Barcoding. *Biology Methods and Protocols*, *5*(1). https://doi.org/10.1093/biomethods/bpaa014

Gabriel, C., Blome, S., Malogolovkin, A., Parilov, S., Kolbasov, D., Teifke, J. P., & Beer, M. (2011). Characterization of African swine fever virus caucasus isolate in European wild boars. *Emerging Infectious Diseases*, *17*(12), 2342–2345. https://doi.org/10.3201/eid1712.110430

Galindo, I., & Alonso, C. (2017). African swine fever virus: A review. In *Viruses* (Vol. 9, Issue 5). MDPI AG. https://doi.org/10.3390/v9050103

Galindo-Cardiel, I., Ballester, M., Solanes, D., Nofrarías, M., López-Soria, S., Argilaguet, J. M., Lacasta, A., Accensi, F., Rodríguez, F., & Segalés, J. (2013). Standardization of pathological investigations in the framework of experimental ASFV infections. In *Virus Research* (Vol. 173, Issue 1, pp. 180–190). https://doi.org/10.1016/j.virusres.2012.12.018

Gallardo, C., Mwaengo, D. M., MacHaria, J. M., Arias, M., Taracha, E. A., Soler, A., Okoth, E., Martín, E., Kasiti, J., & Bishop, R. P. (2009). Enhanced discrimination of African swine fever virus isolates through nucleotide sequencing of the p54, p72, and pB602L (CVR) genes. *Virus Genes*, *38*(1), 85–95. https://doi.org/10.1007/s11262-008-0293-2

Gallardo, C., Nieto, R., Soler, A., Pelayo, V., Fernández-Pinero, J., Markowska-Daniel, I., Pridotkas, G., Nurmoja, I., Granta, R., Simón, A., Pérez, C., Martín, E., Fernández-Pacheco, P., & Arias, M. (2015). Assessment of African swine fever diagnostic techniques as a response to the epidemic outbreaks in eastern european union countries: How to improve surveillance and control programs. *Journal of Clinical Microbiology*, *53*(8), 2555–2565. https://doi.org/10.1128/JCM.00857-15

Gallardo, C., Soler, A., Nurmoja, I., Cano-Gómez, C., Cvetkova, S., Frant, M., Woźniakowski, G., Simón, A., Pérez, C., Nieto, R., & Arias, M. (2021). Dynamics of African swine fever virus (ASFV) infection in domestic pigs infected with virulent, moderate virulent and attenuated genotype II ASFV European isolates. *Transboundary and Emerging Diseases*, *68*(5), 2826–2841. https://doi.org/10.1111/tbed.14222

Gallardo, M. C., Reoyo, A. de la T., Fernández-Pinero, J., Iglesias, I., Muñoz, M. J., & Arias, M. L. (2015). African swine fever: A global view of the current challenge. In *Porcine Health Management* (Vol. 1). BioMed Central Ltd. https://doi.org/10.1186/s40813-015-0013-y

Ganges, L., Crooke, H. R., Bohórquez, J. A., Postel, A., Sakoda, Y., Becher, P., & Ruggli, N. (2020). Classical swine fever virus: the past, present and future. *Virus Research*, *289*. https://doi.org/10.1016/j.virusres.2020.198151

Gaudreault, N. N., Cool, K., Trujillo, J. D., Morozov, I., Meekins, D. A., McDowell, C., Bold, D., Carossino, M., Balaraman, V., Mitzel, D., Kwon, T., Madden, D. W., Artiaga, B. L., Pogranichniy, R. M., Roman-Sosa, G., Wilson, W. C., Balasuriya, U. B. R., García-Sastre, A., & Richt, J. A. (2022). Susceptibility of sheep to experimental co-infection with the ancestral lineage of SARS-CoV-2 and its alpha variant. *Emerging Microbes & Infections*, *11*(1), 662–675. https://doi.org/10.1080/22221751.2022.2037397

Gaudreault, N. N., Madden, D. W., Wilson, W. C., Trujillo, J. D., & Richt, J. A. (2020). African Swine Fever Virus: An Emerging DNA Arbovirus. In *Frontiers in Veterinary Science* (Vol. 7). Frontiers Media S.A. https://doi.org/10.3389/fvets.2020.00215

Gaudreault, N. N., Trujillo, J. D., Carossino, M., Meekins, D. A., Morozov, I., Madden, D. W., Indran, S. V, Bold, D., Balaraman, V., Kwon, T., Artiaga, B. L., Cool, K., García-Sastre, A., Ma, W., Wilson, W. C., Henningson, J., Balasuriya, U. B. R., & Richt, J. A. (2020). SARS-CoV-2 infection, disease and transmission in domestic cats. *Emerging Microbes & Infections*, *9*(1), 2322–2332. https://doi.org/10.1080/22221751.2020.1833687

Giménez-Lirola, L. G., Mur, L., Rivera, B., Mogler, M., Sun, Y., Lizano, S., Goodell, C., Harris, D. L. H., Rowland, R. R. R., & Gallardo, C. (2016). Detection of African swine fever virus antibodies in serum and oral fluid specimens using a recombinant protein 30 (p30) dual matrix indirect ELISA. *PLoS One*, *11*(9), e0161230.

Gogin, A., Gerasimov, V., Malogolovkin, A., & Kolbasov, D. (2013). African swine fever in the North Caucasus region and the Russian Federation in years 2007-2012. In *Virus Research* (Vol. 173, Issue 1, pp. 198–203). https://doi.org/10.1016/j.virusres.2012.12.007

Gonzales, W., Moreno, C., Duran, U., Henao, N., Bencosme, M., Lora, P., Reyes, R., Núñez, R., de Gracia, A., & Perez, A. M. (2021). African swine fever in the Dominican Republic. *Transboundary and Emerging Diseases*, *68*(6), 3018–3019. https://doi.org/10.1111/tbed.14341

Gu, W., Miller, S., & Chiu, C. Y. (2024). *Clinical Metagenomic Next-Generation Sequencing for Pathogen Detection*. https://doi.org/10.1146/annurev-pathmechdis

Guinat, C., Gogin, A., Blome, S., Keil, G., Pollin, R., Pfeiffer, D. U., & Dixon, L. (2016). Transmission routes of African swine fever virus to domestic pigs: Current knowledge and future research directions. In *Veterinary Record* (Vol. 178, Issue 11, pp. 262–267). British Veterinary Association. https://doi.org/10.1136/vr.103593

Guinat, C., Reis, A. L., Netherton, C. L., Goatley, L., Pfeiffer, D. U., & Dixon, L. (2014). Dynamics of African swine fever virus shedding and excretion in domestic pigs infected by intramuscular inoculation and contact transmission. *Veterinary Research*, *45*(1). https://doi.org/10.1186/s13567-014-0093-8

Güner, H. R., Hasanoğlu, İ., & Aktaş, F. (2020). COVID-19: Prevention and control measures in community. *Turkish Journal of Medical Sciences*, *50*(9), 571–577.

Haines, F. J., Hofmann, M. A., King, D. P., Drew, T. W., & Crooke, H. R. (2013). Development and Validation of a Multiplex, Real-Time RT PCR Assay for the Simultaneous Detection of Classical and African Swine Fever Viruses. *PLoS ONE*, *8*(7). https://doi.org/10.1371/journal.pone.0071019

Hale, V. L., Dennis, P. M., McBride, D. S., Nolting, J. M., Madden, C., Huey, D., Ehrlich, M., Grieser, J., Winston, J., Lombardi, D., Gibson, S., Saif, L., Killian, M. L., Lantz, K., Tell, R. M., Torchetti, M., Robbe-Austerman, S., Nelson, M. I., Faith, S. A., & Bowman, A. S. (2022). SARS-CoV-2 infection in free-ranging white-tailed deer. *Nature*, *602*(7897), 481–486. https://doi.org/10.1038/s41586-021-04353-x

Halwe, N. J., Cool, K., Breithaupt, A., Schön, J., Trujillo, J. D., Nooruzzaman, M., Kwon, T., Ahrens, A. K., Britzke, T., McDowell, C. D., Piesche, R., Singh, G., Pinho dos Reis, V., Kafle, S., Pohlmann, A., Gaudreault, N. N., Corleis, B., Ferreyra, F. M., Carossino, M., … Richt, J. A. (2024). H5N1 clade 2.3.4.4b dynamics in experimentally infected calves and cows. *Nature*. https://doi.org/10.1038/s41586-024-08063-y

Harrison, A. G., Lin, T., & Wang, P. (2020). Mechanisms of SARS-CoV-2 Transmission and Pathogenesis. *Trends in Immunology*, *41*(12), 1100–1115. https://doi.org/https://doi.org/10.1016/j.it.2020.10.004

Harvey, W. T., Carabelli, A. M., Jackson, B., Gupta, R. K., Thomson, E. C., Harrison, E. M., Ludden, C., Reeve, R., Rambaut, A., Peacock, S. J., Robertson, D. L., & Consortium, C.-19 G. U. K. (COG-U. (2021). SARS-CoV-2 variants, spike mutations and immune escape. *Nature Reviews Microbiology*, *19*(7), 409–424. https://doi.org/10.1038/s41579-021-00573-0

Heather, J. M., & Chain, B. (2016a). The sequence of sequencers: The history of sequencing DNA. *Genomics*, *107*(1), 1–8. https://doi.org/10.1016/J.YGENO.2015.11.003

Heather, J. M., & Chain, B. (2016b). The sequence of sequencers: The history of sequencing DNA. In *Genomics* (Vol. 107, Issue 1, pp. 1–8). Academic Press Inc. https://doi.org/10.1016/j.ygeno.2015.11.003

Heilmann, M., Lkhagvasuren, A., Adyasuren, T., Khishgee, B., Bold, B., Ankhanbaatar, U., Fusheng, G., Raizman, E., & Dietze, K. (2020). African swine fever in Mongolia: Course of the epidemic and applied control measures. *Veterinary Sciences*, *7*(1). https://doi.org/10.3390/vetsci7010024

Hernández-Neuta, I., Magoulopoulou, A., Pineiro, F., Lisby, J. G., Gulberg, M., & Nilsson, M. (2023). Highly multiplexed targeted sequencing strategy for infectious disease surveillance. *BMC Biotechnology*, *23*(1), 31. https://doi.org/10.1186/s12896-023-00804-7

Hilt, E. E., & Ferrieri, P. (2022). Next Generation and Other Sequencing Technologies in Diagnostic Microbiology and Infectious Diseases. In *Genes* (Vol. 13, Issue 9). MDPI. https://doi.org/10.3390/genes13091566

Höper, D., Hoffmann, B., & Beer, M. (2011). A Comprehensive Deep Sequencing Strategy for Full-Length Genomes of Influenza A. *PLOS ONE*, *6*(4), e19075-. https://doi.org/10.1371/journal.pone.0019075

Hou, Y. J., Chiba, S., Halfmann, P., Ehre, C., Kuroda, M., Dinnon Iii, K. H., Leist, S. R., Schäfer, A., Nakajima, N., Takahashi, K., Lee, R. E., Mascenik, T. M., Graham, R., Edwards, C. E., Tse, L. V, Okuda, K., Markmann, A. J., Bartelt, L., De Silva, A., … Baric, R. S. (n.d.). *SARS-CoV-2 D614G variant exhibits efficient replication ex vivo and transmission in vivo*. https://www.science.org

Hou, Y.-C. C., Neidich, J. A., Duncavage, E. J., Spencer, D. H., & Schroeder, M. C. (2022). Clinical whole-genome sequencing in cancer diagnosis. *Human Mutation*, *43*(11), 1519–1530. https://doi.org/https://doi.org/10.1002/humu.24381

Hu, B., Guo, H., Zhou, P., & Shi, Z.-L. (2021). Characteristics of SARS-CoV-2 and COVID-19. *Nature Reviews Microbiology*, *19*(3), 141–154. https://doi.org/10.1038/s41579-020-00459-7

Hu, T., Chitnis, N., Monos, D., & Dinh, A. (2021). Next-generation sequencing technologies: An overview. *Human Immunology*, *82*(11), 801–811. https://doi.org/10.1016/j.humimm.2021.02.012

Hu, Z., Tian, X., Lai, R., Wang, X., & Li, X. (2023). Current detection methods of African swine fever virus. *Frontiers in Veterinary Science*, *10*. https://www.frontiersin.org/journals/veterinary-science/articles/10.3389/fvets.2023.1289676

Huang, Y. L., Pang, V. F., Pan, C. H., Chen, T. H., Jong, M. H., Huang, T. S., & Jeng, C. R. (2009). Development of a reverse transcription multiplex real-time PCR for the detection and genotyping of classical swine fever virus. *Journal of Virological Methods*, *160*(1–2), 111–118. https://doi.org/10.1016/j.jviromet.2009.04.029

Huang, Z.-Z., Tan, J., Huang, P., Li, B.-S., Guo, Q., & Liang, L.-J. (2024). The evolutionary features and roles of single nucleotide variants and charged amino acid mutations in influenza outbreaks during NPI period. *Scientific Reports*, *14*(1), 20418. https://doi.org/10.1038/s41598-024-71349-8

Hurtado, C., Bustos, M. J., & Carrascosa, A. L. (2010). The use of COS-1 cells for studies of field and laboratory African swine fever virus samples. *Journal of Virological Methods*, *164*(1–2), 131–134. https://doi.org/10.1016/j.jviromet.2009.11.030

Illumina. (2010). *Technology Spotlight: Illumina ® Sequencing*.

James, H. E., Ebert, K., McGonigle, R., Reid, S. M., Boonham, N., Tomlinson, J. A., Hutchings, G. H., Denyer, M., Oura, C. A. L., Dukes, J. P., & King, D. P. (2010). Detection of African swine fever virus by loop-mediated isothermal amplification. *Journal of Virological Methods*, *164*(1), 68–74. https://doi.org/https://doi.org/10.1016/j.jviromet.2009.11.034

Juul, S., Izquierdo, F., Hurst, A., Dai, X., Wright, A., Kulesha, E., Pettett, R., & Turner, D. J. (2015). What's in my pot? Real-time species identification on the MinION™. *BioRxiv*, 030742. https://doi.org/10.1101/030742

Kata, F., Cameron, P., Rachel, W., Natasha, A.-S., Irene, B., R, B. M., Hubert, D., S, G. J. M., L, K. J., S, K. M., Igor, P., Rich, S., J, W. M., Nick, W., & L, J. D. (2023). Rapid Assessment of SARS-CoV-2 Variant-Associated Mutations in Wastewater Using Real-Time RT-PCR. *Microbiology Spectrum*, *11*(1), e03177-22. https://doi.org/10.1128/spectrum.03177-22

Kevadiya, B. D., Machhi, J., Herskovitz, J., Oleynikov, M. D., Blomberg, W. R., Bajwa, N., Soni, D., Das, S., Hasan, M., Patel, M., Senan, A. M., Gorantla, S., McMillan, J., Edagwa, B., Eisenberg, R., Gurumurthy, C. B., Reid, S. P. M., Punyadeera, C., Chang, L., & Gendelman, H. E. (2021). Diagnostics for SARS-CoV-2 infections. *Nature Materials*, *20*(5), 593–605. https://doi.org/10.1038/s41563-020-00906-z

Khoo, C. K., Norlina, D., Roshaslinda, D., Siti Suraya Hani, M. S., Zunaida, B., Mohd Hasrul, A. H., Pauzi, N. A. S., Roslina, H., Faizah Hanim, M. S., & Leow, B. L. (2021). African swine fever in backyard pigs of Sabah state, East Malaysia, 2021. *Tropical Biomedicine*, *38*(4), 499–504. https://doi.org/10.47665/tb.38.4.095

Kim, H. J., Cho, K. H., Lee, S. K., Kim, D. Y., Nah, J. J., Kim, H. J., Kim, H. J., Hwang, J. Y., Sohn, H. J., Choi, J. G., Kang, H. E., & Kim, Y. J. (2020). Outbreak of African swine fever in South Korea, 2019. *Transboundary and Emerging Diseases*, *67*(2), 473–475. https://doi.org/10.1111/tbed.13483

Kim, Y. Il, Kim, S. G., Kim, S. M., Kim, E. H., Park, S. J., Yu, K. M., Chang, J. H., Kim, E. J., Lee, S., Casel, M. A. B., Um, J., Song, M. S., Jeong, H. W., Lai, V. D., Kim, Y., Chin, B. S., Park, J. S., Chung, K. H., Foo, S. S., … Choi, Y. K. (2020). Infection and Rapid Transmission of SARS-CoV-2 in Ferrets. *Cell Host and Microbe*, *27*(5), 704-709.e2. https://doi.org/10.1016/j.chom.2020.03.023

King, D. P., Reid, S. M., Hutchings, G. H., Grierson, S. S., Wilkinson, P. J., Dixon, L. K., Bastos, A. D. S., & Drew, T. W. (2003). Development of a TaqMan® PCR assay with internal amplification control for the detection of African swine fever virus. *Journal of Virological Methods*, *107*(1), 53–61. https://doi.org/https://doi.org/10.1016/S0166-0934(02)00189-1

Koh, E., Tan, A. K. S., Yeo, D., Lau, C., Tan, L. Y., Ng, O. W., Ong, J., Chong, S., Toh, S., Chen, J., Wong, W. K., Tan, B. Z. Y., He-Lee, C., Heng, Z. P., Liang, I., Fernandez, C. J., Chang, S. F., & Er, K. B. H. (2023). Detection of African Swine Fever Virus from Wild Boar, Singapore, 2023. *Emerging Infectious Disease Journal*, *29*(12), 2580. https://doi.org/10.3201/eid2912.230966

Kosmidou, A., Ahl, R., Thiel, H.-J., & Weiland, E. (1995). Differentiation of classical swine fever virus (CSFV) strains using monoclonal antibodies against structural glycoproteins. *Veterinary Microbiology*, *47*(1), 111–118. https://doi.org/https://doi.org/10.1016/0378-1135(95)00054-E

Kuchipudi, S. V, Surendran-Nair, M., Ruden, R. M., Yon, M., Nissly, R. H., Vandegrift, K. J., Nelli, R. K., Li, L., Jayarao, B. M., Maranas, C. D., Levine, N., Willgert, K., Conlan, A. J. K., Olsen, R. J., Davis, J. J., Musser, J. M., Hudson, P. J., & Kapur, V. (2022). Multiple

spillovers from humans and onward transmission of SARS-CoV-2 in white-tailed deer. *PNAS*, *119*(6). https://doi.org/10.1073/pnas.2121644119/-/DCSupplemental

Lai, C. K. C., & Lam, W. (2021). Laboratory testing for the diagnosis of COVID-19. *Biochemical and Biophysical Research Communications*, *538*, 226–230. https://doi.org/https://doi.org/10.1016/j.bbrc.2020.10.069

Langelier, C., Zinter, M. S., Kalantar, K., Yanik, G. A., Christenson, S., O'Donovan, B., White, C., Wilson, M., Sapru, A., & Dvorak, C. C. (2018). Metagenomic sequencing detects respiratory pathogens in hematopoietic cellular transplant patients. *American Journal of Respiratory and Critical Care Medicine*, *197*(4), 524–528.

Lattwein, E., Klemens, O., Schwindt, S., Becher, P., & Tautz, N. (2012). Pestivirus Virion Morphogenesis in the Absence of Uncleaved Nonstructural Protein 2-3. *Journal of Virology*, *86*(1), 427–437. https://doi.org/10.1128/jvi.06133-11

Le, V. P., Ahn, M. J., Kim, J. S., Jung, M. C., Yoon, S. W., Trinh, T. B. N., Le, T. N., Kim, H. K., Kang, J. A., Lim, J. W., Yeom, M., Na, W., Xie, X., Feng, Z., Song, D., & Jeong, D. G. (2023). A Whole-Genome Analysis of the African Swine Fever Virus That Circulated during the First Outbreak in Vietnam in 2019 and Subsequently in 2022. *Viruses*, *15*(9). https://doi.org/10.3390/v15091945

Lee, H. S., Bui, V. N., Dao, D. T., Bui, N. A., Le, T. D., Kieu, M. A., Nguyen, Q. H., Tran, L. H., Roh, J. H., So, K. M., Hur, T. Y., & Oh, S. I. (2021). Pathogenicity of an African swine fever virus strain isolated in Vietnam and alternative diagnostic specimens for early detection of viral infection. *Porcine Health Management*, *7*(1). https://doi.org/10.1186/s40813-021-00215-0

Leifer, I., Blome, S., Beer, M., & Hoffmann, B. (2011). Development of a highly sensitive real-time RT-PCR protocol for the detection of Classical swine fever virus independent of the 5′ untranslated region. *Journal of Virological Methods*, *171*(1), 314–317. https://doi.org/https://doi.org/10.1016/j.jviromet.2010.11.014

Leifer, I., Hoffmann, B., Höper, D., Rasmussen, T. B., Blome, S., Strebelow, G., Höreth-Böntgen, D., Staubach, C., & Beer, M. (2010). Molecular epidemiology of current classical swine fever virus isolates of wild boar in Germany. *Journal of General Virology*, *91*(11), 2687–2697. https://doi.org/10.1099/vir.0.023200-0

Leifer, I., Lange, E., Reimann, I., Blome, S., Juanola, S., Duran, J. P., & Beer, M. (2009). Modified live marker vaccine candidate CP7_E2alf provides early onset of protection against lethal challenge infection with classical swine fever virus after both intramuscular and oral immunization. *Vaccine*, *27*(47), 6522–6529. https://doi.org/https://doi.org/10.1016/j.vaccine.2009.08.057

Leitão, A., Cartaxeiro, C., Coelho, R., Cruz, B., Parkhouse, R. M. E., Portugal, F. C., Vigário, J. D., & Martins, C. L. V. (2001). The non-haemadsorbing African swine fever virus isolate ASFV/NH/P68 provides a model for defining the protective anti-virus immune response. *Journal of General Virology*, *82*(3), 513–523. https://doi.org/10.1099/0022-1317-82-3-513

Li, Y., Shen, L., Sun, Y., Yuan, J., Huang, J., Li, C., Li, S., Luo, Y., & Qiu, H. J. (2013). Simplified serum neutralization test based on enhanced green fluorescent protein-tagged classical swine fever virus. *Journal of Clinical Microbiology*, *51*(8), 2710–2712. https://doi.org/10.1128/JCM.00859-13

Li, Z., Chen, W., Qiu, Z., Li, Y., Fan, J., Wu, K., Li, X., Zhao, M., Ding, H., Fan, S., & Chen, J. (2022). African Swine Fever Virus: A Review. In *Life* (Vol. 12, Issue 8). Multidisciplinary Digital Publishing Institute (MDPI). https://doi.org/10.3390/life12081255

Liao, H., Cai, D., & Sun, Y. (2022). VirStrain: a strain identification tool for RNA viruses. *Genome Biology*, *23*(1). https://doi.org/10.1186/s13059-022-02609-x

Lim, J. W., Vu, T. T. H., Le, V. P., Yeom, M., Song, D., Jeong, D. G., & Park, S. K. (2023). Advanced Strategies for Developing Vaccines and Diagnostic Tools for African Swine Fever. In *Viruses* (Vol. 15, Issue 11). Multidisciplinary Digital Publishing Institute (MDPI). https://doi.org/10.3390/v15112169

Liu, L., Xia, H., Belák, S., & Widén, F. (2009). Development of a primer-probe energy transfer real-time PCR assay for improved detection of classical swine fever virus. *Journal of Virological Methods*, *160*(1–2), 69–73. https://doi.org/10.1016/j.jviromet.2009.04.019

Liu, Y., Bahoussi, A. N., Wang, P.-H., Wu, C., & Xing, L. (n.d.). *Complete genome sequences of classical swine fever virus: Phylogenetic and evolutionary analyses*.

Liu, Y., Zhang, X., Qi, W., Yang, Y., Liu, Z., An, T., Wu, X., & Chen, J. (2021). Prevention and control strategies of african swine fever and progress on pig farm repopulation in China. In *Viruses* (Vol. 13, Issue 12). MDPI. https://doi.org/10.3390/v13122552

Logunov, D. Y., Dolzhikova, I. V, Shcheblyakov, D. V, Tukhvatulin, A. I., Zubkova, O. V, Dzharullaeva, A. S., Kovyrshina, A. V, Lubenets, N. L., Grousova, D. M., Erokhova, A. S., Botikov, A. G., Izhaeva, F. M., Popova, O., Ozharovskaya, T. A., Esmagambetov, I. B., Favorskaya, I. A., Zrelkin, D. I., Voronina, D. V, Shcherbinin, D. N., … Gintsburg, A. L. (2021). Safety and efficacy of an rAd26 and rAd5 vector-based heterologous prime-boost COVID-19 vaccine: an interim analysis of a randomised controlled phase 3 trial in Russia. *The Lancet*, *397*(10275), 671–681. https://doi.org/https://doi.org/10.1016/S0140-6736(21)00234-8

Loman, N. J., Misra, R. V, Dallman, T. J., Constantinidou, C., Gharbia, S. E., Wain, J., & Pallen, M. J. (2012). Performance comparison of benchtop high-throughput sequencing platforms. *Nature Biotechnology*, *30*(5), 434–439. https://doi.org/10.1038/nbt.2198

Lu, R., Zhao, X., Li, J., Niu, P., Yang, B., Wu, H., Wang, W., Song, H., Huang, B., Zhu, N., Bi, Y., Ma, X., Zhan, F., Wang, L., Hu, T., Zhou, H., Hu, Z., Zhou, W., Zhao, L., … Tan, W. (2020). Genomic characterisation and epidemiology of 2019 novel coronavirus: implications for virus origins and receptor binding. *The Lancet*, *395*(10224), 565–574. https://doi.org/https://doi.org/10.1016/S0140-6736(20)30251-8

Lv, J.-X., Liu, X., Pei, Y.-Y., Song, Z.-G., Chen, X., Hu, S.-J., She, J.-L., Liu, Y., Chen, Y.-M., & Zhang, Y.-Z. (2024). *Evolutionary trajectory of diverse SARS-CoV-2 variants at the beginning of COVID-19 outbreak*. https://www.gisaid.org/

Madden, D. W., Sunwoo, S.-Y., Gaudreault, N. N., Trujillo, J. D., Morozov, I., Gallardo, C., & Richt, J. A. (2022). Development of a chromatographic lateral flow immunoassay for detection of African swine fever virus antigen in blood. *Animal Diseases*, *2*(1), 14. https://doi.org/10.1186/s44149-022-00045-9

Malogolovkin, A., Burmakina, G., Tulman, E. R., Delhon, G., Diel, D. G., Salnikov, N., Kutish, G. F., Kolbasov, D., & Rock, D. L. (2015). African swine fever virus CD2v and C-type lectin gene loci mediate serological specificity. *Journal of General Virology*, *96*(4), 866–873. https://doi.org/10.1099/jgv.0.000024

Margulies, M., Egholm, M., Altman, W. E., Attiya, S., Bader, J. S., Bemben, L. A., Berka, J., Braverman, M. S., Chen, Y.-J., Chen, Z., Dewell, S. B., Du, L., Fierro, J. M., Gomes, X. V, Godwin, B. C., He, W., Helgesen, S., Ho, C. H., Irzyk, G. P., … Rothberg, J. M. (2005).

Genome sequencing in microfabricated high-density picolitre reactors. *Nature*, *437*(7057), 376–380. https://doi.org/10.1038/nature03959

Markov, P. V., Ghafari, M., Beer, M., Lythgoe, K., Simmonds, P., Stilianakis, N. I., & Katzourakis, A. (2023). The evolution of SARS-CoV-2. In *Nature Reviews Microbiology* (Vol. 21, Issue 6, pp. 361–379). Nature Research. https://doi.org/10.1038/s41579-023-00878-2

McDowell, C. D., Bold, D., Trujillo, J. D., Meekins, D. A., Keating, C., Cool, K., Kwon, T., Madden, D. W., Artiaga, B. L., Balaraman, V., Ankhanbaatar, U., Zayat, B., Retallick, J., Dodd, K., Chung, C. J., Morozov, I., Gaudreault, N. N., Souza-Neto, J. A., & Richt, J. A. (2022a). Experimental Infection of Domestic Pigs with African Swine Fever Virus Isolated in 2019 in Mongolia. *Viruses*, *14*(12). https://doi.org/10.3390/v14122698

McDowell, C. D., Bold, D., Trujillo, J. D., Meekins, D. A., Keating, C., Cool, K., Kwon, T., Madden, D. W., Artiaga, B. L., Balaraman, V., Ankhanbaatar, U., Zayat, B., Retallick, J., Dodd, K., Chung, C. J., Morozov, I., Gaudreault, N. N., Souza-Neto, J. A., & Richt, J. A. (2022b). Experimental Infection of Domestic Pigs with African Swine Fever Virus Isolated in 2019 in Mongolia. *Viruses*, *14*(12). https://doi.org/10.3390/v14122698

McGinnis, S., & Madden, T. L. (2004). BLAST: at the core of a powerful and diverse set of sequence analysis tools. *Nucleic Acids Research*, *32*(suppl_2), W20–W25. https://doi.org/10.1093/nar/gkh435

Meekins, D. A., Gaudreault, N. N., & Richt, J. A. (2021). Natural and experimental sars-cov-2 infection in domestic and wild animals. In *Viruses* (Vol. 13, Issue 10). MDPI. https://doi.org/10.3390/v13101993

Mercier, J. F., & Slater, G. W. (2005). Solid Phase DNA Amplification: A Brownian Dynamics Study of Crowding Effects. *Biophysical Journal*, *89*(1), 32–42. https://doi.org/10.1529/BIOPHYSJ.104.051904

Meyer, D., Fritsche, S., Luo, Y., Engemann, C., Blome, S., Beyerbach, M., Chang, C.-Y., Qiu, H.-J., Becher, P., & Postel, A. (2017). The double-antigen ELISA concept for early detection of Erns-specific classical swine fever virus antibodies and application as an accompanying test for differentiation of infected from marker vaccinated animals. *Transboundary and Emerging Diseases*, *64*(6), 2013–2022. https://doi.org/https://doi.org/10.1111/tbed.12611

Meyerowitz, E. A., Richterman, A., Gandhi, R. T., & Sax, P. E. (2020). Transmission of SARS-CoV-2: A Review of Viral, Host, and Environmental Factors. *Annals of Internal Medicine*, *174*(1), 69–79. https://doi.org/10.7326/M20-5008

Michael, J. J., & L, A. S. (2007). 16S rRNA Gene Sequencing for Bacterial Identification in the Diagnostic Laboratory: Pluses, Perils, and Pitfalls. *Journal of Clinical Microbiology*, *45*(9), 2761–2764. https://doi.org/10.1128/jcm.01228-07

Mighell, E., & Ward, M. P. (2021). African Swine Fever spread across Asia, 2018–2019. *Transboundary and Emerging Diseases*, *68*(5), 2722–2732. https://doi.org/10.1111/tbed.14039

Milicévić, V., Kureljušić, B., Maksimović Zorić, J., Savić, B., Stanojević, S., & Milakara, E. (2019). First Occurence of African Swine Fever in Serbia. In *Acta Veterinaria* (Vol. 69, Issue 4, pp. 443–449). Sciendo. https://doi.org/10.2478/acve-2019-0038

Mistry, P., Barmania, F., Mellet, J., Peta, K., Strydom, A., Viljoen, I. M., James, W., Gordon, S., & Pepper, M. S. (2022). SARS-CoV-2 Variants, Vaccines, and Host Immunity. *Frontiers in Immunology*, *12*. https://www.frontiersin.org/journals/immunology/articles/10.3389/fimmu.2021.809244

Mittelholzer, C., Moser, C., Tratschin, J.-D., & Hofmann, M. A. (2000). Analysis of classical swine fever virus replication kinetics allows differentiation of highly virulent from avirulent strains. *Veterinary Microbiology*, *74*(4), 293–308. https://doi.org/https://doi.org/10.1016/S0378-1135(00)00195-4

Moennig, V. (2015a). The control of classical swine fever in wild boar. In *Frontiers in Microbiology* (Vol. 6, Issue NOV). Frontiers Research Foundation. https://doi.org/10.3389/fmicb.2015.01211

Moennig, V. (2015b). The control of classical swine fever in wild boar. In *Frontiers in Microbiology* (Vol. 6, Issue NOV). Frontiers Research Foundation. https://doi.org/10.3389/fmicb.2015.01211

Moennig, V., & Becher, P. (2015). Pestivirus control programs: how far have we come and where are we going? *Animal Health Research Reviews*, *16*(1), 83–87.

Moennig, V., Floegel-Niesmann, G., & Greiser-Wilke, I. (2003). Clinical Signs and Epidemiology of Classical Swine Fever: A Review of New Knowledge. *The Veterinary Journal*, *165*(1), 11–20. https://doi.org/https://doi.org/10.1016/S1090-0233(02)00112-0

Morgulis, A., Coulouris, G., Raytselis, Y., Madden, T. L., Agarwala, R., & Schäffer, A. A. (2008). Database indexing for production MegaBLAST searches. *Bioinformatics*, *24*(16), 1757–1764. https://doi.org/10.1093/bioinformatics/btn322

Mulumba-Mfumu, L. K., Achenbach, J. E., Mauldin, M. R., Dixon, L. K., Tshilenge, C. G., Thiry, E., Moreno, N., Blanco, E., Saegerman, C., Lamien, C. E., & Diallo, A. (2017). Genetic assessment of african swine fever isolates involved in outbreaks in the Democratic Republic Of Congo between 2005 and 2012 reveals co-circulation of p72 genotypes I, IX and XIV, including 19 variants. *Viruses*, *9*(2). https://doi.org/10.3390/v9020031

Muzykina, L., Barrado-Gil, L., Gonzalez-Bulnes, A., Crespo-Piazuelo, D., Cerón, J. J., Alonso, C., & Montoya, M. (2024a). Overview of Modern Commercial Kits for Laboratory Diagnosis of African Swine Fever and Swine Influenza A Viruses. In *Viruses* (Vol. 16, Issue 4). Multidisciplinary Digital Publishing Institute (MDPI). https://doi.org/10.3390/v16040505

Muzykina, L., Barrado-Gil, L., Gonzalez-Bulnes, A., Crespo-Piazuelo, D., Cerón, J. J., Alonso, C., & Montoya, M. (2024b). Overview of Modern Commercial Kits for Laboratory Diagnosis of African Swine Fever and Swine Influenza A Viruses. In *Viruses* (Vol. 16, Issue 4). Multidisciplinary Digital Publishing Institute (MDPI). https://doi.org/10.3390/v16040505

Naccache, S. N., Federman, S., Veeraraghavan, N., Zaharia, M., Lee, D., Samayoa, E., Bouquet, J., Greninger, A. L., Luk, K.-C., & Enge, B. (2014). A cloud-compatible bioinformatics pipeline for ultrarapid pathogen identification from next-generation sequencing of clinical samples. *Genome Research*, *24*(7), 1180–1192.

Nerenz, R. D., Hubbard, J. A., & Cervinski, M. A. (2022). Review of SARS-CoV-2 Antigen and Antibody Testing in Diagnosis and Community Surveillance. *Clinics in Laboratory Medicine*, *42*(4), 687–704. https://doi.org/https://doi.org/10.1016/j.cll.2022.09.018

Nguyen, N. H., Nguyen, B. T. P., Do, D. T., Nguyen, T. Q., Nguyen, D. T. M., & Nguyen, M. N. (2021). Genetic diversity and molecular characterization of classical swine fever virus envelope protein genes E2 and Erns circulating in Vietnam from 2017 to 2019. *Infection, Genetics and Evolution*, *96*, 105140. https://doi.org/10.1016/J.MEEGID.2021.105140

Nogales, A., & Dediego, M. L. (2019). Host single nucleotide polymorphisms modulating influenza a virus disease in humans. In *Pathogens* (Vol. 8, Issue 4). MDPI AG. https://doi.org/10.3390/pathogens8040168

Nyrén, P., & Lundin, A. (1985). Enzymatic method for continuous monitoring of inorganic pyrophosphate synthesis. *Analytical Biochemistry*, *151*(2), 504–509. https://doi.org/10.1016/0003-2697(85)90211-8

O'Donnell, V. K., Mayr, G. A., Sturgill Samayoa, T. L., Dodd, K. A., & Barrette, R. W. (2020). Rapid sequence-based characterization of African swine fever virus by use of the Oxford Nanopore MiniOn sequence sensing device and a companion analysis software tool. *Journal of Clinical Microbiology*, *58*(1). https://doi.org/10.1128/JCM.01104-19

Oleaga, A., Pérez Sánchez, R., & Encinas Grandes, A. (1990). *Distribution and biology of Ornithodoros erraticus in parts of Spain affected by African swine fever*.

Olivero, N. B., Gonzalez-Reiche, A. S., Re, V. E., Castro, G. M., Pisano, M. B., Sicilia, P., Barbas, M. G., Khan, Z., van de Guchte, A., Dutta, J., Cortes, P. R., Hernandez-Morfa, M., Zappia, V. E., Ortiz, L., Geiger, G., Rajao, D., Perez, D. R., van Bakel, H., & Echenique, J. (2022). Phylogenetic analysis and comparative genomics of SARS-CoV-2 from survivor and non-survivor COVID-19 patients in Cordoba, Argentina. *BMC Genomics*, *23*(1). https://doi.org/10.1186/s12864-022-08756-6

Onyilagha, C., Nguyen, K., Luka, P. D., Hussaini, U., Adedeji, A., Odoom, T., & Ambagala, A. (2022). Evaluation of a Lateral Flow Assay for Rapid Detection of African Swine Fever Virus in Multiple Sample Types. *Pathogens*, *11*(2). https://doi.org/10.3390/pathogens11020138

P, P. F., J, T. S., Nicholas, K., Judith, A., Alejandra, G., Stephen, L., L, P. J., Gonzalo, P. M., D, M. E., Cristiano, Z., Ruth, B., A, S. K., Satrajit, R., Kenneth, K., Ping, L., V, K. W., David, C., W, F. R., L, H. L., … C, G. W. (2020). Safety and Efficacy of the BNT162b2 mRNA Covid-19 Vaccine. *New England Journal of Medicine*, *383*(27), 2603–2615. https://doi.org/10.1056/NEJMoa2034577

Palmer, M. V., Martins, M., Falkenberg, S., Buckley, A., Caserta, L. C., Mitchell, P. K., Cassmann, E. D., Rollins, A., Zylich, N. C., Renshaw, R. W., Guarino, C., Wagner, B., Lager, K., & Diel, D. G. (2021). Susceptibility of White-Tailed Deer (Odocoileus

virginianus) to SARS-CoV-2. *Journal of Virology*, *95*(11). https://doi.org/10.1128/jvi.00083-21

Parida, M., Sannarangaiah, S., Dash, P. K., Rao, P. V. L., & Morita, K. (2008). Loop mediated isothermal amplification (LAMP): a new generation of innovative gene amplification technique; perspectives in clinical diagnosis of infectious diseases. *Reviews in Medical Virology*, *18*(6), 407–421. https://doi.org/https://doi.org/10.1002/rmv.593

Pastor, M. J., Arias, M., & Escribano, J. M. (1990). Comparison of two antigens for use in an enzyme-linked immunosorbent assay to detect African swine fever antibody. *American Journal of Veterinary Research*, *51*(10), 1540–1543. https://doi.org/10.2460/ajvr.1990.51.10.1540

Patel, R., Kaki, M., Potluri, V. S., Kahar, P., & Khanna, D. (2022). A comprehensive review of SARS-CoV-2 vaccines: Pfizer, Moderna & Johnson & Johnson. *Human Vaccines & Immunotherapeutics*, *18*(1), 2002083. https://doi.org/10.1080/21645515.2021.2002083

Paton, D. J., & Greiser-Wilke, I. (2003). Classical swine fever - An update. In *Research in Veterinary Science* (Vol. 75, Issue 3, pp. 169–178). Elsevier. https://doi.org/10.1016/S0034-5288(03)00076-6

Paton, D. J., McGoldrick, A., Greiser-Wilke, I., Parchariyanon, S., Song, J.-Y., Liou, P. P., Stadejek, T., Lowings, J. P., Björklund, H., & Belák, S. (2000). Genetic typing of classical swine fever virus. *Veterinary Microbiology*, *73*(2), 137–157. https://doi.org/https://doi.org/10.1016/S0378-1135(00)00141-3

Pearson, J. D., Trcka, D., Lu, S., Hyduk, S. J., Jen, M., Aynaud, M.-M., Hernández, J. J., Peidis, P., Barrios-Rodiles, M., Chan, K., Woodgett, J., Mazzulli, T., Attisano, L., Pelletier, L., Cybulsky, M. I., Wrana, J. L., & Bremner, R. (2021). Comparison of SARS-CoV-2 indirect and direct RT-qPCR detection methods. *Virology Journal*, *18*(1), 99. https://doi.org/10.1186/s12985-021-01574-4

Penrith, M.-L., & Vosloo, W. (2009). Review of African swine fever: transmission, spread and control. In *Tydskr.S.Afr.vet.Ver* (Vol. 58, Issue 2). www.oie.int

Pickering, B., Lung, O., Maguire, F., Kruczkiewicz, P., Kotwa, J. D., Buchanan, T., Gagnier, M., Guthrie, J. L., Jardine, C. M., Marchand-Austin, A., Massé, A., McClinchey, H., Nirmalarajah, K., Aftanas, P., Blais-Savoie, J., Chee, H.-Y., Chien, E., Yim, W., Banete, A., … Bowman, J. (2022). Divergent SARS-CoV-2 variant emerges in white-tailed deer with

deer-to-human transmission. *Nature Microbiology*, *7*(12), 2011–2024. https://doi.org/10.1038/s41564-022-01268-9

Porte, L., Legarraga, P., Vollrath, V., Aguilera, X., Munita, J. M., Araos, R., Pizarro, G., Vial, P., Iruretagoyena, M., Dittrich, S., & Weitzel, T. (2020). Evaluation of a novel antigen-based rapid detection test for the diagnosis of SARS-CoV-2 in respiratory samples. *International Journal of Infectious Diseases*, *99*, 328–333. https://doi.org/https://doi.org/10.1016/j.ijid.2020.05.098

Postel, A., Austermann-Busch, S., Petrov, A., Moennig, V., & Becher, P. (2018). Epidemiology, diagnosis and control of classical swine fever: Recent developments and future challenges. *Transboundary and Emerging Diseases*, *65*, 248–261. https://doi.org/10.1111/tbed.12676

Postel, A., Nishi, T., Kameyama, K., Meyer, D., Suckstorff, O., & Becher, P. (2019). Reemergence of Classical Swine Fever, Japan, 2018. *Emerging Infectious Disease Journal*, *25*(6), 1228. https://doi.org/10.3201/eid2506.181578

Postel, A., Schmeiser, S., Bernau, J., Meindl-Boehmer, A., Pridotkas, G., Dirbakova, Z., Mojzis, M., & Becher, P. (2012). *Improved strategy for phylogenetic analysis of classical swine fever virus based on full-length E2 encoding sequences*. http://www.veterinaryresearch.org/content/43/1/50

Pozzi, C., Sarti, R., Levi, R., Mollura, M., Azzolini, E., Barbieri, R., Mantovani, A., & Rescigno, M. (2023). Association Between Duration of SARS-CoV-2 Positivity and Long COVID. *Clinical Infectious Diseases*, *77*(11), 1531–1533. https://doi.org/10.1093/cid/ciad434

Prather, K. A., Wang, C. C., & Schooley, R. T. (2020). Reducing transmission of SARS-CoV-2. *Science*, *368*(6498), 1422–1424. https://doi.org/10.1126/science.abc6197

Prince, T., Smith, S. L., Radford, A. D., Solomon, T., Hughes, G. L., & Patterson, E. I. (2021). Sars-cov-2 infections in animals: Reservoirs for reverse zoonosis and models for study. In *Viruses* (Vol. 13, Issue 3). MDPI AG. https://doi.org/10.3390/v13030494

Probst, C., Globig, A., Knoll, B., Conraths, F. J., & Depner, K. (2017). Behaviour of free ranging wild boar towards their dead fellows: potential implications for the transmission of African swine fever. *Royal Society Open Science*, *4*(5), 170054.

Qiagen. (2024). *CLC Genomics Workbench USER MANUAL Manual for*.

Quick, J. (2020). *nCoV-2019 sequencing protocol v1*. https://doi.org/10.17504/protocols.io.bbmuik6w

Quick, J., Loman, N. J., Duraffour, S., Simpson, J. T., Severi, E., Cowley, L., Bore, J. A., Koundouno, R., Dudas, G., Mikhail, A., Ouédraogo, N., Afrough, B., Bah, A., Baum, J. H. J., Becker-Ziaja, B., Boettcher, J. P., Cabeza-Cabrerizo, M., Camino-Sánchez, Á., Carter, L. L., … Carroll, M. W. (2016). Real-time, portable genome sequencing for Ebola surveillance. *Nature*, *530*(7589), 228–232. https://doi.org/10.1038/nature16996

R, B. L., M, E. S. H., Brandon, E., Karen, K., Sharon, F., Rick, N., David, D., A, S. S., Nadine, R., Buddy, C. C., John, M., Shishir, K., Nathan, S., Joel, S., Adam, B., Carlos, F., Howard, S., Kathleen, N., Lawrence, C., … Tal, Z. (2021). Efficacy and Safety of the mRNA-1273 SARS-CoV-2 Vaccine. *New England Journal of Medicine*, *384*(5), 403–416. https://doi.org/10.1056/NEJMoa2035389

Rai, A., Pruitt, S., Ramirez-Medina, E., Vuono, E. A., Silva, E., Velazquez-Salinas, L., Carrillo, C., Borca, M. V., & Gladue, D. P. (2020). Identification of a continuously stable and commercially available cell line for the identification of infectious African swine fever virus in clinical samples. *Viruses*, *12*(8). https://doi.org/10.3390/v12080820

Rajala, E., Gröndal, H., & Sternberg Lewerin, S. (2023). The first outbreak of African swine fever in Sweden: a survey of pig farmers' perceptions of information received, risks, biosecurity measures and future prospects. *Acta Veterinaria Scandinavica*, *65*(1). https://doi.org/10.1186/s13028-023-00722-w

Rajukumar, K., Senthilkumar, D., Venkatesh, G., Singh, F., Patil, V. P., Kombiah, S., Tosh, C., Dubey, C. K., Sen, A., Barman, N. N., Chakravarty, A., Dutta, B., Pegu, S. R., Bharali, A., & Singh, V. P. (2021). Genetic characterization of African swine fever virus from domestic pigs in India. *Transboundary and Emerging Diseases*, *68*(5), 2687–2692. https://doi.org/10.1111/tbed.13986

Ramirez-Medina, E., O'Donnell, V., Silva, E., Espinoza, N., Velazquez-Salinas, L., Moran, K., Daite, D. A., Barrette, R., Faburay, B., Holland, R., Gladue, D. P., & Borca, M. v. (2022). Experimental Infection of Domestic Pigs with an African Swine Fever Virus Field Strain Isolated in 2021 from the Dominican Republic. *Viruses*, *14*(5), 1090. https://doi.org/10.3390/v14051090

Rios, L., Núñez, J. I., Díaz de Arce, H., Ganges, L., & Pérez, L. J. (2018). Revisiting the genetic diversity of classical swine fever virus: A proposal for new genotyping and subgenotyping

schemes of classification. *Transboundary and Emerging Diseases*, *65*(4), 963–971. https://doi.org/10.1111/tbed.12909

Rossi, S., Staubach, C., Blome, S., Guberti, V., Thulke, H. H., Vos, A., Koenen, F., & Le Potier, M. F. (2015). Controlling of CSFV in European wild boar using oral vaccination: A review. In *Frontiers in Microbiology* (Vol. 6, Issue OCT). Frontiers Media S.A. https://doi.org/10.3389/fmicb.2015.01141

Rothberg, J. M., Hinz, W., Rearick, T. M., Schultz, J., Mileski, W., Davey, M., Leamon, J. H., Johnson, K., Milgrew, M. J., Edwards, M., Hoon, J., Simons, J. F., Marran, D., Myers, J. W., Davidson, J. F., Branting, A., Nobile, J. R., Puc, B. P., Light, D., … Bustillo, J. (2011). An integrated semiconductor device enabling non-optical genome sequencing. *Nature*, *475*(7356), 348–352. https://doi.org/10.1038/nature10242

Rozek, W., Kwasnik, M., Socha, W., Sztromwasser, P., & Rola, J. (2021). Analysis of single nucleotide variants (Snvs) induced by passages of equine influenza virus h3n8 in embryonated chicken eggs. *Viruses*, *13*(8). https://doi.org/10.3390/v13081551

Salas, M. L., & Andrés, G. (2013). African swine fever virus morphogenesis. In *Virus Research* (Vol. 173, Issue 1, pp. 29–41). https://doi.org/10.1016/j.virusres.2012.09.016

Salguero, F. J. (2020). Comparative Pathology and Pathogenesis of African Swine Fever Infection in Swine. In *Frontiers in Veterinary Science* (Vol. 7). Frontiers Media S.A. https://doi.org/10.3389/fvets.2020.00282

Sánchez-Cordón, P. J., Montoya, M., Reis, A. L., & Dixon, L. K. (2018). African swine fever: A re-emerging viral disease threatening the global pig industry. In *Veterinary Journal* (Vol. 233, pp. 41–48). Bailliere Tindall Ltd. https://doi.org/10.1016/j.tvjl.2017.12.025

Sánchez-Cordón, P. J., Nunez, A., Neimanis, A., Wikström-Lassa, E., Montoya, M., Crooke, H., & Gavier-Widén, D. (2019). African swine fever: Disease dynamics in wild boar experimentally infected with ASFV isolates belonging to genotype I and II. In *Viruses* (Vol. 11, Issue 9). MDPI AG. https://doi.org/10.3390/v11090852

Sánchez-Cordón, P. J., Vidaña, B., Neimanis, A., Núñez, A., Wikström, E., & Gavier-Widén, D. (2021). 4. Pathology of African swine fever. In *Understanding and combatting African Swine Fever* (pp. 87–139). Wageningen Academic Publishers. https://doi.org/10.3920/978-90-8686-910-7_4

Sánchez-Vizcaíno, J. M., Mur, L., Gomez-Villamandos, J. C., & Carrasco, L. (2015). An update on the epidemiology and pathology of African swine fever. In *Journal of Comparative Pathology* (Vol. 152, Issue 1, pp. 9–21). W.B. Saunders Ltd. https://doi.org/10.1016/j.jcpa.2014.09.003

Sánchez-Vizcaíno, J. M., Mur, L., & Martínez-López, B. (2013). African swine fever (ASF): Five years around Europe. In *Veterinary Microbiology* (Vol. 165, Issues 1–2, pp. 45–50). https://doi.org/10.1016/j.vetmic.2012.11.030

Sanger, F., Nicklen, S., & Coulson, A. R. (1977). *DNA sequencing with chain-terminating inhibitors (DNA polymerase/nucleotide sequences/bacteriophage 4X174)* (Vol. 74, Issue 12).

Sarker, R., Roknuzzaman, A. S. M., Nazmunnahar, Shahriar, M., Hossain, Md. J., & Islam, Md. R. (2023). The WHO has declared the end of pandemic phase of COVID-19: Way to come back in the normal life. *Health Science Reports*, *6*(9), e1544. https://doi.org/https://doi.org/10.1002/hsr2.1544

Sastre, P., Gallardo, C., Monedero, A., Ruiz, T., Arias, M., Sanz, A., & Rueda, P. (2016). Development of a novel lateral flow assay for detection of African swine fever in blood. *BMC Veterinary Research*, *12*(1), 206. https://doi.org/10.1186/s12917-016-0831-4

Sauter-Louis, C., Forth, J. H., Probst, C., Staubach, C., Hlinak, A., Rudovsky, A., Holland, D., Schlieben, P., Göldner, M., Schatz, J., Bock, S., Fischer, M., Schulz, K., Homeier-Bachmann, T., Plagemann, R., Klaaß, U., Marquart, R., Mettenleiter, T. C., Beer, M., … Blome, S. (2021). Joining the club: First detection of African swine fever in wild boar in Germany. *Transboundary and Emerging Diseases*, *68*(4), 1744–1752. https://doi.org/10.1111/tbed.13890

Schadt, E. E., Turner, S., & Kasarskis, A. (2010). A window into third-generation sequencing. *Human Molecular Genetics*, *19*(R2), R227–R240. https://doi.org/10.1093/hmg/ddq416

Shastry, B. S. (2009). SNPs: Impact on Gene Function and Phenotype. In A. A. Komar (Ed.), *Single Nucleotide Polymorphisms: Methods and Protocols* (pp. 3–22). Humana Press. https://doi.org/10.1007/978-1-60327-411-1_1

Shi, J., Wen, Z., Zhong, G., Yang, H., Wang, C., Huang, B., Liu, R., He, X., Shuai, L., Sun, Z., Zhao, Y., Liu, P., Liang, L., Cui, P., Wang, J., Zhang, X., Guan, Y., Tan, W., Wu, G., …

Bu, Z. (2020). *Susceptibility of ferrets, cats, dogs, and other domesticated animals to SARS-coronavirus 2*. https://www.science.org

Shi, X., Liu, X., Wang, Q., Das, A., Ma, G., Xu, L., Sun, Q., Peddireddi, L., Jia, W., Liu, Y., Anderson, G., Bai, J., & Shi, J. (2016). A multiplex real-time PCR panel assay for simultaneous detection and differentiation of 12 common swine viruses. *Journal of Virological Methods*, *236*, 258–265. https://doi.org/10.1016/j.jviromet.2016.08.005

Smith, L. M., Sanders, J. Z., Kaiser, R. J., Hughes, P., Dodd, C., Connell, C. R., Heiner, C., Kent, S. B. H., & Hood, L. E. (1986). Fluorescence detection in automated DNA sequence analysis. *Nature*, *321*(6071), 674–679. https://doi.org/10.1038/321674a0

Sohn, J., & Nam, J.-W. (2018). The present and future of de novo whole-genome assembly. *Briefings in Bioinformatics*, *19*(1), 23–40. https://doi.org/10.1093/bib/bbw096

Spinard, E., Dinhobl, M., Tesler, N., Birtley, H., Signore, A. V., Ambagala, A., Masembe, C., Borca, M. V., & Gladue, D. P. (2023). A Re-Evaluation of African Swine Fever Genotypes Based on p72 Sequences Reveals the Existence of Only Six Distinct p72 Groups. *Viruses*, *15*(11). https://doi.org/10.3390/v15112246

Spinard, E., O'Donnell, V., Vuono, E., Rai, A., Davis, C., Ramirez-Medina, E., Espinoza, N., Valladares, A., Borca, M. V, & Gladue, D. P. (2023). Full genome sequence for the African swine fever virus outbreak in the Dominican Republic in 1980. *Scientific Reports*, *13*(1), 1024. https://doi.org/10.1038/s41598-022-25987-5

Steiner, S., Kratzel, A., Barut, G. T., Lang, R. M., Aguiar Moreira, E., Thomann, L., Kelly, J. N., & Thiel, V. (2024). SARS-CoV-2 biology and host interactions. *Nature Reviews Microbiology*, *22*(4), 206–225. https://doi.org/10.1038/s41579-023-01003-z

Stüder, F., Petit, J.-L., Engelen, S., & Mendoza-Parra, M. A. (2021). Real-time SARS-CoV-2 diagnostic and variants tracking over multiple candidates using nanopore DNA sequencing. *Scientific Reports*, *11*(1), 15869. https://doi.org/10.1038/s41598-021-95563-w

Subbarao, K. (2021). The success of SARS-CoV-2 vaccines and challenges ahead. *Cell Host & Microbe*, *29*(7), 1111–1123. https://doi.org/https://doi.org/10.1016/j.chom.2021.06.016

Subedi, D., Subedi, S., & Karki, S. (2022). First outbreak of African swine fever in Nepal. *Transboundary and Emerging Diseases*, *69*(5), e3334–e3335. https://doi.org/10.1111/tbed.14616

Sunwoo, S. Y., Pérez-Núñez, D., Morozov, I., Sánchez, E. G., Gaudreault, N. N., Trujillo, J. D., Mur, L., Nogal, M., Madden, D., Urbaniak, K., Kim, I. J., Ma, W., Revilla, Y., & Richt, J. A. (2019a). Dna-protein vaccination strategy does not protect from challenge with African swine fever virus Armenia 2007 strain. *Vaccines*, *7*(1). https://doi.org/10.3390/vaccines7010012

Sunwoo, S. Y., Pérez-Núñez, D., Morozov, I., Sánchez, E. G., Gaudreault, N. N., Trujillo, J. D., Mur, L., Nogal, M., Madden, D., Urbaniak, K., Kim, I. J., Ma, W., Revilla, Y., & Richt, J. A. (2019b). Dna-protein vaccination strategy does not protect from challenge with African swine fever virus Armenia 2007 strain. *Vaccines*, *7*(1). https://doi.org/10.3390/vaccines7010012

Tamura, K., Stecher, G., & Kumar, S. (2021). MEGA11: Molecular Evolutionary Genetics Analysis Version 11. *Molecular Biology and Evolution*, *38*(7), 3022–3027. https://doi.org/10.1093/molbev/msab120

Tao, K., Tzou, P. L., Nouhin, J., Gupta, R. K., de Oliveira, T., Kosakovsky Pond, S. L., Fera, D., & Shafer, R. W. (2021). The biological and clinical significance of emerging SARS-CoV-2 variants. In *Nature Reviews Genetics* (Vol. 22, Issue 12, pp. 757–773). Nature Research. https://doi.org/10.1038/s41576-021-00408-x

Tatsi, E.-B., Filippatos, F., & Michos, A. (2021). SARS-CoV-2 variants and effectiveness of vaccines: a review of current evidence. *Epidemiology and Infection*, *149*, e237. https://doi.org/DOI: 10.1017/S0950268821002430

Terpstra, C., Bloemraad, M., & Gielkens, A. L. J. (1984). The neutralizing peroxidase-linked assay for detection of antibody against swine fever virus. *Veterinary Microbiology*, *9*(2), 113–120.

Thiel, H. J., Stark, R., Weiland, E., Rümenapf, T., & Meyers, G. (1991). Hog cholera virus: molecular composition of virions from a pestivirus. *Journal of Virology*, *65*(9), 4705–4712. https://doi.org/10.1128/jvi.65.9.4705-4712.1991

Thiel, H.-J., Stark, R., Weiland, E., Rumenapf, T., & Meyers, G. (1991). Hog Cholera Virus: Molecular Composition of Virions from a Pestivirus. In *JOURNAL OF VIROLOGY* (Vol. 65, Issue 9). https://journals.asm.org/journal/jvi

Töpfer, A., Höper, D., Blome, S., Beer, M., Beerenwinkel, N., Ruggli, N., & Leifer, I. (2013). Sequencing approach to analyze the role of quasispecies for classical swine fever. *Virology*, *438*(1), 14–19. https://doi.org/10.1016/j.virol.2012.11.020

Tran, D. H., Tran, H. T., Le, U. P., Vu, X. D., Trinh, T. B. N., Do, H. D. K., Than, V. T., Bui, L. M., Vu, V. Van, Nguyen, T. L., Phung, H. T. T., & Le, V. P. (2021). Direct colorimetric LAMP assay for rapid detection of African swine fever virus: A validation study during an outbreak in Vietnam. *Transboundary and Emerging Diseases*, *68*(4), 2595–2602. https://doi.org/10.1111/tbed.13879

Tran, H. N. T., Le, N.-C. T., Pham, B. P., Luu, V. Q., & Nguyen, V.-L. (2021). Evaluation of an automated insulated isothermal polymerase chain reaction system for rapid and reliable, on-site detection of African swine fever virus. *Journal of the American Veterinary Medical Association*, *259*(6), 662–668. https://doi.org/10.2460/javma.259.6.662

Tran, X. H., Phuong, L. T. T., Huy, N. Q., Thuy, D. T., Dung, N. van, Quang, P. H., Ngôn, Q. V., Rai, A., Gay, C. G., Gladue, D. P., & Borca, M. V. (2022). Evaluation of the Safety Profile of the ASFV Vaccine Candidate ASFV-G-ΔI177L. *Viruses*, *14*(5). https://doi.org/10.3390/v14050896

Trinh, T. B. N., Truong, T., Nguyen, V. T., Vu, X. D., Dao, L. A., Nguyen, T. L., Ambagala, A., Babiuk, S., Oh, J., Song, D., & Le, V. P. (2021). Development of a novel real-time PCR assay targeting p54 gene for rapid detection of African swine fever virus (ASFV) strains circulating in Vietnam. *Veterinary Medicine and Science*, *7*(6), 2268–2272. https://doi.org/10.1002/vms3.605

Ulrich, L., Halwe, N. J., Taddeo, A., Ebert, N., Schön, J., Devisme, C., Trüeb, B. S., Hoffmann, B., Wider, M., Fan, X., Bekliz, M., Essaidi-Laziosi, M., Schmidt, M. L., Niemeyer, D., Corman, V. M., Kraft, A., Godel, A., Laloli, L., Kelly, J. N., … Benarafa, C. (2022). Enhanced fitness of SARS-CoV-2 variant of concern Alpha but not Beta. *Nature*, *602*(7896), 307–313. https://doi.org/10.1038/s41586-021-04342-0

USDA. (2013). *Goals of a CSF Response*.

USDA. (2023). *African swine fever Response Plan: The Red Book*. www.aphis.usda.gov/fadprep.

van Dijk, E. L., Auger, H., Jaszczyszyn, Y., & Thermes, C. (2014). Ten years of next-generation sequencing technology. *Trends in Genetics*, *30*(9), 418–426. https://doi.org/https://doi.org/10.1016/j.tig.2014.07.001

Van Oirschot, J. T., & Terpstra, C. (1977). A congenital persistent swine fever infection. I. Clinical and virological observations. *Veterinary Microbiology*, *2*(2), 121–132. https://doi.org/https://doi.org/10.1016/0378-1135(77)90003-7

Vilem, A., Nurmoja, I., Niine, T., Riit, T., Nieto, R., Viltrop, A., & Gallardo, C. (2020a). Molecular characterization of African swine fever virus isolates in Estonia in 2014–2019. *Pathogens*, *9*(7), 1–13. https://doi.org/10.3390/pathogens9070582

Vilem, A., Nurmoja, I., Niine, T., Riit, T., Nieto, R., Viltrop, A., & Gallardo, C. (2020b). Molecular characterization of African swine fever virus isolates in Estonia in 2014–2019. *Pathogens*, *9*(7), 1–13. https://doi.org/10.3390/pathogens9070582

Voelkerding, K. V, Dames, S. A., & Durtschi, J. D. (2009). Next-Generation Sequencing: From Basic Research to Diagnostics. *Clinical Chemistry*, *55*(4), 641–658. https://doi.org/10.1373/clinchem.2008.112789

Wagner, K., Springer, B., Pires, V. P., & Keller, P. M. (2018). Molecular detection of fungal pathogens in clinical specimens by 18S rDNA high-throughput screening in comparison to ITS PCR and culture. *Scientific Reports*, *8*(1), 6964. https://doi.org/10.1038/s41598-018-25129-w

Wang, D., Yu, J., Wang, Y., Zhang, M., Li, P., Liu, M., & Liu, Y. (2020). Development of a real-time loop-mediated isothermal amplification (LAMP) assay and visual LAMP assay for detection of African swine fever virus (ASFV). *Journal of Virological Methods*, *276*, 113775. https://doi.org/https://doi.org/10.1016/j.jviromet.2019.113775

Wang, L., Ganges, L., Dixon, L. K., Bu, Z., Zhao, D., Truong, Q. L., Richt, J. A., Jin, M., Netherton, C. L., Benarafa, C., Summerfield, A., Weng, C., Peng, G., Reis, A. L., Han, J., Penrith, M. L., Mo, Y., Su, Z., Vu Hoang, D., … Shi, J. (2024). 2023 International African Swine Fever Workshop: Critical Issues That Need to Be Addressed for ASF Control. *Viruses*, *16*(1). https://doi.org/10.3390/v16010004

Wang, N., Zhao, D., Wang, J., Zhang, Y., Wang, M., Gao, Y., Li, F., Wang, J., Bu, Z., Rao, Z., & Wang, X. (2019). *Architecture of African swine fever virus and implications for viral assembly*. www.oie.int/en/animal-

Wang, X., Wang, X., Zhang, X., He, S., Chen, Y., Liu, X., & Guo, C. (2022a). *Genetic Characterization and Variation of African Swine Fever Virus China/GD/2019 Strain in Domestic Pigs*. https://doi.org/10.3390/pathogens

Wang, X., Wang, X., Zhang, X., He, S., Chen, Y., Liu, X., & Guo, C. (2022b). *Genetic Characterization and Variation of African Swine Fever Virus China/GD/2019 Strain in Domestic Pigs*. https://doi.org/10.3390/pathogens

Wang, Y., Zhao, Y., Bollas, A., Wang, Y., & Au, K. F. (2021). Nanopore sequencing technology, bioinformatics and applications. *Nature Biotechnology*, *39*(11), 1348–1365. https://doi.org/10.1038/s41587-021-01108-x

Weesendorp, E., Backer, J., Stegeman, A., & Loeffen, W. (2011). Transmission of classical swine fever virus depends on the clinical course of infection which is associated with high and low levels of virus excretion. *Veterinary Microbiology*, *147*(3), 262–273. https://doi.org/https://doi.org/10.1016/j.vetmic.2010.06.032

Westhaus, S., & Rabenau, H. F. (2022). Neutralization Assay for SARS-CoV-2 Infection: Plaque Reduction Neutralization Test. In J. J. H. Chu, B. A. Ahidjo, & C. K. Mok (Eds.), *SARS-CoV-2: Methods and Protocols* (pp. 353–360). Springer US. https://doi.org/10.1007/978-1-0716-2111-0_20

Wheeler, D. A., Srinivasan, M., Egholm, M., Shen, Y., Chen, L., McGuire, A., He, W., Chen, Y.-J., Makhijani, V., Roth, G. T., Gomes, X., Tartaro, K., Niazi, F., Turcotte, C. L., Irzyk, G. P., Lupski, J. R., Chinault, C., Song, X., Liu, Y., … Rothberg, J. M. (2008). The complete genome of an individual by massively parallel DNA sequencing. *Nature*, *452*(7189), 872–876. https://doi.org/10.1038/nature06884

Wilson, M. R., Suan, D., Duggins, A., Schubert, R. D., Khan, L. M., Sample, H. A., Zorn, K. C., Rodrigues Hoffman, A., Blick, A., & Shingde, M. (2017). A novel cause of chronic viral meningoencephalitis: C ache Valley virus. *Annals of Neurology*, *82*(1), 105–114.

WOAH. (2024, November 24). *OIE World Animal Health Information System [WWW Document]. WAHIS Interface*. Https://Wahis.Woah.Org/#/Event-Management. https://wahis.woah.org/#/event-management

WOAH: Manual of Diagnostic Tests and Vaccines for Terrestrial Animals. (2023a). *3.9.1 African Swine Fever (Infection with African Swine Fever Virus*.

WOAH: Manual of Diagnostic Tests and Vaccines for Terrestrial Animals. (2023b). *3.9.3 Classical Swine Fever (Infection with Classical Swine Fever Virus)*.

Wood, D. E., & Salzberg, S. L. (2014). Kraken: ultrafast metagenomic sequence classification using exact alignments. *Genome Biology*, *15*, 1–12.

World Health Organization. (2023). *Updated working definitions and primary actions for SARS-CoV-2 variants, 4 October 2023*. https://www.who.int/publications/m/item/updated-working-definitions-and-primary-actions-for--sars-cov-2-variants

World Health Organization. (2025). *Tracking SARS-CoV-2 Variants*. WHO Activities. https://www.who.int/activities/tracking-SARS-CoV-2-variants

World Organization for Animal Health. (2023). *SARS-COV-2 IN ANIMALS-SITUATION REPORT 22*. https://doi.org/10.2807/1560-7917.ES.2020.25.23.2001005#html_fulltext

Wu, K., Liu, J., Wang, L., Fan, S., Li, Z., Li, Y., Yi, L., Ding, H., Zhao, M., & Chen, J. (2020). Current state of global african swine fever vaccine development under the prevalence and transmission of ASF in China. In *Vaccines* (Vol. 8, Issue 3, pp. 1–26). MDPI AG. https://doi.org/10.3390/vaccines8030531

Wu, Z., & McGoogan, J. M. (2020). Characteristics of and Important Lessons From the Coronavirus Disease 2019 (COVID-19) Outbreak in China: Summary of a Report of 72 314 Cases From the Chinese Center for Disease Control and Prevention. *JAMA*, *323*(13), 1239–1242. https://doi.org/10.1001/jama.2020.2648

Yadegari, H., Mohammadi, M., Maghsood, F., Ghorbani, A., Bahadori, T., Golsaz-Shirazi, F., Zarnani, A.-H., Salimi, V., Jeddi-Tehrani, M., Amiri, M. M., & Shokri, F. (2023). Diagnostic performance of a novel antigen-capture ELISA for the detection of SARS-CoV-2. *Analytical Biochemistry*, *666*, 115079. https://doi.org/https://doi.org/10.1016/j.ab.2023.115079

Yamashita, M., Iwamoto, S., Ochiai, M., Yamamoto, A., Sudo, K., Narushima, R., Nagasaka, T., Saito, A., Oba, M., Omatsu, T., Mizutani, T., & Yamamoto, K. (2024). Pathogenicity of genotype 2.1 classical swine fever virus isolated from Japan in 2019 in pigs. *Microbiology and Immunology*, *68*(8), 267–280. https://doi.org/https://doi.org/10.1111/1348-0421.13160

Yang, H., & Rao, Z. (2021). Structural biology of SARS-CoV-2 and implications for therapeutic development. *Nature Reviews Microbiology*, *19*(11), 685–700. https://doi.org/10.1038/s41579-021-00630-8

Yüce, M., Filiztekin, E., & Özkaya, K. G. (2021). COVID-19 diagnosis —A review of current methods. *Biosensors and Bioelectronics*, *172*, 112752. https://doi.org/https://doi.org/10.1016/j.bios.2020.112752

Zhang, Y., Li, Q., Wang, R., Wang, L., Wang, X., Luo, J., Xing, G., Zheng, G., Wan, B., Guo, J., & Zhang, G. (2022). Differentiation of Classical Swine Fever Virus Virulent and Vaccine Strains by CRISPR/Cas13a. *Microbiology Spectrum*, *10*(5). https://doi.org/10.1128/spectrum.00891-22

Zhang, Z., Schwartz, S., Wagner, L., & Miller, W. (2000). A Greedy Algorithm for Aligning DNA Sequences. *Journal of Computational Biology*, *7*(1–2), 203–214. https://doi.org/10.1089/10665270050081478

Zhao, D., Liu, R., Zhang, X., Li, F., Wang, J., Zhang, J., Liu, X., Wang, L., Zhang, J., Wu, X., Guan, Y., Chen, W., Wang, X., He, X., & Bu, Z. (2019). Replication and virulence in pigs of the first African swine fever virus isolated in China. *Emerging Microbes and Infections*, *8*(1), 438–447. https://doi.org/10.1080/22221751.2019.1590128

Zhao, D., Sun, E., Huang, L., Ding, L., Zhu, Y., Zhang, J., Shen, D., Zhang, X., Zhang, Z., Ren, T., Wang, W., Li, F., He, X., & Bu, Z. (2023a). Highly lethal genotype I and II recombinant African swine fever viruses detected in pigs. *Nature Communications*, *14*(1). https://doi.org/10.1038/s41467-023-38868-w

Zhao, D., Sun, E., Huang, L., Ding, L., Zhu, Y., Zhang, J., Shen, D., Zhang, X., Zhang, Z., Ren, T., Wang, W., Li, F., He, X., & Bu, Z. (2023b). Highly lethal genotype I and II recombinant African swine fever viruses detected in pigs. *Nature Communications*, *14*(1). https://doi.org/10.1038/s41467-023-38868-w

Zhao, Y., Liu, F., Li, Q., Wu, M., Lei, L., & Pan, Z. (2019). A multiplex RT-PCR assay for rapid and simultaneous detection of four RNA viruses in swine. *Journal of Virological Methods*, *269*, 38–42. https://doi.org/10.1016/j.jviromet.2019.04.001

Zheng, H. H., Zhang, S. J., Cui, J. T., Zhang, J., Wang, L., Liu, F., & Chen, H. Y. (2020). Simultaneous detection of classical swine fever virus and porcine circovirus 3 by SYBR green I-based duplex real-time fluorescence quantitative PCR. *Molecular and Cellular Probes*, *50*. https://doi.org/10.1016/j.mcp.2020.101524

Zhou, B. (2019). Classical Swine Fever in China-An Update Minireview. *Frontiers in Veterinary Science*, *6*. https://www.frontiersin.org/journals/veterinary-science/articles/10.3389/fvets.2019.00187

Zhou, B., Thao, T. T. N., Hoffmann, D., Taddeo, A., Ebert, N., Labroussaa, F., Pohlmann, A., King, J., Steiner, S., Kelly, J. N., Portmann, J., Halwe, N. J., Ulrich, L., Trüeb, B. S., Fan,

X., Hoffmann, B., Wang, L., Thomann, L., Lin, X., … Beer, M. (2021). SARS-CoV-2 spike D614G change enhances replication and transmission. *Nature*, *592*(7852), 122–127. https://doi.org/10.1038/s41586-021-03361-1

Zimmerman, J. J., Karriker, L. A., Ramirez, A., Schwartz, K. J., Stevenson, G. W., & Zhang, J. Q. (2019). *African swine fever: Diseases of Swine*. New Jersey (NJ: John Wiley & Sons, Inc.

Zou, T., Deng, J., Li, X., Zhang, S., Chen, L., Hao, L., Zhuang, J., Wang, H., Zhang, G., Ge, S., & Tian, K. (2022). Development of a fluorescent probe hydrolysis-insulated isothermal PCR for rapid and sensitive on-site detection of African swine fever virus. *Virologica Sinica*, *37*(3), 462–464. https://doi.org/https://doi.org/10.1016/j.virs.2022.03.002

Zsak, L., Borca, M. V., Risatti, G. R., Zsak, A., French, R. A., Lu, Z., Kutish, G. F., Neilan, J. G., Callahan, J. D., Nelson, W. M., & Rock, D. L. (2005). Preclinical diagnosis of African swine fever in contact-exposed swine by a real-time PCR assay. *Journal of Clinical Microbiology*, *43*(1), 112–119. https://doi.org/10.1128/JCM.43.1.112-119.2005